Review of oceanic mesoscale processes in the North Pacific:

2 physical and biogeochemical impacts

3

1

- 4 Hiromichi Uenoa*, Annalisa Braccob*, John A. Barthc, Maxim V. Budyanskyd, Daisuke
- 5 Hasegawa^e, Sachihiko Itoh^f, Sung Yong Kim^g, Carol Ladd^h, Xiaopei Linⁱ, Young-Gyu Park^j,
- 6 Sergey Prants^d, Tetjana Ross^k, Irina Rypina^l, Yoshikazu Sasai^m, Olga O. Trusenkova^d, Elena I.
- 7 Ustinovaⁿ, Yisen Zhong^o

8

- 9 ^a Faculty of Fisheries Sciences, Hokkaido University, 3-1-1 Minato-cho, Hakodate, 041-8611
- 10 Japan
- 11 b School of Earth and Atmospheric Sciences, Georgia Institute of Technology, 311 Ferst Dr.,
- 12 Atlanta, GA, 30332-0340, U.S.A.
- 13 ° College of Earth, Ocean, and Atmospheric Sciences, Oregon State University, 104 CEOAS
- 14 Admin. Bldg., Corvallis, OR, 97331-5503, U.S.A.
- 15 d V.I. Il'ichev Pacific Oceanological Institute, FEB RAS, 43 Baltiyskaya St., Vladiyostok,
- 16 Primorsky Kray, 690041, Russia
- 17 ^e Fisheries Resources Institute, Japan Fisheries Research and Education Agency (FRA), 3-27-5
- 18 Shinhama-cho, Shiogama, Miyagi, 985-0001, Japan
- 19 f Atmosphere and Ocean Research Institute, The University of Tokyo, 5-1-5 Kashiwanoha,
- 20 Kashiwa, Chiba, 277-8564, Japan
- 21 g Department of Mechanical Engineering, School of Mechanical and Aerospace Engineering,
- 22 Korea Advanced Institute of Science and Technology, 291 Daehak-ro, Yuseong-gu, Daejeon
- 23 34141, Republic of Korea
- 24 h§ Pacific Marine Environmental Laboratory, National Oceanic and Atmospheric Administration,
- 25 7600 Sand Point Way NE, Seattle, WA, 98115, U.S.A.
- ¹ College of Physical and Environmental Oceanography, Ocean University of China, 238 Songling
- 27 Rd., Laoshan District, Qingdao, Shandong, 266100, People's Republic of China
- 28 ^j Ocean Circulation Research Center, Korea Institute of Ocean Science and Technology, 385
- 29 Haeyang-ro, Yeongdo-gu, Busan, 49111, Republic of Korea
- 30 k Institute of Ocean Sciences, Fisheries and Oceans Canada, P.O. Box 6000, Sidney, BC, V8L
- 31 4B2, Canada
- 32 Physical Oceanography Department, Woods Hole Oceanographic Institution, 266 Woods Hole
- 33 rd, MS#21, Woods Hole, MA, 02543, U.S.A.

- ^m Japan Agency for Marine-Earth Science and Technology, 2-15, Natsushima-cho, Yokosuka,
- **35** Kanagawa, 237-0061, Japan
- 36 ⁿ Laboratory of Fisheries Oceanography, Pacific branch of Russian Federal Research Institute of
- 37 Fisheries and Oceanography, 4 Shevchenko Alley, Vladivostok, Primorsky Kray, 690091, Russia
- ^o School of Oceanography, Shanghai Jiao Tong University, 1954 Huashan Rd., Shanghai, 200030,
- 39 China

40

- *Corresponding authors, at: Faculty of Fisheries Sciences, Hokkaido University, 3-1-1 Minato-
- 42 cho, Hakodate, 041-8611 Japan (H. Ueno); School of Earth and Atmospheric Sciences, Georgia
- 43 Institute of Technology, 311 Ferst Dr., Atlanta, GA, 30332-0340, U.S.A. (A. Bracco).
- 44 E-mail addresses: ueno@fish.hokudai.ac.jp (H. Ueno), abracco@gatech.edu (A. Bracco).

45

46 § Retired.

47

- 48 Keywords: Mesoscale processes, North Pacific, fishery, biophysical interactions, climate
- 49 variability and change

50

51

ABSTRACT

- 52 Physical transport dynamics occurring at the ocean mesoscale (~ 20 km 200 km) largely
- determine the environment in which biogeochemical processes occur. As a result, understanding
- and modeling mesoscale transport is crucial for determining the physical modulations of the
- marine ecosystem. This review synthesizes current knowledge of mesoscale eddies and their
- 56 impacts on the marine ecosystem across most of the North Pacific and its marginal Seas. The
- North Pacific domain north of 20°N is divided in four regions, and for each region known,
- unknowns and known-unknowns are summarized with a focus on physical properties, physical-
- biogeochemical interactions, and the impacts of climate variability and change on the eddy field
- and on the marine ecosystem.

61

1. Introduction

The role that the ocean circulation plays on the living marine resources is widely recognized, but often not coherently integrated. This review aims at synthesizing the physical knowledge across a large portion of the North Pacific and its marginal Seas, focusing on mesoscale eddies and their impacts on the marine ecosystem. Oceanic mesoscale eddies with radii between *ca.* 20 and 200 km are ubiquitous features of the world ocean (e.g., Robinson, 1983). They are typically produced by instability processes and are in approximate geostrophic balance in the horizontal and in hydrostatic balance in the vertical (e.g., McGillicuddy, 2016). High-resolution sea surface height (SSH) fields constructed by merging measurements from two or more simultaneously operating altimeters have revealed that SSH variability throughout most of the world ocean is dominated by westward-propagating nonlinear mesoscale eddies that trap fluid at their core (Chelton et al., 2007; 2011b). Recent progress on eddy detection and tracking algorithms has helped clarify eddy formation mechanisms and location, their propagation, amplitude, radius, and evolution (Chelton et al., 2007; 2011b).

Mesoscale eddies influence the marine ecosystems in many ways; foremost by altering phytoplankton (chlorophyll) concentrations in the euphotic layer. This is achieved through at least six mechanisms (McGillicuddy, 2016). The first two are related to eddy advection. On time scales longer than 2-3 weeks, the dominant impact on surface chlorophyll variability is that of eddyinduced horizontal advection by the rotational velocities of the eddies (Chelton, 2011a). These rotational motions redistribute the chlorophyll creating a dipole pattern but likely no net increase in primary productivity; following Gaube et al. (2014), in this paper, this mechanism is referred to as eddy stirring. The second advective mechanism is eddy trapping. Most extratropical eddies are formed because of nonlinear instabilities that occur in presence of strong currents and/or bathymetric features and therefore relatively close to coastal, nutrient rich areas (Chelton et al., 2011b). The eddies in which the nutrients are trapped inside are transported away from their formation region, creating patches of high chlorophyll in otherwise less productive areas. This mechanism does not augment primary productivity globally either, but contributes significantly to regional budgets. The following four mechanisms increase primary productivity, rather than just moving nutrients and chlorophyll around horizontally. Eddy pumping, the third mechanism described by Falkowski et al. (1991), occurs when a cyclonic eddy intensifies and upwelling occurs in its core, resulting in enhanced chlorophyll growth. The fourth mechanism is eddyinduced Ekman pumping and is controlled by the surface stress differences around the eddy, by the interaction of the surface stress with the surface current vorticity gradient, and, to a lesser extent, by the eddy-induced spatial variability of sea surface temperature (SST) (Gaube et al., 2015). The fifth mechanism is associated with the change of mixed-layer depth due to the presence of mesoscale eddies, with shallow mixed layers tending to have higher chlorophyll levels and vice versa. The mixed layer depth in eddies is influenced directly by isopycnal displacement and indirectly by changing propagation characteristics of near-inertial waves and by SST, as summarized in McGillicuddy (2016). This mechanism is important in the Southern Ocean, where it has been linked to changes in light and micro-nutrient availability that impact the near-surface chlorophyll concentration (Song et al., 2018). The sixth mechanism is due to processes that occur at scales of few kilometers (submesoscales) around the eddy periphery and include streamers and local upwelling, which may enhance chlorophyll production (McGillicuddy et al., 1995; McGillicuddy, 2016; Zhong et al., 2017; Liu et al., 2021).

Eddies further impact zooplankton, fish, marine mammals, and seabirds. The zooplankton modulation was first supported by observations in the Gulf Stream region, where Wiebe et al. (1976) reported that in a cold core cyclonic eddy or "ring" a zooplankton assemblage persisted longer than a phytoplankton assemblage. Mesoscale eddies can have both positive and negative impacts on fish recruitment via retention of fish larvae at their interior. For example, in the Kuroshio region, Kasai et al. (2002) found that eddies contribute to fish recruitment because they tend to recirculate in the coastal nursery area. On the other hand, in the Leeuwin Current system in the Indian Ocean the entrainment of larvae and eggs of teleost populations in a warm core eddy had a negative impact on recruitment (Gaughan, 2007). Mesoscale eddies may also influence higher trophic levels. For example, in the Gulf of Mexico the catch per unit effort (CPUE) of Atlantic bluefin tuna is significantly higher in cyclonic eddies (Teo and Block, 2010). In the Southern Ocean, mesoscale eddies and (sub-)mesoscale features ensure that king penguins and elephant seals have access to localized areas with high concentrations of prey (Cotté et al., 2007; 2015).

In the North Pacific, which is a source of "food, economic benefit and recreation, primarily through the abundant living marine resources" for all the Nations that surround it (PICES, 2004) and the target region for this paper, many recurrent eddies have been observed and have been shown to impact the ecosystems. Warm-core and cold-core rings in the Kuroshio and Oyashio Extension (KOE) Region are among the most extensively studied mesoscale eddies because their peripheries are excellent fishing grounds for pelagic fish, such as skipjack, mackerel, flying squid

and saury (e.g., Saitoh et al., 1986; Sugimoto and Tameishi, 1992; Prants et al., 2014a). In the California Current System (CCS) larval abundance of Pacific sardine is greater in offshore eddies relative to the inshore, slope and surrounding offshore waters (Logerwell et al., 2001) due to high survival rate supported by enhanced primary production in their interior (Logerwell and Smith, 2001). The Gulf of Alaska is recognized as a high-nutrient low-chlorophyll region (Nishioka et al., 2001) due to limited iron availability, and eddies formed along its coastlines contribute to the transport of iron from the coastal to the offshore ocean (Johnson et al., 2005). These eddies are so transformative that they are named based on their formation area; Haida, Sitka, and Yakutat eddies form off Haida Gwaii, Sitka and Yakutat, respectively (Crawford, 2002; Tabata, 1982; Ladd et al., 2005a).

126

127

128

129

130

131

132

133

134

135

136

137

138

139

140

141

142

143

144

145

146

147

148

149

150

151

152

153

154

155

156

Mesoscale eddies in the North Pacific have been investigated mainly from the perspective of their formation area, that is, many regional studies have been written on the properties and impacts of eddies formed in a given region. Few inter-comparisons have been conducted, but within specific areas (e.g., Henson and Thomas, 2008 in the Gulf of Alaska; Itoh and Yasuda, 2010a in the Kuroshio/Oyashio and their extension regions; Cheng et al., 2014 in the offshore North Pacific) and with a narrow focus, usually on physical properties. Existing inter-comparisons are also often limited to the analysis of satellite data (e.g., Kouketsu et al., 2015). This paper, on the other hand, synthesizes physical knowledge on mesoscale eddies and their impacts on the marine ecosystem across a range of scales and data types across most of the North Pacific focusing on the region north of 20°N (next referred simply as North Pacific). First, we divide the North Pacific area of interest into four regions, and for each region briefly discuss eddy formation (type and timing) and how long they last using eddy track data (Chelton et al., 2011b) (Section 2). Then we review the impact of mesoscale eddies on the marine ecosystem as well as their physical characteristics within each region (Section 3), summarizing findings in four tables that focus on known and unknowns in each region. Finally, we discuss the similarities and differences across regions, highlighting where observations/studies are mostly needed (Section 4). Although the target of this paper is mesoscale processes and their impacts, we introduce submesoscale processes as well whenever possible (see McWilliams, 2016 for a review of submesoscale circulations). Additionally, we provide information, when useful and available, about climate trends that may directly or indirectly, i.e. through changes in mesoscale activity, impact the marine ecosystem.

2. General characteristics of mesoscale eddies in the North Pacific and their impact on chlorophyll-a distribution

In this synthesis, the North Pacific has been divided into 4 regions (Figs. 1 and 2). Region 1 covers the CCS. Its northern boundary was determined by evaluating the correlation between SSH and surface chlorophyll-a (Chl-a) anomalies (Fig. 1) and selecting the latitude at which negative correlations appear (up to 45°–50°N) (Gaube et al., 2014; Kouketsu et al., 2015). It includes the west coast of Vancouver Island, that is part of the upwelling dominated CCS (e.g., Denman et al., 1981; Crawford and Thomson, 1991). Region 2 consists of the coastal region to the north of the CCS that extends to the northeastern North Pacific and the Bering Sea, where downwelling due to along-shore wind is prevalent (e.g. Henson and Thomas, 2008). Region 3 covers the western boundary current and includes the marginal seas in the western Pacific where physical and biological processes are strongly influenced by the Kuroshio and Oyashio currents (e.g. Yasuda, 2003). Region 4 covers the open North Pacific with the KOE. Strong eddies are seldom observed in the eastern part of Region 4 (e.g. Cheng et al., 2014).

The most noticeable features in the correlation between SSH and surface Chl-a anomalies in Fig. 1 are the strong negative correlations along the Kuroshio and Kuroshio extension and in the CCS. Gaube et al. (2014) presumed that the negative correlation in the Kuroshio area, which is found for most western boundary currents, results from higher chlorophyll in cyclonic eddies due to upwelling accompanied by eddy intensification and also due to the trapping of coastal waters in these regions, which have higher chlorophyll. In the CCS, on the other hand, eddy stirring and trapping play an important role and the correlation results from a chlorophyll response to the numerous cyclonic eddies (Gaube et al., 2014). Positive correlations are observed along the Alaskan Stream and Alaska Current in Region 2 and along the East Kamchatka and Oyashio currents in Region 3. Here the ambient cross-current Chl-a gradient is negative (i.e. lower Chl-a to the left of the currents) which explains the positive sign of the 4 weeks lag correlation between Chl-a and SSH anomaly (Figs. 5b and 6a in Gaube et al., 2014). Regional studies have shown that micronutrients transported from the shelf region offshore by eddy stirring and trapping support primary production in the Gulf of Alaska (e.g., Crawford et al., 2007; Ladd et al., 2009), as further reviewed in Section 3.2.

Maintaining a dynamic view of the North Pacific system is essential as mesoscale activity may change over time. The last four decades have seen a non-uniform increase in SST over

most of the North Pacific (Fig. 3). The Kuroshio and Oyashio currents and their extensions and adjacent regions experienced the greatest warming (Region 3 and 4), approaching 0.5°C/decade in the marginal seas between 1980 and 2018 (Fig. 3). The SST trend over the CCS (Region 1) and portions of the Alaskan coastlines (Region 2) has been more moderate, but these areas have been hit by extreme warming events in recent years, as we will discuss in Section 3. Warming, whether long term or episodic, and changes in stratification and water masses can modify or modulate the mesoscale distribution, and/or change how the ecosystem responds to the presence of mesoscale eddies.

To begin our review of mesoscale dynamics, we first discuss the relative contribution of each eddy formation area in the North Pacific from the perspective of the frequency of eddy 'spawning' and/or eddy lifetime using Chelton et al. (2011b) version 4 eddy dataset (http://wombat.coas.oregonstate.edu/eddies/AVISO_announcement.html). This dataset covers the period from January 1, 1993 to January 18, 2018 (~25 years) and includes eddies with lifetimes of 4 weeks or longer. To statistically quantify the relative contribution of each eddy formation area, we estimate the "eddy yield", that is, the average yearly lifetime integral of the eddies formed in each 2°×2° box over 25 years.

Figs. 4a and 5a show the formation rate of anticyclonic and cyclonic eddies in each 2°×2° box per year, respectively. While not uniformly, eddies form throughout the open North Pacific, consistent with results by Chelton et al. (2011b) for a shorter 16-year analysis. This agrees with the conclusions that nearly all of the World Oceans are baroclinically unstable (Gill et al., 1974; Robinson and McWilliams, 1974; Stammer, 1998; Smith, 2007b among others). Eddies are formed most frequently (ca. twice per year in the 2°×2° boxes) along the eastern boundary (Region 1 and eastern part of Region 2), along island chains between the open North Pacific and marginal seas (Regions 2 and 3), and near the Hawaiian Islands (~20°N, 155°W) and seamounts west-northwest of Hawaiian Islands (Region 4) (Figs. 4a and 5a). Meandering boundary currents, interactions between currents and topography (e.g., Swaters and Mysak, 1985 in the northeastern Gulf of Alaska), wind forcing effects (e.g., Thomson and Gower, 1998; Ladd and Cheng, 2016 in the northeastern Gulf of Alaska), and tidal mixing (e.g., Ohshima et al., 2005 in the southeastern Sea of Okhotsk) contribute to eddy formation. Eddies form slightly less frequently (ca. more than once per year but less than two in the $2^{\circ} \times 2^{\circ}$ boxes) in the open subtropical gyre west of the eastern boundary (around 20°-40°N, 140°-170°W: eastern part of Region 4). In this area the meridional flow is effective at generating strong eddies (Spall, 2000; Smith, 2007a). Within the western

boundary currents and their extensions (Regions 3 and 4), the eddy formation frequency is high (Chelton et al., 2011b). Eddies seldom form in the center of the Alaskan gyre (~50°N, 160°W). This area is known as an eddy desert (Henson and Thomas, 2008); our analysis indicates that the eddy desert is a region of both rare eddy formation as well as rare eddy propagation.

Overall, the spatial distribution of eddy formation is similar for both anticyclonic and cyclonic eddies (Figs. 4a and 5a), but differs seasonally (Fig. 6). Along the eastern boundary of the North Pacific (northern portion of Region 1 and eastern part of Region 2), anticyclonic eddies form more frequently in winter and spring while cyclonic eddies form more frequently in boreal summer and fall. In the northern part (eastern part of Region 2), anticyclonic eddies are generally thought to be generated in boreal winter, when downwelling-favorable southerly winds are at their maximum (Tabata, 1982; Henson and Thomas, 2008). In the southern part of Region 1 the eddy kinetic energy (EKE) is stronger in summer/fall and has been associated with local upwelling-favorable northerly winds in boreal summer (Marchesiello et al., 2003). Around 20°-30°N and 130°-170°W in the southeastern portion of Region 4, both anticyclonic and cyclonic eddies form frequently in boreal winter and spring. The seasonal variation of eddy formation in the 20°-30°N band of Region 4 is consistent with that of vertical velocity shear and stratification, pointing to baroclinic instability as generation mechanism (Qiu, 1999). Near islands/seamounts/island-chains in Regions 2 and 3, marked seasonal variations in eddy formation are not observed. In the western boundary currents and their extensions in Regions 3 and 4, eddies form slightly more frequently in winter and spring but differences between seasons are small.

The distribution of eddy lifetime is quite different from that of eddy formation rate (Figs. 4 and 5); areas of frequent eddy formation - e.g., eastern boundary of the North Pacific - do not correspond to areas where long-lived eddies are formed. Figs. 4b and 5b show anticyclonic and cyclonic eddy lifetimes averaged within their formation area, respectively; colors in each grid indicate average lifetimes of eddies formed in the grid. The distributions of anticyclonic and cyclonic lifetimes are similar everywhere except in the Gulf of Alaska, and eddies that last more than 100 days preferentially form in the open ocean (Region 4). In the Gulf of Alaska, along the Aleutian Islands in Region 2, to the east off Hokkaido and the Kamchatka peninsula in Region 3, on the other hand, the average lifetime of anticyclonic eddy is longer than that of cyclones, as found in previous studies (Isoguchi and Kawamura, 2003; Henson and Thomas, 2008; Itoh and Yasuda, 2010a; Lyman and Johnson, 2015; Prants et.al., 2018; 2020).

Using the information on eddy formation rate and lifetime, we evaluated eddy yield (sum of lifetime divided by 9149 days (analysis period: 01Jan1993–18Jan2018)) within each 2°×2° formation area (Figs. 4c and 5c), providing a quantitative measure of the importance of the eddies to the circulation (over a 25-yr period). The geographical distributions of eddy yield (Figs. 4c and 5c) are mostly similar to eddy formation rate (Figs. 4a and 5a), except for few areas. Along the eastern boundary of the North Pacific, both anticyclonic and cyclonic eddies formed south of 45°N (in Region 1) can be traced for a long time (averaged lifetimes $> \sim 100$ days, Figs. 4b and 5b). In the area north of 45°N, on the other hand, only anticyclonic eddies are traced for long periods, while the lifetime of cyclonic eddies is relatively short (Fig. 5b). Figs. 4c and 5c also indicate that Region 1 is the most important from the perspective of eddy yield, followed by the eastern part of the Gulf of Alaska and the area along the Aleutian Islands in Region 2, especially for anticyclonic eddies. Eddy yield is high also in Region 4 around 20°-40°N and 160°E-140°W, away from the eddy desert, because moderately long-lived eddies are formed there relatively frequently. Near islands and seamounts, many eddies are formed but their lifetime is generally short, except for those adjacent to the Hawaiian Islands. In the western boundary currents and their extensions (Region 3 and 4), eddy yield is relatively high especially in the Oyashio front region due to frequent eddy formation (Figs. 4a and 5a). Since eddy yield is just a sum of eddy lifetime divided by analysis days, more detailed studies are required to quantify the contribution of each eddy formation area to heat and freshwater transport, primary productivity, etc.

271

272

273

275

276

277

278

279

280

281

252

253

254

255

256

257

258

259

260

261

262

263

264

265

266

267

268

269

270

3. Regional summaries

3.1 Region 1: California Current System region

274 *3.1.1. Introduction*

Region 1 is occupied by the CCS (Figs. 1, 2 and 7) extending from the North Pacific Current (NPC) (about ~50°N) to Baja California, Mexico (about 15°N). Its circulation consists in an equatorward flow that is forced by winds and by the pressure system along the west coast of the North American continent. The CCS is one of the four Eastern Boundary Upwelling Systems (Capone and Hutchins, 2013) and sustains a productive and diverse fishery that relies on the upwelling of nutrient-rich waters into the euphotic layer. More than 60 years ago it was noted that high biomass in the CCS is associated with low water temperatures (Reid et al., 1958). The

source of this cold water is coastal upwelling driven by the longshore component of local wind that results in a divergence of surface water at the coast in turn replaced by cold, nutrient-rich water from greater depths. Near the coast a wind-driven southward flowing jet dominates the dynamics, while further off-shore curl-driven upwelling is predominant (Checkley and Barth, 2009). Underneath the CCS, between 150 and 250 m of depth, the California Undercurrent transports water along the North America continental slope from the equatorial Pacific to Vancouver Island which is warm, salty and nutrient-rich relative to the interior of the subtropical gyre (Fig. 7).

Meandering characterizes both the CCS and the coastal jet, and is accompanied by the generation of vorticity filaments and mesoscale eddies with size comparable to the Rossby radius of deformation (order 100 km) and smaller (10–50 km). The generation of mesoscale eddies is generally higher between boreal late summer to early fall and results from the accumulation of wind-forced energy in the mean flow, as shown by Strub and James (2000) in the first complete assessment of the seasonal evolution of this region. Summer and fall are also, and by far, the most active seasons for California Undercurrent eddy generation (Kurian et al., 2011). The seasonal cycle has stronger amplitude in the California Undercurrent than in the CCS.

3.1.2. Physical properties

In the CCS, the presence and relevance of cyclonic (cold) and anticyclonic (warm) mesoscale eddies has been recognized through observations and modeling since the 1980s (Owen, 1980; Lynn and Simpson, 1987; Batteen, 1997; Huyer et al., 1998; Garfield et al., 1999; Chereskin et al., 2000; Strub and James, 2000; Barth et al., 2005). Owen (1980) enumerated the eddies that occurred in the CalCOFI Atlas (Wyllie, 1966) in the 25°–38°N latitudinal band, finding a predominance of large (> 100 km) cyclones over large anticyclones. In the subsurface, on the other hand, observations in the late 1990s' revealed that warm anticyclonic eddies prevail (Huyer et al., 1998; Garfield et al., 1999; Chereskin et al., 2000). They originate from the California Undercurrent and have been often referred as Cuddies (California Undercurrent Eddies; Garfield et al., 1999; Collins et al., 2013; Pelland et al., 2013). Cuddies are smaller than surface eddies and their representation in ocean model requires submesoscale-resolving meshes (grid sizes below 3 km in the horizontal) to capture the generation process.

Information on the formation areas, propagation, variability, and general physical properties of mesoscale eddies in the CCS has become increasingly available through the satellite altimeter records and the increasing resolution of numerical experiments. Systematic eddy identification and tracking have been conducted using maps of SSH, either observed or modeled (Stegmann and Schwing, 2007; Chaigneau et al., 2009; Kurian et al., 2011; Chelton et al., 2011b). The first satellite-based demography of persistent mesoscale eddies was compiled by Stegmann and Schwing (2007), using altimeter data from 1995 to 2004 over the area 30°-50°N and 130°W to the continent. They showed that both cyclonic and anticyclonic eddies with lifetime >70 days are generated predominantly in areas seaward of the 1000 m isobath, and propagate westward with a speed up to 3.5 km day⁻¹. The sizes (based on close contours) of cyclones and anticyclones are comparable, with mean \pm std of 163 ± 65 km and 166 ± 59 km, respectively, but the mean generation rates are ~13 cyclonic and ~ 6 anticyclonic eddies per year, which is consistent with the analysis by Owen (1980). Long-lived eddies and mesoscale eddy activity in general are greatest roughly between latitudes 32°-40°N, and there is a distinct minimum to the north of approximately 42°N. The main formation area for mesoscale cyclones is 32°-34°N, while for anticyclones eddies is between 38° and 40°N. These contrasts have been confirmed by Chaigneau et al. (2009) and Chelton et al. (2011b), and more recently by Chenillat et al. (2018) for the southern part of the CCS off the Baja California Peninsula. Using both satellite altimetry and a high-resolution numerical model, Kurian et al. (2011) identified eddies both at the surface and at the subsurface. At the surface, long-lived cyclones

312

313

314

315

316

317

318

319

320

321

322

323

324

325

326

327

328

329

330

331

332

333

334

335

336

337

338

339

340

341

342

343

Using both satellite altimetry and a high-resolution numerical model, Kurian et al. (2011) identified eddies both at the surface and at the subsurface. At the surface, long-lived cyclones occur approximately twice as frequently as long-lived anticyclones, whereas at the subsurface, the former are less than 25% of the latter. The difference in dominance of cyclonic/anticyclonic eddies with depth is consistent with previous studies (e.g., Owen, 1980; Huyer et al., 1998; Garfield et al., 1999; Chereskin et al., 2000; Stegmann and Schwing, 2007; Chaigneau et al., 2009; Chelton et al., 2011b). The composites of temperature and salinity profiles clearly show cold/fresh (warm/saline) anomalies for both surface and subsurface anticyclonic (cyclonic) eddies.

As mentioned, subsurface anticyclonic eddies generated by the California Undercurrent are classified as submesoscale coherent vortices and named Cuddies (Garfield et al., 1999; Collins et al., 2013; Pelland et al., 2013). The analysis of a submesoscale-resolving simulation suggests that the subsurface mesoscale anticyclonic eddies with a scale close to the baroclinic radius of deformation emerge from the generation of submesoscale negative-vorticity along the inshore

side of the California Undercurrent (Molemaker et al., 2015) through shear instability. In this region elevated submesoscale variance has indeed been observed (Itoh and Rudnick, 2017).

3.1.3. Physical-biogeochemical interactions

Biological activity along the CCS has been investigated since the late 1940's following the creation of the California Cooperative Oceanic Fisheries Investigation (CalCOFI) by Harald U. Sverdup and others. The eddies formed near shore along the CCS path are primary contributor to long-distance cross-shelf transport and to the redistribution of upwelled water, and they are characterized by enhanced nutrients and therefore elevated biological activity (Marchesiello et al., 2003; Gruber et al., 2011; Chenillat et al., 2018).

Early recognition of spatially correlated mesoscale patterns of cold, upwelled water and enhanced surface pigment concentration goes back decades in this region (e.g., Strub et al., 1990; Abbott and Barksdale, 1991). Current understanding of the biological response to jets, filaments, meanders, fronts and eddies in the CCS has been reviewed by Checkley and Barth (2009). Correlated temperature and surface chlorophyll features are associated with upwelling filaments with widths of ~10 km and lengths of 100s of km extending offshore from the coastline, for example, Heceta Bank (44°N), Cape Blanco (42.8°N), Cape Mendocino (40.4°N) and Point Conception (34.5°N) (Fig. 8). Other large features on the order of 100s of km in the along-coast direction are associated with flow-topography interaction at capes and submarine banks and canyons (e.g., Barth et al., 2005; Stegmann and Schwing, 2007). Mesoscale eddies, both cyclonic and anticyclonic with diameters of 30–50 km show correlated variation of temperature and surface chlorophyll. Cyclonic eddies are regions of surface convergence and therefore enhanced surface chlorophyll. At the finest scales, submesoscale instabilities (Barth, 1994) and eddies with cold water and high chlorophyll are present on the flanks of the meandering jets and filaments. All these features are apparent in Fig. 9.

A recent analysis based on satellite-derived measurements has shown that the longer-lived cyclonic eddies located offshore the CCS but generated near the coast are characterized by higher concentrations of particulate organic carbon than cyclones of similar amplitude generated offshore, and that this particulate organic carbon enrichment can be tracked for 1000 km from the coast (Amos et al., 2019).

3.1.4 Variability

In Region 1 the relation between large-scale climate variability and ocean transport, and therefore marine ecosystems variability, has been widely documented through long-term observing systems (see Di Lorenzo et al., 2013a and citation therein). Relevant large-scale climate modes are the El Niño Southern Oscillation (ENSO), the Pacific Decadal Oscillation (PDO) (Mantua et al., 1997; Mantua and Hare, 2002) and the North Pacific Gyre Oscillation (NPGO) (Di Lorenzo et al., 2008; 2009). The warm phase of ENSO, El Niño, has large and often negative consequences on the CCS ecosystem through both local (see e.g., Alexander et al., 2002) and advective mechanisms (see e.g., Frischkencht et al., 2015). Impacts on the marine ecosystem may occur through the direct influence of ENSO on temperature, dissolved O2, and pH, via food web changes and through changes in advection and therefore transport of organisms (predators, prey, parasites, or pathogens) poleward and/or onshore. The mechanism by which the PDO and NPGO influence the marine ecosystem of the CCS is established through their atmospheric forcing counterparts, the Aleutian Low and the North Pacific Oscillation, respectively, which control the upwelling and downwelling 3-dimensional cells at interannual to decadal scales (Chhak and Di Lorenzo 2007; Chhak et al., 2009; Song et al., 2011; Jacox et al., 2018). The NPGO is key to the upwelling in the CCS, as shown through numerical simulations (Combes et al., 2013). Through its link to the coastal wind stress, the NPGO explains much of the decadal variability of salinity and key biological variables in the CCS (Di Lorenzo et al., 2008). In the last decades the variance of these modes and especially of the NPGO has grown over time in the winter season, as evidenced by both sea level pressure and surface temperature anomalies (Liguori and Di Lorenzo, 2018). It remains to be investigated if and how this increase in variance in the modes impacts mesoscale transport dynamics.

374

375

376

377

378

379

380

381

382

383

384

385

386

387

388

389

390

391

392

393

394

395

396

397

398

399

400

401

402

403

404

405

Advances in regional physical-biological modeling in the past twenty years (see the seminal paper by Marchesiello et al., 2003) have allowed better resolution of how the eddy-scale processes in the CCS modulate the water mass distribution and in turn the marine ecosystem. In terms of ecosystems, transport dynamics control primary productivity through nutrient fluxes associated with upwelling and eddy-pumping, ecosystem connectivity and species distribution (e.g., zooplankton) through changes in alongshore currents, and exchanges of biological properties between the shelves and the open ocean (e.g., iron, phytoplankton, fish larvae, and carbon) via meso- and submeso-scale eddies and fronts (see for a review Di Lorenzo et al., 2013b).

Jets, eddies and filaments are responsible for a high production that is either consumed, is transported horizontally or sinks, at times in a subsiding water mass (Fig. 9). According to model simulations (Plattner et al., 2005; Gruber et al., 2006), mesoscale circulations cause a decoupling between new and export production along the central California coast through the offshore transport of small particles. Cyclonic (cold core) eddies that form offshore of the upwelling jet are usually areas of high primary and secondary production (Huntley et al., 2000). For example, off the coast of Oregon late-stage larvae of Pacific sardines are more abundant offshore in the cyclonic eddies than elsewhere, with eggs being in larger concentrations inshore (Logerwell and Smith, 2001; Fig. 8). This observation has been corroborated by a related modeling study by Logerwell et al. (2001) that attributed the high survival of sardine larvae in offshore, cyclonic eddies, to enhanced production of their planktonic food. Similarly, the strong mesoscale activity in the core of the California Current off central and southern California (Lynn and Simpson, 1987) affects chemical and biological properties (Hayward and Venrick, 1998), and support sardine spawning (Checkley et al., 2000). With a 10-year long integration of a coupled physical-biological model run at 5 km horizontal resolution, Chenillat et al. (2016) showed that cyclonic eddies in the CCS propagate westward across the shelf up to 800 km, transporting coastal planktonic organisms and maintaining locally elevated primary productivity for up to 1 year. Modeled anticyclones, on the other hand, covered about half of the distance during their ~ 6 months lifetime and had a more limited impact on the ecosystem. In this simulation eddies occupied about 8% of the modeled CCS domain at any given time but were responsible for approximately 50% of the nitrate transport. The influence of mesoscale eddies is not limited to primary productivity. Recent in situ and modeling studies have indicated that mesoscale features enhance carbon export in the CCS (Stukel et al., 2017) and are important for understanding trends in ocean acidification in the CCS (Gruber et al., 2012).

406

407

408

409

410

411

412

413

414

415

416

417

418

419

420

421

422

423

424

425

426

427

428

429

430

431

432

433

434

435

436

437

The role of submesoscale variability and overall contribution of submesoscale circulations to the CCS ecosystem remains uncertain. The vertical velocities associated with surface frontogenesis and nonlinear Ekman pumping have been shown to downwell phytoplankton, effectively removing them from the euphotic layer. Gruber et al. (2011) found that the overall CCS productivity decreased in submesoscale permitting simulations compared to mesoscale resolving runs because phytoplankton contained in submesoscale filaments formed at the mesoscale upwelling front were subducted out of the euphotic zone before the nutrients were

fully consumed. An investigation focused on Monterey Bay used numerical simulations together with bio-optical and physical observations to show that the negative impact of submesoscale downwelling is strong in early summer, but the high vertical velocities at the edge of the CCS front have a positive effect on chlorophyll concentrations later in the season, when the mixed-layer depth is shallower than the euphotic depth (Shulman et al., 2015).

In terms of trends, over the last decade the region has experienced dramatic changes in its climate with the occurrence of several record-breaking temperature extremes between 2013–2021, such as the multi-year 2013–15 Northeast Pacific marine heatwave (Bond et al. 2015; Di Lorenzo and Mantua, 2016; McCabe et al., 2016), and the strong 2015-16 El Niño (Jacox et al., 2016). These changes in ocean temperatures influence the metabolic rate and oxygen demand of marine species (e.g., Deutsch et al., 2015), and displace habitats (e.g., Pinsky et al., 2013).

It is known that the eddy circulation statistics are influenced by climate forcing (Davis and Di Lorenzo, 2015). The regional model simulations by Combes et al. (2013), for example, have shown that in the CCS the low-frequency variability of coastal upwelling and the cross-shelf transport of the upwelled water mass depend on the alongshore wind stress in both the northern and southern portions. However, the offshore surface transport is modulated by the mesoscale activity which differs in the two regions. In the south, in particular, cyclonic eddies entrain water masses of southern origin that are then advected poleward by the California Undercurrent, and Kahru et al. (2012) have shown that fronts have increased in frequency over the last couple of decades. This likely happened in response to climate-driven changes in wind and stratification. Building upon these results, Chenillat et al. (2013) investigated the influence of intrinsic and deterministic physical forcing on the ecosystem response in the CCS, again using a circulation model coupled to the North Pacific Ecosystem Model for Understanding Regional Oceanography (NEMURO; Kishi et al., 2007). In their simulation the timing of the onset of the upwelling season in the CCS varies as function of the alongshore winds. The onset, in turn, affects not only the coastal ecosystem during the upwelling season but also the offshore ecosystem year-round. This offshore response can be as much as a factor of two stronger than that at the coast in relative amplitude.

On the marine ecosystem side, drastic changes in the chemistry have been projected, with ocean acidity expected to rise dramatically by 2050 (Gruber et al., 2012). These model projections are limited by resolution and an oversimplified representation of biogeochemical

cycling but have motivated further observational and modeling work. Chan et al. (2017), for example, have been able to describe a remarkable level of spatial variability in the penetration of acidified waters into nearshore habitats across the CCS using a novel coastal ocean acidification observing network. These authors found that in some hotspots, suboptimal conditions for calcifying organisms already extended to up to 56% of the summer season and were accompanied by a great level of pH variability. In other areas, however, persistent refuges were also found, suggesting that local adaptation may persist on longer time scales than predicted by climate models.

3.1.5 Summary

469

470

471

472

473

474

475

476

477

478

479

480

481

482

483

484

485

486

487

488

489

490

491

492

493

494

495

496

497

498

The CCS occupies Region 1 and is a productive Eastern Boundary Upwelling System where eddies are commonly observed. Equatorward winds produce offshore surface Ekman transport and upwelling along the coast, especially during the summer, and bring deep, cold, nutrient-rich waters to the surface. Mesoscale eddies, both cyclonic and anticyclonic, are formed from the CCS meandering as it flows southward along the coast. These eddies redistribute nutrients, transporting the upwelled water hundreds of kilometers offshore from the coastal area into the oligotrophic interior of the Pacific Ocean. Observational and modeling studies have quantified how and how much coastal water is transported by the eddies. The cyclones are areas of elevated primary and secondary production and are preferred nursery ground for late-stage sardine larvae. ENSO, PDO and NPGO, all contribute to the variability of the coastal Ekman upwelling and strongly influence the characteristics of the upwelled waters (temperature, salinity, pH, nutrient and oxygen concentrations), therefore impacting the marine ecosystem of the CCS. The main characteristics of the eddies in this region, knowns and unknows are summarized in Table 1. Overall, research is needed to explore the intrinsic and forced variability of the mesoscale eddy field in the CCS, given its effect on ecosystem productivity. In particular, it is critical to better quantify the intrinsic variability of the eddy field and the relation between climate forcing and this intrinsic variability, which is likely nonlinear. This is particularly urgent considering the increasing frequency in marine heat waves recorded in the last decade (Oliver et al., 2018). Additionally, the contribution of subsurface eddies to the productivity of the area remains unconstrained, and targeted field campaign would improve understanding of the role of these mesoscale circulations on the productivity of the region.

Table 1: Characteristics and impact on the marine ecosystem of eddies in Region 1. Priorities are underlined and doubly underlined (higher priority).

Eddy type	Surface cyclone	Surface	Subsurface
Eddy type	Surface cyclone		
		anticyclone	anticyclone
Formation area	30°–45°N (most	30°-50°N	Along California
	formed at 32°–34°N)	(most formed at	Undercurrent.
	seaward of 1000 m	38°-40°N)	Frequently formed at
	isobath (Stegmann and	seaward of 1000	~34°N and ~40°N
	Schwing, 2007)	m isobath	(Kurian et al., 2011)
		(Stegmann and	
		Schwing, 2007)	
Formation	Baroclinic	Baroclinic	From the
mechanism	instability and flow-	instability of	generation of
	topography interaction	surface-	submesoscale
	of surface-intensified	intensified	negative-vorticity
	California Current and	California Current	along the California
	coastal jets (Checkley	and coastal jets	Undercurrent
	and Barth, 2009)	(Checkley and	through shear
		Barth, 2009)	instability
			(Molemaker et al.
			2015).
Polarity	Cyclonic	Anticyclonic	Anticyclonic
Diameter	163 ± 65 km	166 ± 59 km	59 km (median)
	(Stegmann and	(Stegmann and	(Collins et al.,
	Schwing, 2007)	Schwing, 2007)	2013) ; 20.4 km
			(Pelland et al., 2013)
Propagation	Westward	1	1

Lifetime (years)	Up to 0.8	Up to 1	Up to 1.4 (Collins	
	(Stegmann and	(Stegmann and	et al., 2013)	
	Schwing, 2007)	Schwing, 2007)		
Heat/freshwater	Not yet fully quantified. Observations are		Heat and salt	
transport	needed to validate model estimates over the		fluxed seaward, out	
	whole region and to qua	whole region and to quantify overall		
	submesoscale impacts.		undercurrent	
			(Pelland et al., 2013).	
			More observations	
			are needed for a	
			seasonal	
			quantification.	
Nutrient transport	Offshore transport (Nagai et al., 2015); Offshore transport of			
	carbon (surface cyclone, Barth et al., 2002)			
Impact on	Seaward transport of	<u>Unknown. Likely</u>		
chlorophyll	organisms (e.g. Strub et	less important than		
	and Barksdale, 1991; Logerwell and Smith,		for surface eddies but	
	2001; Checkley and Barth, 2009; Chenillat		could transport	
	et al., 2016)		nutrients.	
Impact on			<u>Unknown.</u>	
zoo/ichthyoplankton			Observational studies	
			to survey	
			<u>zooplankton</u>	
			assemblages inside,	
			around, and outside	
			mesoscale eddies are	
			recommended.	
Impact on higher	Positive impact on sardine survival (surface cyclone: Logerwell			
trophic levels	and Smith 2001) and linked to fur seals migration (Pelland et al.,			

2014, Sterling et al., 2014). <u>Studies targeting other species are</u> recommended. Historical fishery data could be used to this end.

501

502

503

504

505

506

507

508

509

510

511

512

513

514

515

516

517

518

519

520

521

522

523

524

525

526

527

528

3.2 Region 2: Northeastern North Pacific and the Bering Sea

3.2.1 Introduction

Region 2 covers the subarctic North Pacific (Figs. 1, 2 and 10). The northern part of the NPC enters the western edge of this region and flows northwestward along the coast of Canada and US as the Alaska Current, which, in turn, flows west-southwestward as the Alaskan Stream along the southern coast of the Alaska Peninsula and the Aleutian Islands. Part of the Alaskan Stream enters the Bering Sea, flows eastward just north of the Aleutian Islands, turns northwestward and flows along the shelf break of the eastern Bering Sea shelf as the Bering Slope Current. Mesoscale eddies in this region are mostly associated with these three boundary currents (see Fig. 10).

In Region 2, the existence of mesoscale eddies was recognized in the first half of 20th century through analysis of currents flowing in the opposite direction to that of the prevailing flow in the Gulf of Alaska. Based on hydrographic sections across the continental slope, McEwen et al. (1930) reported an eastward current near the continental slope across a section where the westward Alaskan Stream and Alaska Current were dominant. Bennet (1959) identified numerous eddies from hydrographic surveys, and Kirwan et al. (1978) found anticyclonic eddies in the eastern edge of the Gulf of Alaska using satellite tracked drifters. The first comprehensive characterization of the eddy field in the region was realized by Tabata (1982). Analyzing hydrographic data from 1954 to 1967 and drifter observations from 1977, he suggested that the anticyclonic eddies observed off Sitka (Alaska), which he named Sitka eddies, were formed locally and persisted for six months or more. Years later, Gower and Tabata (1993) tracked the motion of anticyclonic eddies through the Gulf of Alaska using observations of the exact repeat mission of the Geosat satellite altimeter, from November 1986 to January 1989. Their analysis showed that more eddies were formed in the ENSO winter of 1986/87 than in the following non-ENSO winter, as summarized by Crawford (2002). Since 1992, when satellite observations by at least two operating altimeters became available, many studies have been published on eddies in the Gulf of Alaska. Among them, Ladd (2007) and

Henson and Thomas (2008) investigated their seasonal and interannual variability, and found that EKE was high in winter/spring but large eddies (diameter $> \sim 80$ km) were fewest in winter.

West of the Gulf of Alaska and south of the Aleutian Islands, mesoscale eddies were first detected after the launch of the Geosat satellite altimeter. Okkonen (1992) first reported the observation of a meander which subsequently separated from the Alaskan Stream as an anticyclonic eddy. More recently, Rogachev et al. (2007) and Saito et al. (2016) investigated eddies in the western subarctic gyre, which mainly form at 170°–175°E south of the Aleutian Islands and supply the East Kamchatka Current with heat, while Ueno et al. (2009) studied the propagation of anticyclonic eddies southwestward in the Alaskan Stream and indicated that eddies form not only off Sitka and Yakutat, but also south of the Alaska Peninsula and Aleutian Islands and then propagate westward beyond 180°.

In the Bering Sea, mesoscale edd¥ies have long been studied. Based on hydrographic data, Kinder et al. (1975) described a mesoscale eddy in the southeastern corner of the Bering Sea basin along the Bering Slope Current system flowing northwestward along the shelf break. Satellite altimetry data further motivated studies to characterize Bering Sea eddies (e.g., wave field satisfying the dispersion relation for topographic planetary waves: Okkonen, 1993) and discuss their spatio-temporal variation along the shelf break, which is related to wind field as well as topography (Okkonen, 2001; Ladd et al., 2012).

Studies on the impact of mesoscale eddies on chemical and biological fields in the subarctic North Pacific started in 1990s. In the southeastern Bering Sea, Schumacher and Stabeno (1994) found an association between high concentrations of pollock larvae and eddies. Springer et al. (1996) summarized how physical processes at the shelf edge, such as intense tidal mixing and eddies in the Bering Slope Current, bring nutrients into the euphotic zone and contribute to enhanced primary and secondary production and elevated biomass of phytoplankton and zooplankton. After Martin et al. (1989) hypothesized that iron is an essential micronutrient that controls phytoplankton growth, iron observations within and around eddies were conducted (e.g., Johnson et al., 2005; Rovegno et al., 2009; Ladd et al., 2009; Tanaka et al., 2012; 2015; 2017) finding that indeed eddies were responsible for transporting both macro- and micronutrients from the shelf region into the basin. Eddies have been shown to contribute to distributions of chlorophyll also in the Gulf of Alaska (e.g., Crawford et al., 2005), south of the Aleutian Islands (Ueno et al., 2010) and in the Bering Sea (e.g., Mizobata et al., 2002), and to

560 be linked to concentrations of zooplankton in the Gulf of Alaska (Mackas and Galbraith, 2002) 561 and south of the Aleutian Islands (Saito et al., 2014), and to concentrations of fish in the Gulf of 562 Alaska (Kline, 2010) and in the Bering Sea (Andreev et al., 2018). Relationships between 563 eddies and marine mammals and seabirds have been also investigated (Ream et al., 2005; 564 Pelland et al., 2014; Paredes et al., 2014; Santora et al., 2018). In most cases, the impact of 565 mesoscale eddies on the marine ecosystem is via micronutrient transport to the high nutrient low 566 chlorophyll (HNLC) area in the middle of the gyre and local enhancement of primary 567 production (e.g., Ladd et al., 2007; Lippiatt et al., 2011), but horizontal advection by mesoscale 568 structures can also influence larval fish assemblages over the shelf and slope (Atwood et al., 569 2010). 570 3.2.2 Physical properties 571 In the subarctic North Pacific, eddy yield is relatively high in the Alaska Current region, at 572 the western edge of the Alaskan Stream region and in the Bering Slope Current region (Figs. 4, 573 5 and 11). This is consistent with the EKE map. In the Alaska Current and Alaskan Stream 574 region, the formation frequency of anticyclonic and cyclonic eddies is similar (Figs. 4 and 5) 575 but anticyclones are longer-lived. As a result, Lyman and Johnson (2015) estimated that only 576 ~37% of all detected eddies were cyclonic in the Gulf of Alaska, and even less (~15%) were 577 identified by Henson and Thomas (2008) using the Okubo-Weiss parameter (Okubo, 1970; 578 Weiss, 1991). Anticyclonic eddies are not only longer-lived, but also substantially larger (Fig. 579 11), and more nonlinear (Fig 2. b and d in Lyman and Johnson, 2015 showing azimuthal 580 velocity divided by translation speed). Cyclonic eddies formed in the Alaskan Stream region 581 west of the Gulf of Alaska have not been discussed in the literature (Henson and Thomas, 2008; 582 Lyman and Johnson, 2015), while in the Alaska Current region, cyclonic eddies form more 583 frequently but have shorter lifetime than anticyclones (Figs. 4b and 5b). Overall, in Region 2 584 cyclonic eddies have received relatively less attention than anticyclonic eddies and should be 585 further investigated. 586 In the Alaska Current region, anticyclonic eddies form frequently off Haida Gwaii, Sitka, and 587 Yakutat (Fig. 11) (Crawford, 2002; Whitney and Robert, 2002). Haida eddies form off the 588 southern tip of Haida Gwaii around 53°N and move mostly westward to the central Gulf of

Alaska (Crawford, 2002; Whitney and Robert, 2002). Sitka eddies form off Sitka around 57°N

and move mostly westward (Gower, 1989; Crawford, 2002), with few moving northwestward

589

590

and becoming embedded in the Alaskan Stream (Crawford et al., 2000; Ueno et al., 2009). Yakutat eddies form at the head of the Gulf of Alaska (141°–144°W) near Yakutat, Alaska, and propagate southwestward along the Alaskan Stream (Okkonen et al., 2003; Ladd et al., 2005a; 2007; Janout et al., 2009; Ueno et al., 2009). These three groups of eddies are primarily distinguished by their origin and share common features, e.g., anticyclonic rotation and ~200 km diameter, but their formation mechanisms differ. The formation of Haida eddies is associated with the mean advection of warmer and fresher water masses around the cape from Hecate Strait between Haida Gwaii and North America (Crawford et al., 2002; Di Lorenzo et al., 2005), while Sitka and Yakutat eddies form via baroclinic instabilities in the northward flowing currents along the shelf associated with coastally trapped Kelvin waves and alongshore downwelling winds that destabilize the Alaska Current by enhancing the velocity shear in the vertical (Thomson and Gower, 1998; Melsom et al., 1999; Murray et al., 2001). The tightly defined Sitka eddy formation region is associated with topographic interactions (Swaters and Mysak, 1985). Ladd et al. (2009) suggested that Yakutat eddies form in shallow shelf water with riverine input, while the Sitka and Haida eddies appear to form in deeper waters. Shore et al. (2008) suggested that barotropic instability (both baroclinic and barotropic instabilities) is (are) important as an energy source for eddies in the north (east) coast of the Gulf of Alaska. Ladd and Cheng (2016) and Ladd et al. (2016) suggested that gap-winds – strong offshoredirected winds channeled through mountain gaps – may play a role in the formation of Sitka and Yakutat eddies and may modify the eddies near Kodiak Island. Haida, Sitka and Yakutat eddies transport heat/freshwater from the coastal region to the deepsea region of the Gulf of Alaska via advection along their outer rim while also trapping coastal water in their center. The latter mechanism has been evaluated based on in-situ and satellite observations. Based on 12 hydrographic sections from 1995 to 2001, the offshore heat and freshwater transport in the top 500 m by a Haida eddy are about 3×10^{19} J and 50 km³ in a typical winter, with a range of $1-10 \times 10^{19}$ J and 0-70 km³ (Crawford, 2005). Ladd et al. (2007) estimated that a Yakutat eddy formed in 2003 contained 5.7×10^{18} J of anomalous heat and 21.1 \times 10¹⁰ kg of anomalous salt between the 25.2 and 27.0 kg m⁻³ isopycnals when it was first sampled in May 2003; the anomalies eroded over time as the eddy was sampled 4 more times through October 2004. Lyman and Johnson (2015) conducted a more comprehensive study on heat and freshwater transport to the basin using eddy trajectories (Chelton et al., 2011a) and Argo profiling float hydrographic data and found $16.2 (\pm 5.6) \times 10^{18}$ J of anomalous heat and –

591

592

593

594

595

596

597

598

599

600

601

602

603

604

605

606

607

608

609

610

611

612

613

614

615

616

617

618

619

620

621

622

623 5.6 (\pm 3.8) km³ of freshwater per eddy and \sim 48.6 \times 10¹⁸ J and \sim -16.8 km³ per year, respectively, 624 between 0 and 900 m. The positive heat flux and negative freshwater flux presumably derive 625 from the Alaska Current and the Alaskan Stream, which both carry subsurface water that is 626 warmer and saltier than that within the center of the gyre (Lyman and Johnson, 2015). Xiu et al. 627 (2011) further suggested the importance of submesoscale processes in the Haida eddy region 628 using numerical simulations. Their model experiment indicates that submesoscale features at the 629 periphery of eddy cores dominate the vertical velocity field, and that the vertical velocity at the 630 eddy centers is about one to two orders of magnitude lower than that in the submesoscale 631 structures. 632 In the Alaskan Stream region, at least three formation sites of long-lifetime anticyclonic 633 eddies have been documented, and the respective eddies have been named Kenai, Alaskan 634 Stream and Aleutian eddies (Fig. 12). The Kenai eddy formation site is near the Kenai 635 Peninsula (~150°W; Rovegno et al., 2009). One well-studied Kenai eddy, containing warm core 636 water with a uniform temperature-salinity relationship near the eddy center, originated there and 637 initially propagated along the Alaskan Stream (Rovegno et al., 2009) and then far to the west 638 (~175°E) with a lifetime of 3.6 years (Ueno et al., 2012). The original warm core water was 639 preserved for 2.7 years but strongly modified by eddy-eddy interaction after that (Ueno et al., 640 2012). Although at least six eddies formed near the Kenai Peninsula over 16 years (Rovegno et 641 al., 2009), their formation mechanism, interannual variation, and heat/freshwater transport 642 remain to be investigated. 643 The Alaskan Stream eddy formation site is south of the Alaska Peninsula and Aleutian 644 Islands between 157° and 169°W (Ueno et al., 2009). Alaskan Stream eddies have been 645 observed to cross the 180° meridian and reach the western subarctic gyre and they contribute 646 warm water to the western subarctic gyre just south of the Aleutian Islands (Ueno et al., 2009). 647 Five Alaskan Stream eddies formed during 1992–2006 and lasted up to five years. Four of the 5 648 eddies formed under negative or weakly positive wind stress curl, which possibly caused the 649 Alaskan Stream to separate from the coast and become unstable (Ueno et al., 2009). A 650 comparison of eddy propagation speeds in the Alaskan Stream with the bottom slope showed 651 that eddies propagated faster over steeper slopes. Finally, the anticyclonic Aleutian eddy 652 formation site is south of the Aleutian Islands at the western edge of the Alaskan Stream 653 between 170° and 175°E (Rogachev et al., 2007; Saito et al., 2016; Budyansky et al., 2022), and 654

Aleutian eddies separate from the main current when it turns north through Near Strait into the

Bering Sea. Using an automatic eddy detection algorithm and altimetry-based daily Lagrangian maps, all long-lived and large-scale anticyclonic Aleutian eddies with size in the range of 100 – 300 km have been identified, tracked and documented during the period 1993 – 2020 (Budyansky et al., 2022). A strong asymmetry between the number of cyclones and anticyclones has been found. After detaching from the Alaskan Stream, the anticyclones propagate southwestward due to the beta-effect. The observations, based on Argo float profiles (Budyansky et al., 2022) and ship measurements (Rogachev et al., 2007; Saito et al., 2016), reveal typical subarctic vertical structure with warm and saline mesothermal water in the intermediate layer. The Aleutian eddies transport warm and saline water under a cold upper layer that eventually contributes to the mesothermal layer of the Western Subarctic Gyre.

In the Bering Slope Current region, frequent eddy generation is associated with the Bering slope canyons (Bering, Pribilof, Zhemchug, Navarin; Okkonen, 2001; Kinney et al., 2009; Ladd et al., 2012, Fig. 13). Eddies in this region have horizontal scales ranging from 10–200 km (Paluszkiewicz and Niebauer, 1984; Stabeno et al., 1999) and vertical scales reaching at least 1000 m (Roden, 1995; Mizobata et al., 2002). The eddy activity is strongest in spring, and instabilities in the Bering Slope Current, wind forcing, topographic interactions and flow through the eastern Aleutian passes have all been suggested as possible generation mechanisms (e.g., Paluszkiewicz and Niebauer, 1984; Schumacher and Stabeno, 1994; Mizobata et al., 2008).

3.2.3 Impact on chemical and biological fields

In the Alaska Current and Alaskan Stream regions, Haida, Sitka, Yakutat and Kenai eddies provide deep-sea waters with macro/micro-nutrients -especially iron - and biota from the coastal areas. Haida (Johnson et al., 2005; Cullen et al., 2009), Sitka (Brown et al., 2012), Yakutat (Crusius et al., 2017) and Kenai eddies (Lippiatt et al., 2011) all contribute to the iron transport, as also indicated by numerical simulations (Combes et al., 2009; Fiechter and Moore, 2012). Johnson et al. (2005) further suggested that upward transport along isopycnals and upwelling within the eddy due to eddy decay (eddy pumping) provide steady fluxes of iron into the euphotic zone from the iron-rich subsurface waters of the eddy cores. Ladd et al. (2009) showed that iron concentrations measured in a Yakutat eddy were higher than any previous Haida eddy measurements (Johnson et al., 2005), including those from an eddy at its formation time, when

biological drawdown had presumably not yet occurred. Therefore, eddies formed on the shelf around Yakutat are key in providing iron to the Gulf of Alaska basin.

In the Bering Sea, eddies can be important for transporting iron and macronutrients to the shelf break as well (Hurst et al., 2010). Eddy induced cross-shelf transport may supply macronutrients (Springer et al., 1996; Mizobata et al., 2006; Mizobata et al., 2008) and iron (Hurst et al., 2010), and cause the highly productive ecosystem found along the edge of the continental shelf in the Bering Sea, in the so-called Green Belt. Additionally, Ladd et al. (2012) showed evidence that eddies trap deeper water from the outer shelf in their core at formation time and carry it with a high nitrate signature off-shelf. All in all, eddies in Region 2 enhance production on-shelf and as well as off-shelf (e.g., Ladd et al., 2005b; Mizobata et al., 2006).

Fig. 1 indicated that chlorophyll concentration is positively correlated with SSH (high chlorophyll associated with anticyclonic eddies) in the Alaska Current, Alaskan Stream and Bering Slope Current regions. This is consistent with previous studies. For example, Crawford et al. (2007) showed that in the Gulf of Alaska more than half of all surface chlorophyll was inside the 4 cm SSH contours of anticyclonic mesoscale eddies (Haida, Sitka and Yakutat eddies), yet these contours enclosed only 10% of the total surface area of offshore waters. They also indicated that macro- and micronutrient transport by eddy trapping, stirring and pumping contribute to the offshore primary production. Lippiatt et al. (2010; 2011) indicated that mesoscale anticyclonic eddies in the Gulf of Alaska are key to the offshore transport of iron-rich coastal waters, enriched by the runoff from glacial rivers and streams. Ueno et al. (2010) confirmed that Alaskan Stream eddies contribute significantly to the Chl-a distribution in the deep-sea region of the subarctic North Pacific based on the climatological Chl-a distributions averaged over space and time. They also suggested that nutrient-rich coastal water is transported offshore via a southward meander of the Alaskan Stream due to Alaskan Stream eddy trapping in the core and eddy stirring in the outer ring. Vertical transport of iron via eddy pumping or eddy-induced Ekman pumping may be another mechanism by which nutrients are supplied to the euphotic layer (Ueno et al., 2010), although Dobashi et al. (2021) indicated that it is not always effective in the offshore region of the western subarctic gyre.

In the Bering Slope Current region, Mizobata and Saitoh (2004) and Mizobata et al. (2008) found that the variability in the eddy field and the primary production along the Bering Sea shelf edge are positively correlated. Increase in Bering Slope Current transport and eddy activity

contributes to vertical nutrient supply to the subsurface layer and to shelf–slope exchanges, thereby maintaining high primary productivity along the shelf edge of the southeastern Bering Sea. Ladd et al. (2012) indicated that the horizontal exchange of water within an eddy may result in the excess nutrients and fresher water within the eddy core, influencing Chl-a distributions throughout the summer months. Tanaka et al. (2012; 2015; 2017) further proposed that tide-induced vertical mixing promotes the iron supply to the euphotic zone in the Bering Slope Current region and sustains local summertime high biological production.

Eddy enhanced primary production and mesoscale advection further impact the marine ecosystem in Region 2. Haida eddies affect zooplankton populations in the offshore regions through supply of shelf- and slope- origin species to offshore regions. Nearshore tracer species are often the dominant or sub-dominant zooplankton within eddies in the first summer after they leave the coast, but their abundances decline rapidly after that (Mackas and Galbraith, 2002). Shelf species of diatoms and calanoid copepods were recorded in Continuous Plankton Recorder (CPR) samples within or near Haida and Sitka eddies and they persisted through the sampling period (Batten and Crawford, 2005). The zooplankton in the Haida eddies are mostly a mixture in both abundance and community composition between the continental margin and offshore source regions, but in about 1/3 of them abundances within-eddy are higher than in either source region (Mackas et al., 2005). Zooplankton assemblages in the Haida and Sitka eddies differ in a statistically significant way, but this is not the case in the Sitka and Yakutat or Yakutat and Haida eddies (Ladd et al., 2009). In the Alaskan Stream region, Saito et al. (2014) reported that large oceanic copepods were more abundant, and some species had accumulated more lipids inside the eddies than outside, a likely reflection of the greater primary production in the eddies.

Mesoscale eddies further impact marine ecosystems by affecting fish distributions. Atwood et al. (2010) indicated that the richness of ichthyoplankton correlates with the distance from eddy centers, and assemblages within eddies are significantly different from those in surrounding basin and shelf waters in the eastern Gulf of Alaska. They also suggested that mesoscale eddies propagating along the continental shelf-break influence larval fish assemblages. In particular, eddies may influence the recruitment of sablefish by increasing nutritional availability and affecting transport (Shotwell et al., 2014), and individual based models indicate that eddies may be key to larval transport of some species (e.g., Stockhausen et al., 2019). Furthermore, Prants et al. (2019) proposed that the observed positive correlations between wind stress curl and

salmon catches in the eastern Bering Sea may result from changes in mesoscale eddy activity. A better understanding of the impact of mesoscale eddies on larval abundance, survival, and transport would contribute to more reliable estimates of recruitment success, potentially improving management decisions in the Gulf of Alaska.

3.2.4 Variability

Mesoscale eddies in Region 2 show seasonal and interannual variations. For example, for the Haida, Sitka and Yakutat eddies EKE and eddy numbers are large in winter and spring, due to their stronger downwelling winds, and low in summer and autumn (Ladd, 2007; Henson and Thomas, 2008). The interannual variability is related to the variability in downwelling winds (Ladd, 2007; Henson and Thomas, 2008) and also to the number of gap-wind events (Ladd and Cheng, 2016). Long-term trends in eddy formation have not been investigated yet in the Alaska Current, Alaskan Stream or Bering Slope Current regions. For the Alaskan Stream, however, Prants et al. (2013) indicated the water flux across the Near Strait, connecting the Pacific Ocean with the Bering Sea, is highly variable and controlled by mesoscale and submesoscale eddies. Interannual variations of heat and freshwater transport for Haida, Sitka, Yakutat and Kenai eddies have been estimated, but solely owing to fluctuations in the number of eddies that are observed in SSH to cross 150°W or offshore of 200 km from the 1000 m isobath (Lyman and Johnson, 2015). Lyman and Johnson (2015) also indicated that heat and freshwater content anomalies of cyclonic eddies are an order of magnitude smaller than those of anticyclonic eddies.

In the Bering Slope Current region, eddy activity is negatively correlated with the North Pacific Index, a measure of the strength of the Aleutian Low (Trenberth and Hurrell, 1994), and positively correlated with Pacific North America Pattern (Barnston and Livezey, 1987). North Pacific Index and Pacific North America Pattern are associated with the wind stress curl over the North Pacific (Ishi and Hanawa, 2005). Indeed, it is suggested that the wind-driven gyre spin-up during the preceding winter may lead to increased eddy activity in the Bering Sea in boreal spring (Ladd et al., 2012). Furthermore, Prants et al. (2019) have shown that eddy activity in the eastern Bering Sea and Alaskan Stream is related to wind stress curl in the northern North Pacific in November-March. Finally, Ding et al. (2018) pointed out that eddy activity increased between 1993 and 2011 across most of the Northeast Pacific. However, in

Region 2 there was longitudinal variability in the increase/decrease of eddy activity with a positive trend around 160°W and negative trend around 170°W (see Ding et al., 2018's Fig. 2).

The effects of mesoscale eddies on ecosystem variability have been studied mainly for upper trophic levels. For example, eddy activity influences the distribution of adult female northern fur seals during their migration between the Bering Sea and the California Current region (Pelland et al., 2014; Ream et al., 2005). Fur seal behavior (foraging) has also been associated with eddy activity, but the quantitative relationship remains unclear and requires further examination of subsurface mesoscale oceanic structures along with behavioral responses or lack thereof. When it comes to bird foraging, black-legged kittiwakes, breeding at the Pribilof Islands in the Bering Sea, often fed near anticyclonic, or inside cyclonic eddies (Paredes et al., 2014). Paredes et al. (2014) also showed that in 2010 high eddy activity in the Bearing Sea, as measured by EKE, coincided with a 63% increase in foraging in the basin by birds from St. Paul compared to 2008, when the EKE was low.

3.2.5 Summary

In the subpolar North Pacific, mesoscale eddies form frequently in the Alaska Current region, at the western edge of the Alaskan Stream region and in the Bering Slope Current area. They typically form by baroclinic instability associated with winds, coastal water outflow, or local topography. In the Alaska Current and Alaskan Stream regions, anticyclonic eddies have longer lifetime and greater size than cyclonic eddies, and most studies to date have focused on them (Table 2). They are named Haida, Sitka, Yakutat, Kenai, Alaskan Stream, and Aleutian eddies, according to their formation area. In the Bering Slope Current region, eddies of both polarities have been investigated. Haida, Aleutian, Bering Slope Current, and some Sitka eddies propagate offshore from the shelf into the basin and transport coastal water to the ocean interior. Yakutat, Kenai, Alaskan Stream and some of the Sitka eddies mostly propagate along the Alaska Current and Alaskan Stream, without detaching from the Alaskan Stream, and therefore do not propagate offshore. All these mesoscale eddies contribute to the transport of iron from the coastal/shelf area to the basin interior and support biological production in the iron-limited HNLC North Pacific subarctic and Bering Sea basins. Mesoscale eddies in Region 2 further impact zooplankton and higher trophic level species such as fish, marine mammals and birds mainly through elevated primary production due to macro- and micro-nutrient trapping in their core and advection into the basin or to the shelf boundaries. We summarize known/unknown

characteristics and impacts of mesoscale eddies in Table 2. Further observational and modeling studies are needed especially in relation to the ecological impacts of the Aleutian eddies. Recently, it was found that the seasonal and interannual variation of the halocline, which affects primary production through pycnocline/mixed layer depth, differ between the western and eastern parts of the subarctic North Pacific (Katsura et al., 2020; Ueno et al., 2022). This eastwest contrast in background physical environment should be considered to better understand the different impacts that mesoscale eddies have on primary production within Region 2.

Table 2: Characteristics and impact on marine ecosystem of eddies in Region 2. Underlining as in Table 1.

Eddy type	Haida/Sitka/Yakutat	Kenai/	Aleutian	BSC
		Alaskan		
		Stream		
Formation	Off Haida Gwaii,	Along the	South of	Along the
area	Sitka and Yakutat in	Alaskan	the Aleutian	eastern shelf-
	the northeastern Gulf	Stream from	Islands	break of the
	of Alaska	the Kenai	between 170°	Bering Sea
		Peninsula to	and 175°E	
		the Aleutian		
		Islands		
Polarity	Anticyclonic	Anticycloni	Mainly	Anticyclonic /
		С	anticyclonic	Cyclonic
Formation	Shelf water	BT and BC	<u>Only</u>	Instabilities
mechanism	advection (Crawford	instabilities	limited	associated with
(BC:	et al., 2002; Di	(Thomson and	theoretical	wind, topography,
baroclinic,	Lorenzo et al., 2005),	Gower, 1998;	understandin	flow through
BT:	BC instabilities	Shore et al.,	g. Realistic	Aleutian passes
barotropic)	associated with waves	2008) and	models that	(e.g.
	and winds (Thomson	instabilities	allow for a	Paluszkiewicz
		associated	direct	and Niebauer,
		with winds	comparison	

Diameter	and Gower, 1998; Shore et al., 2008) Around 100 km on average (Henson and Thomas, 2008)	(Ueno et al., 2009) Around 150 km on average (Ueno et al., 2010; Lippiatt et al., 2011)	with in-situ and satellite observations are needed 80–330 km (Rogachev et al., 2007; Budyansky et al., 2022)	1984; Mizobata et al., 2008). 10–200 km (Ladd et al., 2012)
Propagatio n	To Gulf of Alaska basin, along the Alaskan Stream (Crawford, 2002; Ladd et al., 2007)	Along the Alaskan Stream and sometimes detached from the Alaskan Stream (Ladd et al., 2007; Janout et al., 2009)	To western subarctic basin (Rogachev et al., 2007; Budyansky et al., 2022)	Off-shelf (westward/southw estward) (Ladd et al., 2012)
Lifetime (years)	Up to 5 (Crawford, 2002; Ladd et al., 2007)	Up to 5 (Ueno et al., 2009, 2012)	Up to 4 (Budyansky et al., 2022)	Up to 2 (Chelton et al., 2011b)
Heat/fresh water transport	Seaward warmer, fresher water transport (Crawford, 2005; Ladd et al., 2007)	Seaward warmer, fresher water transport, shelf-basin exchange (Okkonen et al., 2003;	Unknown. Modeling and observational studies are urgently needed.	Shelf-basin exchange (Kinney et al., 2009)

		Ueno et al., 2009)		
Nutrient	Seaward (Whitney	Shelf-basin	<u>Unknown.</u>	Eddy induced
transport	and Robert, 2002;	exchange	<u>In-situ</u>	cross-shelf
	Ladd et al., 2009) and	(Lippiatt et al.,	observations	transport
	upward (Johnson et	2011)	complemente	(Mizobata et al.,
	al., 2005)		<u>d by</u>	2006; Hurst et al.,
	macro/micro-nutrient		modeling	2010)
	transport		investigations	
			are needed.	
Impact on	Enhancing	Enhancing	<u>Unknown.</u>	Maintaining
chlorophyll	production in the Gulf	offshore	Satellite data	high primary
	of Alaska basin	production	<u>analyses</u>	productivity along
	(Whitney and Robert,	(e.g., Ueno et	together with	the shelf edge
	2002; Crawford et al.,	al., 2010)	targeted field	(Springer et al.,
	2007)		campaigns	1996; Ladd et al.,
			and modeling	2012)
			studies are	
			recommende	
			<u>d.</u>	
Impact on	Affecting	<u>Unknown.</u>	Affecting	Affecting
zoo/ichthyopl	zoo/ichthyoplankton	<u>Field</u>	life stage	zoo/ichthyoplankt
ankton	assemblages in Gulf of	campaigns	distribution	on distribution
	Alaska (Mackas and	sampling	of	(Schumacher and
	Galbraith, 2002,	zooplankton	zooplankton	Stabeno, 1994;
	Atwood et al., 2010)	assemblages	(Saito et al.,	Springer et al.,
		inside, outside	2014)	1996)
		and at the		
		boundary of		
		mesoscale		

		eddies are		
		recommended.		
Impact on	Fur seals (Ream et al.	, 2005; Pelland	<u>Unknown.</u>	Fur seals
higher	et al., 2014, Sterling et a	1., 2014),	Ship_	(Nordstrom et al.,
trophic levels	Salmon (Healey et al., 2	000), Steller sea	observations,	2013; Sterling et
	lions (Miller et al., 2005)	bio-logging,	al., 2014), Salmon
			analysis of	(Prants et al.,
			fishery data	2019), Seabirds
			are	(Paredes et al.,
			recommende	2014; Santora et
			<u>d.</u>	al., 2018)

3.3. Region 3: Western boundary of the North Pacific and marginal seas

3.3.1 Introduction

Two strong boundary currents flow along the western edge of the North Pacific: Oyashio and Kuroshio (Fig. 14). The Oyashio Current starts along the west coast of the Kamchatka Peninsula as the East Kamchatka Current, flows along the Kuril Islands and turns to the east near Hokkaido. The Kuroshio Current flows east of Luzon Island and Taiwan, entering the East China Sea through the East Taiwan Channel, flows along the shelf edge of the East China Sea continental shelf, enters the North Pacific Ocean off Kyushu Island, flowing along the south of Japan, and turns to the east near the Boso Peninsula in the southeastern portion of the Honshu Island. Mesoscale eddies are frequently generated along the Kuroshio/Oyashio and their branch currents such as the Tsushima Warm Current. These eddies can influence the volume transports and pathways of the current systems (e.g., Kawabe, 1995, Yin et al., 2019, Sugimoto and Tameishi, 1992). The Tsushima Warm Current diverges into the northward Tsushima Warm Current nearshore branch close to the east coast of Korea and the eastward Tsushima Warm Current offshore branch close to the west coast of Japan. The Tsushima Warm Current nearshore branch is called the East Korea Warm Current, which forms the subpolar front and the Ulleung Warm Eddy when it collides with the North Korea Cold Current.

In one of the first studies in Region 3, Kitano (1975) identified 154 warm-core eddies in the Kuroshio – Oyashio frontal zone over the period 1957–1973 from shipboard observations. Some eddies moved northward and eastward along the Japan Trench from offshore of the Tohoku region and along the southern Kuril-Kamchatka Trench (Yasuda et al., 1992 and references therein). Later studies confirmed that a large number of strong eddies move poleward along the trenches or, less frequently, on a path along the Subarctic Front (e.g., Bulatov and Lobanov, 1983; Yasuda et al., 2000; Rogachev, 2000a; Isoguchi and Kawamura, 2003; Itoh and Yasuda, 2010a, b; Kaneko et al., 2015; Prants et al., 2017a). Additionally, mesoscale eddies have been studied in the marginal seas for more than 30 years. Wakatsuchi and Oshima (1990) observed trains of eddies in the Sea of Okhotsk and suggested they form via barotropic instability of the Soya Warm Current. Dynamic processes vary across Region 3 and the impact of physical phenomena on the marine ecosystem differs depending on the area. Southward western boundary currents such as the East Kamchatka Current, Oyashio, East Sakhalin Current and Primorye (Liman) Current

marine ecosystem differs depending on the area. Southward western boundary currents such as the East Kamchatka Current, Oyashio, East Sakhalin Current and Primorye (Liman) Current contribute to the eddy formation and ecosystem variability north of ~40°N, while changes in the Kuroshio and Tsushima Warm Current are large contributors to the mesoscale and marine ecosystem south of ~40°N. The Tsushima Warm Current also affects the mesoscale variability in the Sea of Okhotsk as the Soya Warm Current and the Kuroshio Warm Core Rings can at times reach the area east of Hokkaido.

Eddies associated with the Oyashio and Kuroshio currents modulate the saury fishing grounds which are located preferentially along fronts where the productive cold waters of the Oyashio Current, the warmer waters of the southern branch of the Soya Warm Current, and waters of warm-core Kuroshio eddies converge (Prants et al., 2014a; Prants et al., 2021). In the Kuroshio region, Kasai et al. (2002) suggested that eddies are important for fish recruitment because they are quasi-stationary and remain in the coastal nursery area.

3.3.2 Physical properties

In the northwest Pacific, east of the Kamchatka Peninsula, Kuril Islands and Japanese Islands, the Oyashio and/or Kuroshio Currents contribute to the generation of a variety of mesoscale eddies. These eddies, also known as rings, can be quasi-stationary or propagate away from their formation regions, transporting mass, momentum, salt, heat, chemical and biological constituents over large distances. Some of them form in the Tohoku region, where the waters of

the Tsugaru Warm Current mix with Oyashio and Kuroshio waters. The Tohoku eddies slowly drift along the Japan Trench to the north against the mean flow (Isoguchi and Kawamura, 2003; Itoh and Yasuda, 2010a, b; Prants et al., 2014b; Kaneko et al., 2015; Prants et al., 2017a). Some rings that split off from the western meander of the Kuroshio Extension also drift along this path. Those that split off from the eastern meander, propagate westward under the influence of the planetary beta effect, reach the Japan Trench, and then turn northward to Hokkaido. The eddies that reach the eastern coast of Hokkaido Island, so-called Hokkaido anticyclonic eddies often stagnate for a while and then drift along the Kuril-Kamchatka Trench to the northeast (Fig. 15) reaching as far as Bussol' Strait, which is the deepest strait connecting the Sea of Okhotsk with the ocean (Bulatov and Lobanov, 1983; Yasuda et al., 2000; Itoh and Yasuda, 2010a, b; Prants et al., 2014a; Prants et al., 2018).

Mesoscale eddies are frequently observed along the Japan and Kuril–Kamchatka Trenches, either quasi-stationary or propagating along the trenches against an opposing mean surface flow (e.g., Kitano, 1975; Yasuda et al., 2000; Itoh and Yasuda, 2010a, b; Kaneko et al., 2015; Prants et al., 2018). Using a Lagrangian eddy monitoring technique (Prants et al., 2017a, d, 2018), it has been possible to investigate in detail life histories of individual eddies including time and locations of their formation, splitting, merging, decay, as well as retention and release of water due to interactions with currents and other eddies. Figs. 15a and 15b show altimetry-based velocities and the Lagrangian origin map, respectively, for August 1, 2010 to exemplify the characteristics of the eddy activity in the area. The warm-core rings with red core in Fig. 15b pinched off from the meanders at the northern flank of the Kuroshio Extension. These rings then propagate westward due to the planetary beta effect (KR1 in Fig. 15b) and once they reach the steep slope of the Japan Trench, they generally turn northward (KR2 to KR3 in Fig. 15) along the Trench (Qiu and Chen, 2005; Sugimoto and Hanawa, 2012; Prants et al., 2014b).

The planetary beta effect should induce a southwestward advection of eddies. Nevertheless, the trench eddies often move northeastward against the southwestward mean flow. The underlying physical mechanisms are complex and are not yet well understood, but the topographic beta effect within the trench appears to dominate the planetary beta effect, and the deep northeastward current at the offshore trench edge guides the eddies poleward (Yasuda et al., 2000).

Kuril eddies form along the Kuril-Kamchatka Trench on the oceanic side of the islands and are characterized by a cold and fresh core. The most energetic among them are the long-lived Bussol' eddies (e.g., Bulatov and Lobanov, 1983; Rogachev, 2000b; Yasuda et al., 2000; Rabinovich et al., 2002; Prants et al., 2016), formed near the Bussol' Strait. Lagrangian maps indicate that the waters in the Bussol' eddy consist of a mixture of cold and fresh water from the Sea of Okhotsk and warmer and more saline water from the East Kamchatka Current (Prants et al., 2016) (shown by green and blue colors, respectively, in Fig. 15b). Eddies formed to the north of the Bussol' Strait drift southwestward with the Oyashio Current and eventually decay, while large-scale long-lived warm-core eddies can reach the area, moving from Hokkaido to the northeast along the trench (Yasuda et al., 2000; Prants et al., 2018). The Bussol' Strait area is therefore a meeting point for eddies drifting from the south and the north, as suggested by earlier studies based on SST, current meter mooring and model data (Bulatov and Lobanov, 1983; Isoguchi and Kawamura, 2003). The northern Kuril-Kamchatka Trench is a catching area for the so-called Kamchatka eddies (eddies KE1 and KE2 in Fig. 15) that move here from the north following the path of the East Kamchatka Current (e.g., Solomon and Ahlnäs, 1978; Stabeno et al., 1994, 1999; Rogachev and Shlyk, 2019). These eddies form due to the intricate coastline of the Kamchatka Peninsula and its irregular nearshore bathymetry that trigger instabilities in the East Kamchatka Current (L'Her et al., 2021). The shedding of anticyclonic eddies occurs mostly between the current and the coast and that of cyclonic eddies offshore of the current. The Kamchatka eddies occasionally merge with quasi-stationary trench eddies and persist from a few months to more than a year, until they eventually shed from the slope and are dispersed into the mean flow (Prants et al., 2020). In the Kuril Basin located in the southwestern Sea of Okhotsk (Fig. 15a), large (100–200 km) anticyclonic eddies can be seen as spiral structures in ice floe patterns, surface drifters and in satellite SST, altimetry, and imagery (e.g., Wakatsuchi and Martin, 1990; Bulatov et al., 1999; Ohshima et al., 2002; Mitnik and Dubina, 2019; Zhabin and Andreev, 2019). These eddies (see Fig. 16) have lifetimes from several months to more than a year, being quasi-stationary or slowly moving northwestward or westward (Bulatov et al., 1999). Ohshima et al. (2005) indicated, through numerical model experiments, that the eddies originating from the area adjacent to the Kuril Straits are generated by baroclinic instability at the front that form between the water around the straits, which is relatively uniform due to the strong tidal mixing, and the

897

898

899

900

901

902

903

904

905

906

907

908

909

910

911

912

913

914

915

916

917

918

919

920

921

922

923

924

925

926

927

928

offshore water. In the southwestern Kuril Basin, the negative wind stress curl, which prevails during the summer season, intensifies the anticyclonic eddies (Zhabin and Andreev, 2019). In the nearshore zone of the Kuril Islands, mesoscale eddies between 35–70 km in diameter are generated by the interaction of large-scale and tidal currents, which are very strong, with topography (Mitnik and Dubina, 2019; Nakamura et al., 2012; Zhabin and Andreev, 2019).

The Soya Warm Current flows into the Sea of Okhotsk through the La Perouse (Soya) Strait and then along the northeastern Hokkaido coast (Fig. 14). Eddies often interact with the Soya Warm Current, and their water turns warmer than ambient (Wakatsuchi and Martin, 1990; Uchimoto et al., 2007; Zhabin and Andreev, 2019). Trains of eddies, with diameters of 45–50 km, have been observed at the boundary between the Soya Warm Current and the colder and less saline offshore water. Barotropic instability of the Soya Warm Current has been suggested as a mechanism for their formation (Wakatsuchi and Oshima, 1990). Saline water can be advected by the offshore Soya Warm Current streamers along the eddies' edges towards the deep Kuril Basin (Zhabin and Andreev, 2019). The colder, nutrient-rich water of the East Sakhalin Current can also be caught in these eddies (Prants et al., 2017c). Overall, eddies in the central Kuril Basin can hold both Soya Warm Current water and colder and fresher water originating from the tidal zone near the Kuril Islands, while eddies in the northern Kuril Basin usually have a cold surface core that traps tidal water, especially in summer (Bulatov et al., 1999).

Around the Subpolar Front located ~40°N, between the Korean Peninsula and the Japanese Islands, frontal eddies have been found in hydrographic surveys, satellite images (Sugimoto and Tameishi, 1992, Takematsu et al., 1999) and in a circulation model (Prants et al., 2015). At least some of them may live over the deep Japan Basin for a few months and they provide an effective mechanism for cross-frontal exchanges in the Subpolar Front. The existence of meridional cross-front transport corridors has been revealed by statistical analysis of Lagrangian transport based on the AVISO satellite altimetry currents (Prants et al., 2017b).

During the cold season, a cluster of warm anticyclonic eddies is regularly detected off the northeastern coast of the Korean Peninsula (e.g., Sugimoto and Tameishi, 1992; Danchenkov et al., 2006). These eddies are forced by the local anticyclonic stress curl of the northwestern wind, which is typical during the winter monsoon (Yoon and Kim, 2009). Warm eddies are also

observed in spring and summer, likely generated by the local anticyclonic stress curl of the western and southwestern winds (Trusenkova et al., 2009).

959

960

961

962

963

964

965

966

967

968

969

970

971

972

973

974

975

976

977

978

979

980

981

982

983

984

985

986

987

988

989

Warm eddies form along the west coast of the Japanese Islands and move westward due to the planetary β-effect or with the intermittent westward Tsushima Warm Current branches off the Tsugaru Strait (Takematsu et al., 1999). They carry salty water from the Tsushima Warm Current that flows off the Japanese Islands. When the water mass cools, it subducts while moving westward, and contributes to the high salinity intermediate water (Danchenkov et al., 2006). Anticyclonic eddies are also frequently detected between the coast and the cold western boundary Primorye Current and North Korea Cold Current (Prants et al., 2011; Ladychenko and Lobanov, 2013). They form through shear instabilities and slowly move southwestward, with translation speeds lower than the surface velocity of the Primorye Current (Prants et al., 2011). In Peter the Great Bay, off Vladivostok, mesoscale eddies carry shelf fresh and warm water to the southwest, into the deep Japan Basin, where they become a source water for the intermediate salinity minimum of the basin (Ladychenko and Lobanov, 2013). Additionally, brine rejections during episodes of sea-ice formation in winter form a cold and saline water, which sinks to intermediate and deep layers (Kim et al., 2002; Talley et al., 2003). Mesoscale anticyclones and submesoscale cyclones then carry this cold and saline water offshore (Fayman et al., 2019a, b). The regional circulation around the Korean Peninsula (Fig. 17) is described by (1) tidedominant currents and seasonal northward warm currents in the Yellow Sea (Hwang et al., 2014), (2) low-frequency geostrophic flows and the subpolar front along the east coast of Korea associated with regional boundary currents with distinct water temperature difference (Danchenkov et al., 2006, Yoo et al., 2018, Lee et al., 2019), and (3) a mixture of tidedominated, geostrophic currents, intermittent fronts and eddies to the south of the Korean peninsula (Kim et al., 2000a; Lie et al., 2015). Tidal fronts and eddies associated with islands and coastal boundaries (Lie, 1989; Hwang et al., 2014; Jeong et al., 2009), the migration of persistent and intermittent fronts over continental shelves (Son et al., 2010; Yang et al., 1998),

least 150 km and a lifetime from several months to more than one year (Chang et al., 2004). It is generated within the anticyclonic meander of the East Korea Warm Current that flows

been observed in this region. An anticyclonic eddy known as the Ulleung Warm Eddy is

and submesoscale frontal eddies associated with baroclinic instability (Yoo et al., 2018) have all

frequently observed east of the Korean Peninsula, centered at 37° – 38° N, with a diameter of at

990 northward as part of the subpolar front (Yoshikawa et al., 2012). The Ulleung Warm Eddy 991 surface signature is often a cold core wrapped by a warm filament (Chang et al., 2004). 992 Lastly, we summarize the mesoscale processes around Kuroshio. To the east of Taiwan, 993 Kuroshio intrusions represent an important mechanism of water exchange between the East 994 China Sea shelf and the western North Pacific Ocean (Matsuno et al., 2009). Kuroshio 995 intrusions are linked to the formation of a cold dome (Shen et al., 2011), a cyclonic circulation 996 that occurs northeast of Taiwan. Kuroshio and its intrusions in this area are affected by the open 997 ocean eddies detached from the Subtropical Counter Current (STCC) and the North Equatorial 998 Current, as described in Sections 3.3.3. Upwelling of subsurface water occurs around the 999 Kuroshio in the East China Sea (e.g., Wong and Zhang, 2003), and eddy-induced lateral mixing 1000 due to the Kuroshio around the Ryukyu Islands in the East China Sea has been recently 1001 investigated using a submesoscale-eddy-resolving model (Kamidaira et al., 2017). 1002 The Kuroshio follows the shelf break of the East China Sea and the south coast of Japan, 1003 passing through Tokara Strait and Izu Ridge, and then moves offshore to the Kuroshio 1004 Extension region. In recent years, several studies focused on sub-mesoscale processes 1005 associated with flow-topography interactions around the ridges (e.g., Nagai et al., 2021, 1006 Hasegawa et al., 2021). Along the south coast of Japan, the Kuroshio Current follows two major 1007 paths, characterized by a large or small meander (e.g., Kawabe, 1995). In the small meander 1008 configuration, a cyclonic eddy propagates the Kuroshio path to the east (Nagano and Kawabe, 1009 2004). In the large meander pathway, a large cyclonic circulation forms between the meandered 1010 Kuroshio and the coast, as captured by satellite data analysis (e.g., Ebuchi and Hanawa, 2000; 1011 Kobashi and Kawamura, 2001). 1012 3.3.3 Impact on biogeochemical and marine ecosystem fields 1013 In the open North Pacific, the Kuroshio rings transport subtropical water with 1014 biogeochemical properties that differ from ambient waters (e.g., Tomosada, 1986; Sugimoto 1015 and Tameishi, 1992; Kaneko et al., 2015). Some rings reach subpolar latitudes up to 46.5°N at 1016 Bussol' Strait (Bulatov and Lobanov, 1983; Rogachev, 2000a; Yasuda et al., 2000; Itoh and 1017 Yasuda, 2010a) and greatly modify fishing grounds and ecosystems (Saitoh et al., 1986; 1018 Sugimoto and Tameishi, 1992; Prants et al., 2021). For example, the ring WCR86, formed in 1019 1986 at approximately 37°N (Sugimoto and Tameishi, 1992), moved along the Japan and Kuril-1020 Kamchatka Trenches and reached as far as 46.5°N at the Bussol' Strait; despite having travelled

a long way from its origin, it still contained warm, salty water in its upper layer (Yasuda et al., 2000; Rogachev, 2000a). Offshore of southeastern Hokkaido, warm core rings often block the coastal branch of the nutrient-rich Oyashio Current causing a change of the migration routes of pelagic species and a shift of the richest fishing grounds offshore (Saitoh et al., 1986; Sugimoto et al., 1992; Prants et al., 2014a; Prants et al., 2021).

The large Kuril eddies on the Pacific Ocean side of Kuril Islands influence transport pathways, water masses, nutrient distributions and chlorophyll concentrations. Near the coast, they can block the coastal flow and thus intensify the offshore branches of the East Kamchatka and Oyashio Currents (see Figs. 15 and 16). Due to strong mixing, the Kuril eddies affect the distributions and vertical fluxes of dissolved oxygen, nutrients and dissolved inorganic carbon in the Oyashio region, and thus the plankton blooms. Using in situ observation and satellite data, it has been found that the boundaries of the Kuril eddies are enriched in nutrients and characterized by high biological productivity (Kusakabe et al., 2002).

The impact of meso- and submeso-scale processes on the marine ecosystem is remarkable in the northwestern Sea of Okhotsk, namely in the Sakhalin Bay, where the Amur River enters the Sea (Zhabin et al., 2010). The region northwestward of the Sakhalin Bay around the Bolshoy Shantar Island is highly productive; e.g., it is a bowhead whale feeding ground (Rogachev et al., 2008). It has been shown that submesoscale eddies in this area are generated by the interaction of Amur River freshwater, strong tidal currents, and topographic torque induced by the bathymetry, resulting in intensive vertical mixing and abundant nutrient supply to the euphotic layer (Rogachev et al., 2008; Zhabin et al., 2010).

Around the Korean Peninsula, the temporal and spatial variability of surface phytoplankton blooms has been observed using ocean color (e.g., Kim et al., 2000b; Yamada et al., 2004, 2005; Kim et al., 2007; Park et al., 2012b; Shi and Wang, 2012; Lee and Kim, 2018). Park et al. (2012b) showed that satellite Chl-a concentrations correlate with numerous eddies during the phytoplankton spring bloom in the East Korea Warm Current region. These data also indicate that along the southeast coast of the Korean Peninsula, the biological productivity is enhanced mainly by wind-driven upwelling (Yoo and Park, 2009), submesoscale eddies and shear currents (Lee and Kim, 2018). In summer, surface Chl-a is low in the Ulleung Warm Eddy interior due to the strong vertical stratification and nutrient depletion inside the eddy. However, a strong Chl-a maximum has been observed in the subsurface layer, which is attributed to an

intrathermocline eddy formed within the Ulleung Warm Eddy mixing surface and deep-ocean waters and supplying sufficient nutrients. This suggests a key ecological role of the Ulleung Warm Eddy (Kim et al., 2012). Moreover, the regional spring and fall blooms are more significant within 40 km of the coast than offshore because of more energetic submesoscale horizontal shear and vortical phenomena onshore as well as their propagation in the cross-shore direction. Specifically, the regional spring bloom starts offshore and migrates onshore with a time delay of about one month, resulting from the onshore propagation of geostrophic currents, the deepening of the mixed layer, and favorable nutrient fluxes from the subsurface (Lee and Kim, 2018).

To the northeast of Taiwan, the Kuroshio intrusions to the East China Sea shelf and its mesoscale dynamics sustain the local biogeochemical fluxes, biological productivity, spawning grounds, larval transport routes, and habitat conditions (temperature and food) of commercial fish (e.g., Liu et al., 1992; Gong et al., 1997; Liu et al., 2010; Sassa et al., 2008; Sassa and Tsukamoto, 2010). Mesoscale eddies are also likely to contribute to the indirect transport of terrigenous particles from the East China Sea shelf and slope to the southern Okinawa Trough and the Pacific Ocean, as evidenced by the observation of suspended matter collected in August 1994 in a cyclonic eddy, linked to the Kuroshio intrusion (Hsu et al., 1998). Wong and Zhang (2003) surveyed the distribution of iodine, governed by biological activities, in a transect across the southern East China Sea shelf off the northeast of Taiwan, and suggested that the exchange between the open ocean and marginal sea due to mesoscale fluctuations of the Kuroshio is an important source. Miller et al. (2002) found that the widespread distribution of marine eels in the East China Sea is linked to the transport by the Kuroshio and Tsushima Warm Current. Sassa et al. (2008) and Sassa and Tsukamoto (2010) reported that the spawning ground and habitat condition (temperature and food) of larval fish (jack mackerel and chub mackerel) vary from year to year due to the warm Kuroshio intrusion in the northern Taiwan.

The southern coast of Japan is a major spawning ground for pelagic fishes such as sardines and anchovies (e.g., Kimura et al., 2000; Nakata et al., 2000; Kasai et al., 2002), due in large part to mesoscale activity. Mesoscale eddies induced by frontal disturbances of the Kuroshio Current can stimulate local biological production that results, in turn, in an increase of the number of anchovy larvae (Kimura et al., 2000). These eddies also have implications for larval transport, distribution and food availability for anchovy in the Enshu-nada Sea (Nakata et al., 2000). Kasai et al. (2002) showed that the primary production in the subsurface layer is

enhanced when the nutrient-rich coastal water is entrained into Kuroshio frontal eddies. Furthermore, the Kuroshio Current plays a crucial role in supplying nutrient to the shelf-slope region off the southern coast of Japan (e.g., Kuroda et al., 2018). Kuroda et al. (2014, 2018) investigated through modeling the circulation of Tosa Bay and revealed that when the Kuroshio takes a stable near-shore path, nitrate was frequently uplifted around the Kuroshio front and horizontally transported along the front and into the bay via the counterclockwise circulation within the bay, and at times it was further uplifted onto the shelf.

3.3.4 Variability

The coastal areas of the western North Pacific Ocean underwent significant warming in the past three decades. Its manifestation is a decreasing trend in seasonal sea ice in the Sea of Okhotsk, since, at least, the 1970s. As reported by the Japan Meteorological Agency, the reduction of the maximum sea ice extent from 1970 onwards is equivalent to a 3.9% decrease of the ice cover per decade (https://www.data.jma.go.jp/gmd/kaiyou/english/seaice okhotsk/series okhotsk e.html). The positive SST trend results from the weakening of the East Asian winter monsoon, in turn linked to the abrupt decline of the Siberian high, the cold-core high pressure system that modulates air temperatures in boreal winter with a center located in the northwestern Mongolia region (Park et al., 2012a). The SST warming during winter then persists throughout the year in the coastal areas. Since 1990, the ocean dynamical response to the Aleutian Low variability has strengthened, and the PDO influence on SST in Region 3 has increased. This increase in the relative role of ocean (PDO-mediated) versus atmospheric (East Asian winter monsoonmediated) influences has been interpreted as a response to the weakening of the Siberian highpressure system. To our knowledge, the impacts of these changes on mesoscale variability, eddy formation and ecosystem functioning in Region 3 have not been investigated.

To date, the interannual to seasonal variability in eddy activity in Region 3 has only been studied in the upstream Kuroshio region (Chang et al., 2015; Yin et al., 2017; Yin et al., 2019). Chang et al. (2015) concluded that the change of the Kuroshio transport is locally caused by mass convergence and divergence produced by the mesoscale eddies and is therefore non-uniform. In eddy-rich years, the Kuroshio is generally stronger upstream. The large number of warm eddies to the east of Taiwan and Luzon Island further strengthens the jet, whereas the larger number of cold eddies to the east of the Luzon Strait weakens the Kuroshio in the Luzon

1115 Strait. Yin et al. (2017) analyzed the impact of mesoscale eddies on the Kuroshio intrusion 1116 variability northeast of Taiwan, finding that cyclonic (anticyclonic) eddy increase (decrease) the 1117 Kuroshio intrusion. Yin et al. (2019) found that the seasonality of the relative number of 1118 anticyclonic and cyclonic eddies, which strengthen the Kuroshio between June and August and 1119 weaken the Kuroshio between February and April in the East Taiwan Channel, is determined by 1120 the number of cyclonic eddies. 1121 The Kuroshio and its intrusions northeast of Taiwan are affected by open ocean eddies from 1122 the STCC and North Equatorial Current regions. The Kuroshio volume transport at the entrance 1123 to the East China Sea has a remarkable 100-day variability of ± 10 Sv (Johns et al., 2001), which 1124 has been attributed to open ocean mesoscale eddies (Zhang et al., 2001). Anticyclonic 1125 (cyclonic) eddies enhance (weaken) the Kuroshio transport, as shown through observations 1126 (Vélez-Belchí et al., 2013) and modelling (using HYCOM, Yin et al., 2017). Additionally, in 1127 the model it has been found that the arrival of cyclonic eddies introduces a positive potential 1128 vorticity flux and weakens the cross-slope potential vorticity gradient, favoring the onshore 1129 intrusion of Kuroshio water. The modulation of the Kuroshio front is important for the cross-1130 shelf exchange of heat, salt and nutrients. The seasonal cycle in SST in the Bohai Sea, Yellow 1131 Sea and East China Sea depends on the frontal structure and physical mechanisms responsible 1132 for the front formation, e.g., tidal mixing, water mass convergence, river runoff, and deep-water 1133 mass convection (Belkin et al., 2009; Shi and Wang, 2012). 1134 Summer marine heatwaves have been observed during 2010–2016 in the Oyashio region, and 1135 may be responsible for an increase of yellowtail catch in the waters surrounding northern Japan 1136 (Miyama et al., 2021). The heatwaves might have been caused by a weakened southward 1137 intrusion of the Oyashio near the coast, accompanied by an increase in anticyclonic eddies from 1138 the Kuroshio Extension (Miyama et al., 2021). Interactions between the Oyashio and mesoscale 1139 eddies result in an interdecadal shift in the cold-water intrusion of the Oyashio to the area off 1140 the southwestern coast of Hokkaido, and large areas of favorable potential fishing grounds near 1141 the Hokkaido coast have disappeared in the 2010s (Kuroda and Yokouchi, 2017; Prants et al., 1142 2021). Although the variability of the western Oyashio front may be controlled by decadal 1143 modulations of mesoscale activity in the upstream Kuroshio Extension (Qiu et al., 2017), further 1144 studies are needed to identify the driver for the warming in summer and increased anticyclonic 1145 eddies after 2010 (Miyama et al., 2021). Using 1993-2020 altimetry data, Trusenkova and 1146 Kaplunenko (2022) demonstrated the existence of quasi-biennial (in 1995–1998), interannual

1147 (3–7 years; since 2002), and decadal (8–10 years; in 2002–2014) fluctuations of EKE in the area 1148 west of Hokkaido between the Korean Peninsula and the Japanese Islands.

3.3.5. Summary

Mesoscale eddies in Region 3 are influenced by coastal processes such as tidal and topographic mixing, sea ice formation and melting, typhoon upwelling, weather events and terrestrial inputs of fresh water. The interaction of eddies, often generated over the shelves, with the western boundary currents occurs frequently and characterizes the circulation of this region. The Japan and Kuril–Kamchatka Trenches tend to catch mesoscale eddies, which stagnate or propagate over the trenches. Eddies are essential to exchanging waters between adjacent enclosed basins and the open ocean, inshore to offshore, and shallow to deep. Owing to the technological developments of satellite remote sensing, advances in modeling, newly developed analytical methods such as Lagrangian eddy monitoring, and tremendous efforts in in-situ observations, a large amount of information on the eddy activities and their influences has been accumulated for Region 3. several questions are still open due to the complex interactions of multiscale, nonlinear and highly diverse processes, including eddy-eddy interactions, eddy-merging and dipole-eddy processes.

The marine ecosystems in the western North Pacific and marginal seas are influenced by local changes in the convergence of water masses around eddies on the open-ocean fronts and upwelling and tidal mixing on the coastal fronts, as well as the interactions and exchanges between the local/coastal ecosystems and the open ocean ones. In recent years, changes attributable to global warming have become more apparent, including an increase in the frequency of extreme events in both the atmosphere and the ocean that threatens marine ecosystems. Climate projections show monotonic increases in ocean warming and frequency of extreme events, such as marine heat waves.

Again, we summarize main eddy characteristics in the Table below. In this region the physical properties have been generally sampled and quantified, while open questions remain on the overall impacts on the ecosystem, especially on zooplankton and higher trophic levels. Given the economic and social role played by fishery in this area, it is imperative to close these gaps with targeted campaigns and repeated and mooring observations, noting that simulations of zooplankton dynamics would also benefit greatly from the data collected. Constraining plankton cycling will help forecasting climate change impacts on the fishery of Region 3.

Table 3: Characteristics and impact on marine ecosystem of eddies in Region 3. Underlining as in Table 1.

	Cold dome	Kuroshio	Ulleung	Coastal eddies	Eddies along the	Eddies in
	off	small meander	Warm Eddy	off the	Kuril –	the Kuril
Eddy type	northeastern			northeastern	Kamchatka	Basin
	Taiwan			coast of Korea	Trench*	
	Off	Kuroshio	East of the	Coastal areas	Local or within	Local
Formation	northeastern	south coast of	Korea	near the East	the Kuroshio	
area	Taiwan	Kyushu	Peninsula	Coast Warm	Extension	
				Current		
	Cyclonic	Cyclonic	Anticycloni	Anticyclonic/Cy	Anticyclonic	Anticyclo
Polarity			С	clonic		nic/Cyclo
						nic
	Interaction	Advection of	Potential	Baroclinic	Boundary current	Baroclinic
	between	positive PV	vorticity	instability (Yoo	instability	/
i	Kuroshio	caused by the	balance (Jo	et al., 2018)	(Yasuda et al.,	barotropic
	current and	propagation of	et al., 2017)		2000)	instability,
	East China	cyclonic				tidal
Formation	Sea shelf	eddies (Usui				processes,
mechanism	(Shen et al.,	et al. 2008)				topographi
	2011)					c torque
						(Ohshima
						et al.,
						2005)
	70 km (Hsu	50–100 km	86 km	3–15 km (Yoo	100–350 km	~100 km
Diam -t	et al., 1998)	(Nagano and	(average,	et al., 2018)	(Yasuda et al.,	(Ohshima
Diameter		Kawabe,	Lee et al.,		2000)	et al.,
		2004)	2019)			2005)
	Stationary	Eastward	Quasi	Onshore and	Stationary or	Quasi
Propagation	(Chuang et	(Nagano and	stationary	offshore	moving towards	stationary
	al., 1993)			propagations	the Bussol' Strait	(Wakatsuc

		Kawabe,	(Chang et	(Yoo et al.,	(Isoguchi and	hi and
		2004)	al., 2004)	2018)	Kawamura, 2003;	Martin,
					Prants et al.,	1991;
					2020)	Ohshima
						et al.,
						2002)
	Summer	1 – a few	From	A few days to a	From several	From
		months	several	few weeks (Yoo	months to more	several
		(Nagano and	months to	et al., 2018)	than a year	months to
Lifetime		Kawabe,	more than a		(Rogachev,	more than
Lifetime		2004)	year (Chang		2000a; Prants et	a year
			et al., 2004)		al. (2020);	(Bulatov
						et al.,
						1999)
	Decreasing	Affecting	<u>Unknown.</u>	Vertical	Resulting in	Transporti
	surface	winter mixed	Heat and	transport (Yoo	latitudinal	ng Soya
	temperature	layer in the	salt budget	et al., 2018)	transports (Itoh	Warm
	due to	shelf-slope	analysis		and Yasuda,	Current
	vertical	waters facing	based on		2010b)	and waters
	mixing	the Kuroshio	<u>data</u>			round
Heat/freshw	(Shen et al.,	(Kuroda et al.,	assimilated			Kuril
ater	2011).	2014)	products			Islands
transport	<u>Further</u>		that capture			offshore
	evaluations		the			(Bulatov
	to verify		<u>variability</u>			et al.,
	generality		of the eddy			1999)
	are needed.		field is			
			recommend			
			ed.			
Nutrient	Offshore	Supplying	Supplying	Vertical	Advecting coastal	Offshore
transport	transport of	nutrient to the	nutrient to	transport (Lee	high productivity	transport
панэрон	terrigenous	shelf-slope	the	and Kim, 2018)	waters offshore	of

	material	region	subsurface		(Kusakabe at al.,	nutrients
	(Hsu et al.,	(Kuroda et al.,	layer (Kim		2002)	(Zhabin
	1998)	2018)	et al., 2012)			and
						Andreev,
						2019)
	Enhanced	Enhanced	Enhanced	Correlated with	Advecting coastal	Enhanced
	through	(Kimura et al.,	(Kim et al.,	submesoscale	high productivity	(Zhabin
	upwelling	2000; Kasai et	2012)	horizontal shear,	waters offshore	and
	(Gong et al.,	al., 2002)		vortical	(Kusakabe at al.,	Andreev,
Impact on	1997)			phenomena,	2002)	2019)
chlorophyll				their cross-shore		
				propagations		
				(Lee and Kim,		
				2018)		
	Affected	Impacting on	Influencing	<u>Unknown.</u>	Unknown. Field car	mpaigns
	through	the spawning	latitudinal	Expected to	targeting zooplankto	on_
Impact on	upwelling	ground for	heterogeneit	yield blooming	assemblages in and around	
zoo/ichthyo-	(Sassa and	pelagic fishes	y of	of zooplankton;	mesoscale structures are	
plankton	Tsukamoto,	(Kimura et al.,	plankton	further studies	recommended.	
	2010)	2000; Kasai et	(Kang et al.,	<u>are</u>		
		al., 2002)	2004)	recommended.		
	Fishing	Anchovy	<u>Unknown.</u>	<u>Unknown.</u>	Pacific saury	<u>Unknown.</u>
	(Shen et al.,	recruitment	Expected to	Expected to	(Prants et al.,	Analysis
	2011)	(Nakata et al.,	<u>yield slow</u>	yield rapid	2014a; Prants et	of fishing
Impact on		2000)	blooming	blooming of the	al., 2021)	data and
_			of the	higher trophic		<u>oceanogra</u>
higher trophic			<u>higher</u>	levels; in-situ		phic data
levels			trophic	concurrent		<u>is</u>
ieveis			levels; in-	observations		recommen
			<u>situ</u>	(e.g., physical		ded.
			concurrent	quantities and		
			observations			

	<u>(e.g.,</u>	fishing data) are	
	physical	required.	
	quantities		
	and fishing		
	data) are		
	required.		

^{*}Including warm-core ring (eddy), Kuril eddy, Bussol' eddy and Kamchatka eddy.

3.4 Region 4: Extratropical open North Pacific

3.4.1 Introduction

Region 4 covers the extratropical open North Pacific (Fig. 1 and 2). It includes the KOE, the NPC, the STCC and the area east of 170°W. While eddies in these four areas often interact with each other, here we characterize their mesoscale features separately, as their background conditions, such as flow field and stratification, are considerably different.

The KOE is the downstream part of the Kuroshio and the Oyashio currents, flowing eastward after separating from Japan at around 35°N and 42°N. It includes strong frontal boundaries between warm and salty subtropical waters, and cold and fresh subpolar waters (Yuan and Talley, 1996; Yasuda, 2003; Bishop and Watts, 2014). Intense mesoscale eddies, both warmand cold-core rings, are often shed from these currents (Mizuno and White, 1983; Yasuda et al., 1996; Itoh and Yasuda, 2010a; Sasaki and Minobe, 2015; Dong et al., 2017). The energy of the KOE decreases as it moves eastward; east of the dateline the KOE becomes the broad NPC¹ (Qiu, 2002). Finally, the STCC is a shallow eastward current flowing between 18°N and 28°N at a speed of a few centimeters per second that is counter to the westward current predicted by wind-driven ocean circulation theory. This counter current is formed due to the combined forcing of surface wind and heat fluxes (Kobashi and Kubokawa, 2012).

indicate the downstream part of KOE.

¹ Although the NPC definition varies among published literature, we use here the term to

1199 The EKE estimated from SSH (Qiu, 2002, Fig. 18) or a high resolution numerical model (Qiu 1200 et al., 2018) is highest along the KOE, followed by the STCC. The high EKE within the KOE is 1201 partly attributed to variability of the currents themselves, but contributions from detached 1202 eddies, especially warm and cold-core rings shed from the northern and southern side of the 1203 Kuroshio Extension, are likely significant (Yasuda et al., 1992; Okuda et al., 2001; Qiu et al., 1204 2006; Itoh and Yasuda, 2010a). The EKE level in the NPC is lower than that in the KOE, and so 1205 is the amplitude of the eddies shed by it (Itoh and Yasuda, 2010a; Dong et al., 2017). 1206 Nonetheless, moderate amplitude eddies occur frequently in the NPC (Sasaki and Minobe, 1207 2015). They form either in this area or to the west of it (and then propagate into the region). 1208 While the formation rate of eddies generated in the NPC is low, their lifetime is long (Figs. 4 1209 and 5). 1210 Transport properties of oceanic systems involving strong meandering jets and associated 1211 eddies, such as KOE, NPC and the warm-/cold-core rings that detach from them, have been the 1212 subject of research and debate for more than thirty years, starting with the seminal paper by 1213 Bower et al. (1985). Do meandering jets enhance or inhibit transport in the cross-stream 1214 direction, i.e., are they "barriers or blenders"? This is an important question from both 1215 oceanographic and biological prospective because jets and eddies contribute to the redistribution 1216 of both physical and bio-geo-chemical tracers in the ocean, as well as to the transport of slowly-1217 swimming biological organisms such as fish larvae (Rypina et al., 2014; 2016; 2019). 1218 East of 170°W, the offshore North Pacific is largely an eddy desert (see e.g., Fig. 4 in Cheng 1219 et al., 2014). There is a long history of authors noting the large difference in eddy activity 1220 between the western and eastern North Pacific. Dantzler (1976) was among the first; he showed 1221 the amplitude of the structure function of dynamic height dropped more than one order of 1222 magnitude when comparing similar regions east and west of 170°W. Bernstein and White 1223 (1977) called the region 30°-40°N, 170°-140°W an eddy void and they also found an order of 1224 magnitude difference in eddy energy at wavelengths greater than 300 km between the eastern 1225 and western North Pacific. In subsequent years, many other authors used different datasets to 1226 demonstrate the same (e.g., Kirwan et al., 1978; Emery, 1983; Holloway, 1986). A particularly 1227 compelling instance was provided by an array of moorings showing that the EKE starts 1228 dropping east of 152°E and decreases by a factor of 4 by 165°E, and by a factor of 50 (100) by 1229 152°W for abyssal (near-surface) data (Schmitz, 1988).

1230 *3.4.2 Physical properties*

1260

1231 In this region, distant from shore, direct observations of mesoscale eddies have been limited 1232 compared to the other nearshore regions, with very few observations until satellite altimetry and 1233 the Argo float array became available. Since the early 1990s, the basic characteristics of eddies 1234 such as number, lifetime and formation/transit patterns have been increasingly investigated 1235 (e.g., Chelton et al., 2011b; Cheng et al., 2014). 1236 The governing dynamics for the KOE eddies are diverse. The Kuroshio Extension is an 1237 inertial jet providing energy for large-amplitude meanders and eddies (Qiu, 2002). Using linear 1238 stability analysis Kouketsu et al. (2008) found that the unstable waves in the KOE with 1239 wavelength of ~200 km (Kouketsu et al., 2005; 2007) were caused mainly by baroclinic 1240 instability. Furthermore, baroclinic instabilities due to the intense KOE density front and 1241 barotropic instabilities due to horizontal shears north and south of the jet play important roles 1242 (Yang and San Liang, 2018; Ji et al., 2018). Within the STCC, the meridional potential vorticity 1243 gradient is positive, but down below the surface the potential vorticity gradient is negative due 1244 to the westward North Equatorial Current. Baroclinic instability occurs due to the reversal in the 1245 potential vorticity gradient, inducing high eddy activity (Qiu, 1999; Roemmich and Gilson, 1246 2001; Kobashi and Kawamura, 2002; Chang and Oey, 2014). 1247 Satellite-based eddy identification and tracking can be used to derive an eddy census through 1248 metrics such as number, size, amplitude, lifetime, propagation speed, and 1249 appearance/disappearance, which are often projected onto geographical/hydrographical maps 1250 (e.g., Figs. 4, 5 and 6). Such altimeter-based eddy censuses have been compiled for the 1251 KOE/NPC (Itoh and Yasuda, 2010a; Sasaki and Minobe, 2015; Ji et al., 2018) and STCC 1252 domains (Liu et al., 2012). Cheng et al. (2014) conducted a comprehensive statistical analysis 1253 on the mesoscale eddies in the North Pacific. They indicated that cyclonic eddies are more 1254 numerous than anticyclones in Region 4 and the number of eddies decreases with latitude, as 1255 well as their size, speed and travel distance in accordance with the Rossby deformation radius 1256 and the phase speed of the baroclinic Rossby waves. The lifespan of the eddies does not show 1257 latitudinal dependence. In the case of lifespan, EKE, travel distance, and amplitude, the standard 1258 deviations are as large as the mean values; therefore, the mean values have low significance 1259 (Cheng et al., 2014). These censuses update and expand earlier studies based on limited

hydrographic surveys (Mizuno and White, 1983; Maximenko et al., 2001).

1261 As mentioned, temperature and salinity profiles of the eddies in Region 4 were sparse until 1262 the development of Argo floats. Exceptions are those collected by the Japanese and Soviet 1263 Union campaigns that extended observations offshore of Region 3, in the northern part of KOE 1264 (Tomosada, 1986; Yasuda et al., 1992; Yasuda et al., 2000; Rogachev, 2000b; Maximenko et 1265 al., 2001; Komatsu et al., 2004). In the transition zone from the Kuroshio Extension to the 1266 Oyashio Extension, intense anticyclonic eddies are often observed, which have warm and saline 1267 core water with a thickness of several hundreds of meters, originating from the Kuroshio 1268 Extension (Tomosada, 1986; Yasuda et al., 1992). A Soviet hydro-physical experiment 1269 "Megapolygon-87" conducted around the subarctic frontal zone also captured several mesoscale 1270 eddies (Maximenko et al., 2001). In this area, a comparable number of warm anticyclonic and 1271 cold cyclonic eddies were observed, but the anticyclones were more distinct and persistent 1272 (Maximenko et al., 2001). Many of these anticyclonic eddies originate from the Kuroshio 1273 Extension, but there are some formed in the Sea of Okhotsk, Bering Sea and Alaskan Stream 1274 (Rogachev, 2000b; Yasuda et al., 2000; Rogachev et al., 2007), and migrate in Region 4 from 1275 Regions 2 and 3 (see Section 3.2.2 and 3.3.2 and references therein). Those from the Sea of 1276 Okhotsk or the Bering Sea are cold/fresh-core anticyclonic eddies (Rogachev, 2000b; Yasuda et 1277 al., 2000; Rogachev et al., 2007), while anticyclonic eddies originating from the Alaskan Stream 1278 have a warm and saline core (Rogachev et al., 2007). 1279 Since the early 2000s, Argo floats have considerably increased the availability of 1280 temperature/salinity profiles within the eddies in Region 4. Combining satellite information on 1281 positioning and Argo data, it has been possible to compile profiles near the eddy center or 1282 composites of the three-dimensional structure. Itoh and Yasuda (2010b) analyzed the 1283 temperature and salinity profiles of mesoscale eddies near their center, and found anticyclonic 1284 eddies with a cold and saline core also in the KOE. In addition, some anticyclonic eddies with a 1285 distinct warm core in an upper layer have a cold and fresh core in a lower layer, which is likely 1286 formed through the interaction of eddies originating from the Kuroshio Extension and the Sea of 1287 Okhotsk. 1288 As to how mesoscale structures impact transport in this region, evidence suggests that at the 1289 ocean surface, strong oceanic jets such as the Kuroshio act as permeable transport barriers (e.g.,

Rypina et al., 2011; 2013; 2018 and references therein). However, the existence of such barriers

at depth is less understood and remains the subject of ongoing research. Burkholder and Lozier

(2011, 2014) and Garraffo et al. (2014) showed that although jets may act as barriers at the

1290

1291

1292

surface, the cross-stream transport and exchange is stronger along subsurface isopycnals. On the other hand, recent work by Cedarholm et al. (2019) suggests that along the 26.5 σ_{θ} isopycnal surface (that lays deeper than 500 m between 140°E and 180°E at 30°N), fluid parcel trajectories are unlikely to cross the Kuroshio Extension west of 155°–160°E, and therefore most of the simulated trajectories cross the front from the northern flank to the southern one in a limited longitudinal band east of 160°E, and then remain to the south of the front.

The suppression of the cross-jet transport near the Kuroshio Extension core, and more generally near the shearless cores of all strong oceanic jets, agrees with the strong Kolmogorov-Arnold-Moser stability arguments (Rypina et al., 2007), although the latter only rigorously applies to spatially periodic flows. It is also in line with the critical layer theory results of Ferrari and Nikurashin (2010) and Chen et al. (2014), who found limited subsurface cross-Kuroshio Extension transport west of ~155°E, with enhanced meridional transport at this longitude. Eddies, therefore, play an important role in enhancing (or strengthening) cross frontal transport. Budyansky et al. (2015) demonstrated that anticyclonic Kuroshio warm core rings transported Fukushima-derived cesium, that was subducted and trapped in the subsurface core and intermediate water layers (100~500 m), northward of the subarctic front.

While EKE is weak to the east of 170°W, mooring data from 49.55°N, 138.6°W reveal that occasional eddy events still dominate the depth-averaged kinetic energy budget (Freeland, 1993). Eddies are seldom observed around the center of the eastern part of the North Pacific subarctic gyre (Cheng et al., 2014); almost all eddies generated in the North Pacific travel westward (meaning many enter this area from the coastal regions indicated as Regions 1 and 2 in this work). When this happens, eddies contribute nutrients and elevated productivity by transporting coastal, nutrient rich waters.

The exception to the east of 170°W being an eddy desert is given by the seamount generated eddies north and west of the Hawaiian Islands. As early as 1974, Bernstein (1974) confirmed that eddies existed in this area and observed them drifting westward at 4.6 cm/s using temperature observations collected northeast of the Hawaiian Islands. Shortly thereafter, Royer (1978) showed that baroclinic eddies along 158°W north of Hawaii were correlated with upstream seamounts and pointed to Huppert and Bryan's (1976) theoretical work for eddy generation by seamounts to explain their formation. Later, the analysis of mooring data from

1323 28°N, 152°W showed that all these eddies propagated southwest-ward and derived energy
1324 baroclinically from the mean flow (Niiler and Hall, 1988).

3.4.3 Impact on chemical and biological fields

In Region 4, the relationship between eddies and the surface Chl-a concentration is spatially variable (Fig. 1). Negative correlations between SSH and Chl-a are most prominent along the stream of the Kuroshio Extension, typically west of 160°E, which corresponds to the mid-zone of the KOE. These negative correlations are primarily attributable to the eddy pumping effect. Upwelling and downwelling within cyclonic and anticyclonic eddies during their formation phase are likely responsible for the increase and decrease in primary productivity, respectively (Kouketsu et al., 2015). Because of the prominent impact of cyclonic eddies on primary productivity, their structure and contribution to nutrient transport and subsequent enhancement of primary production have been highlighted (Sasai et al., 2010; Nakano et al., 2013; Honda et al., 2018). Numerical experiments revealed that core waters of cyclonic eddies consist mainly of waters from the northern side of the Kuroshio Extension (Nakano et al., 2013), pointing to the importance of horizontal advection (eddy-trapping) in addition to vertical pumping.

Away from the center of the Kuroshio Extension, either northward, southward or eastward, the negative correlation gradually weakens (Fig. 1). This is because fewer eddies form in the areas around the Kuroshio Extension, and therefore there is less eddy-induced transport of nutrients, both vertically and horizontally (Kouketsu et al., 2015; Nakano et al., 2013). An exception is found in the southern part of the recirculation gyre (around 30°N, 140°–150°E) where slight positive correlations occur. This is partly due to horizontal advection by anticyclonic eddies that entrain nutrient-rich waters from the north (Kouketsu et al., 2015), and partly to cross-stream transport caused by quasi-steady recirculations. For the northern area of the KOE, where slight positive correlations are observed, it has been suggested that cold anticyclonic eddies that originate in the marginal seas contribute nutrient rich waters (Yasuda et al., 2000; Rogachev, 2000b; Itoh and Yasuda, 2010b; Prants et al., 2016). In the area east of 170°W, except for the region near Hawaii, the relationship between SSH anomaly and Chl-a is weak (Fig. 1). The sparsity of the eddies as well as small eddy amplitude especially in the northern part (e.g., Chelton et al., 2011b; Cheng et al., 2014) explain this weak relation.

South of the recirculation gyre (i.e. south of ~30°N), the correlation map transitions in sign near 23°–24°N and again around 17°–18°N, with correlation coefficients changing from

negative to positive, and then positive to negative again (Fig. 1). The positive band around 18°–23°N roughly corresponds to the STCC region, although the pattern is not clear at the western end. The eddy pumping mechanism does not explain the positive correlation, but it should be kept in mind that both cyclonic and anticyclonic eddies are generated along the STCC (Yang et al., 2013; Chang et al., 2017). The analysis of the cross correlation of Chl-a and eddy-induced Ekman pumping (Fig. 1d in Gaube et al., 2014) suggests that eddy current-induced Ekman pumping at the ocean surface may be responsible for the positive correlation in Fig. 1.

1354

1355

1356

1357

1358

1359

1360

1361

1362

1363

1364

1365

1366

1367

1368

1369

1370

1371

1372

1373

1374

1375

1376

1377

1378

1379

1380

1381

1382

1383

1384

1385

The eddy field near Hawaii is important biologically; decades of observations in this region suggest that anticyclonic and cyclonic eddies increase local primary productivity, change phytoplankton assemblages to favor larger species (diatoms) and increase nitrogen fixation. Venrick (1990) was among the first to point out the correlation between mesoscale patterns of dynamic topography (eddies) and chlorophyll distributions west of the Hawaiian Ridge, and postulated that eddy activity accounts for some of the variation in productivity in the Central North Pacific. Allen et al. (1996) noted that near the island of Hawaii, area-averaged photosynthetic rates were one third higher at the edge of a cyclonic eddy and 2/3 higher in the center than outside the eddy. In another study, vertically integrated nutrient and chlorophyll concentrations were shown to be enhanced in the center of a cyclonic eddy (Vaillancourt et al., 2003). The presence of eddies also impacts phytoplankton community structure, with large (>3 μm) phytoplankton enhanced within the eddy while small ones are enhanced outside of it. This effect was confirmed by Brown et al. (2008), but only for deep waters within the eddy; they observed a deep chlorophyll maximum in the center of a cold-core cyclonic eddy in the lee of the Hawaiian Islands that was comprised primarily of chain-forming diatoms. This contrasted with the upper mixed-layer populations within the eddy, which were similar to populations in the upper mixed-layer outside the eddy. The impact of anticyclonic eddies was demonstrated by Fong et al. (2008), who observed increased near-surface chlorophyll (5-fold) and increased nitrogen fixation (2–18 fold) in an anticyclonic eddy just north of Hawaii. Likewise, Guidi et al. (2012) observed increased nitrogen fixation (and high chlorophyll) caused by eddies, but at the interface between an anticyclonic and a cyclonic eddy and they attribute the increase to horizontal stirring. Eddy-eddy interaction has also been proposed for episodic injection of nutrients, perhaps due to surface frontogenesis and nonlinear Ekman pumping in the complex eddy field near Hawaii (Calil and Richards, 2010), and observed as nitrate variability by profiling floats (Ascani et al., 2013).

While cyclonic eddies in the KOE and NPC often enhance primary production through eddy pumping of nutrients, water trapping and more frequent water exchanges in the frontal structure surrounding both cyclonic and anticyclonic eddies are important for higher trophic levels as well. Warm anticyclonic eddies are often pinched off from the Kuroshio Extension and stay in the northern KOE for more than one year. They trap warm and saline water masses within their core, while interacting with the Kuroshio Extension, the surrounding Oyashio waters, and also with other anticyclonic eddies (Saitoh et al., 1986; Yasuda et al., 1992; Itoh et al., 2011; Kaneko et al., 2015). These processes are linked to the thriving of a unique community of zooplankton (Yamamoto and Nishizawa, 1986; Tsuda and Nemoto, 1992; Terazaki, 1992). As eddies in the offshore areas generally propagate westward, they are assumed to play important roles in transporting large copepods westward (Shimode et al., 2012).

Anticyclonic eddies and mesoscale fronts are also important for fish migration across the Kuroshio and Oyashio regions. Sugimoto and Tameishi (1992) revealed that various fish

Anticyclonic eddies and mesoscale fronts are also important for fish migration across the Kuroshio and Oyashio regions. Sugimoto and Tameishi (1992) revealed that various fish species, such as skipjack, mackerel, flying squid and saury use different parts of these vortical features for foraging. Since some fish species aggregates in and/or around eddies, their positions, observed through satellite altimetry, are used in forecasting fishing grounds of some species, such as Pacific saury in the northern KOE (Yasuda and Watanabe, 1994; Yasuda and Kitagawa, 1996; Prants et al., 2014a; Syah et al., 2016) and neon flying squid in the KOE/NPC (Alabia et al., 2015).

Although the trophic productivity in the STCC is generally lower than in the KOE/NPC, some migratory species use STCC eddies for their migration or larval transport. Chang et al. (2018) suggested that larval growth of Japanese eel that spawned west of the Mariana Islands is more successful if the larvae are trapped within mesoscale eddies, as they are confined within the food-rich cyclonic eddy environment. Mugo et al. (2010) found that the preferred habitat of the skipjack tuna in the western North Pacific can be successfully estimated by a geo-statistical model if information on SST, SSH and EKE from satellite remote sensing is properly accounted for. Skipjack tuna fishing sets were made in areas with low to moderate EKE, indicating that there were instances when catches were associated with eddies (Mugo et al., 2010).

In the case of the Hawaiian eddies, some observations suggest that they also impact higher trophic levels through entrapment and/or transport of zooplankton and larval fish. Several studies have found zooplankton and larval fish biomass to be enhanced inside cyclonic cold-

core eddies relative to outside around Hawaii (Lobel and Robinson, 1988; Landry et al., 2008). Lobel and Robinson (1986) used a combination of drogues and net sampling to illustrate how zooplankton and larval fish can be trapped inside an eddy; for larval reef fish, this meant that they would be retained near natal reefs long enough to complete their pelagic development phase. Later, Lobel (2011) showed that larval lizardfish were ready to settle at a younger age when a cyclonic eddy was present, indicating that the eddy influences not only retention but also larval plasticity. However, not all studies have found that cyclonic cold-core eddies positively influence fish recruitment; Fox et al. (2012) found that the presence of cyclonic cold-core eddies was negatively correlated with fish recruitment and Vaz et al. (2013) found both positive (increased connectivity between populations on the island of Hawaii) and negative (entrapping larvae and transporting them away from the coast) influences. Finally, some work has shown a positive correlation between fish catches and the presence of cyclonic eddies (e.g., Seki et al., 2002).

3.4.4 Variability

Neither altimetry data nor high resolution model outputs have long enough time series to investigate trends beyond the past two decades in Region 4. Climate models suggest that under global warming scenarios the southern half of the subtropical North Pacific Gyre will weaken while the northern one will intensify and shift northward (Cheon et al., 2012). Whether such a change would be conducive to changes in mesoscale activities has yet to be proved; to date global climate models have too coarse resolution to explicitly represent eddy processes.

Recently, Ding et al. (2018) found a significant increase in eddy activity north of the Hawaiian islands, in the Hawaiian – Emperor seamount chain (triangle with the vertices 30°N,142°W; 30°N,175°W; 48°N,175°W) over the period 1993–2011, and attributed the change to increasing eddy lifetime caused by weakening wind speed over the region, which was possibly linked to sea surface warming.

At interannual scales, the EKE in the KOE and NPC undergoes a multi-year modulation (Qiu and Chen, 2005; Nonaka et al., 2008). The EKE is inversely proportional to the strength of the Kuroshio Extension jet. When the Kuroshio Extension jet and recirculation gyre are weaker than the mean (for example during 1996–2001), the regional EKE level is high, and vice versa. This behavior results from the migration of the Kuroshio Extension jet inflow over the Izu–Ogasawara Ridge extending from Japan southward along 140°E rather than from intrinsic

1448 baroclinic instability of the Kuroshio Extension jet (Qiu and Chen, 2005). Wang et al. (2016) 1449 also reported that baroclinic instability is not the dominant contributor, and that barotropic 1450 instability prevails. 1451 In the STCC area, interannual variations are driven by the vertical shear between the STCC 1452 and the subsurface westward-flowing North Equatorial Current, which is due to surface Ekman 1453 temperature gradient convergence within the STCC band of 18°-28°N. Such shear induces 1454 baroclinic instability that in turn drives variability in the mesoscale eddy field (Qiu and Chen, 1455 2010; Liu et al., 2012). In the Hawaiian Lee Countercurrent (17°N–21.7°N and 170E°–160°W), 1456 Yoshida et al. (2011) found a low-frequency modulation linked to the PDO, with greater 1457 vertical shear, enhancement of conditions favorable to baroclinic instability, and positive EKE 1458 anomalies during the positive phase of the PDO, and vice versa for periods of negative PDO. 1459 At seasonal scales, altimetry data show that in the KOE and NPC the EKE maximum occurs 1460 in summer and the minimum in winter (Tai and White, 1990; Stammer and Wunsch, 1999; 1461 Ducet and Le Traon, 2001; Scharffenberg and Stammer, 2010; Zhai, 2017). Bishop et al. (2013) 1462 reported that the seasonal cycle in the KOE and NPC is associated with baroclinic instability 1463 based on the analysis of current- and pressure-equipped inverted echo sounders (CPIES) data. 1464 Yang and San Liang (2018) have used the HYCOM reanalysis to suggest that both baroclinic 1465 and barotropic instabilities are responsible for the observed seasonality. 1466 In the STCC, the EKE maximum occurs in May and the minimum in December (Qiu et al., 1467 2014; Liu et al., 2012; Chang and Oey, 2014). This is because cooling during fall and winter 1468 brings the meridional tilt of the upper thermocline at its maximum in early spring, just before 1469 warming starts; vertical shear is intensified and baroclinic instability occurs, intensifying the 1470 EKE one or two months later (Kobashi and Kawamura, 2002; Qiu, 1999; Qiu et al., 2008; Qiu 1471 and Chen, 2010; Liu et al., 2012; Chang and Oey, 2014). Furthermore, Chang and Oey (2014) 1472 proposed that the intensification of the SST front in winter and spring accelerates the eddy 1473 growth rate. 1474 The seasonality reported from the analysis of altimetry data may be biased because its spatial 1475 resolution, order 150 km, is not enough to fully account for the mesoscale variability. High 1476 resolution modeling studies show that the timing and the strength of the seasonality signal 1477 changes among years due to the cascade of kinetic energy occurring in submesoscale eddies 1478 (Qiu et al., 2014; Sasaki et al., 2014; 2017). A recent high-resolution ocean-only model

simulation has shown that the EKE peaks around May–June for the Kuroshio Extension, around April for the STCC and in January–February for the Oyashio Extension (Sasaki et al., 2017; see their Fig. 5), with minima in fall–early winter. Considering the dominant role of baroclinic instabilities in all Region 4 subregions, the difference in the phase across the different domains may be caused by the different seasonality in stratification and/or phase speed of Rossby waves. Submesoscale permitting simulations used to investigate the interannual to decadal variations of submescale motions in the subtropical Northwestern and Northeastern Pacific (Sasaki et al., 2020, 2022) have shown that these variations were modulated by the PDO or ENSO.

Eddy variability in the lee of the Hawaiian Islands has been found to be strongest at seasonal and sub-seasonal scales. Calil et al. (2008) attributed it to the regional, orographic wind forcing using a regional model and modifying the wind field. Yoshida et al. (2010) confirmed this result by performing a statistical analysis of weekly satellite SSH images, and further showed that the variability of the ocean eddy population around Hawaii has distinguishable time scales at 60 and 100 days: 100-day period eddies are found west of 160°W and their variability is generated by instabilities in the shear of the mean flow (similar to the analysis by Niiler and Hall, 1988), while 60-day eddies are found close to the island Hawaii and their variability is linked to wind stress curl anomalies associated to the blocking of the trades by the island orography.

3.4.5 Summary

In the extratropical open North Pacific, the EKE is relatively strong in the southwestern part and weak in the northeastern part as suggested in Fig. 18. The eddy activity is strongest along the KOE, where an inertial jet provides energy for strong meanders and eddies, and baroclinic and barotropic instabilities due to strong fronts and shears contribute to eddy formation. Eddy activity is weaker in the NPC, the downstream end of the KOE. High eddy activity is also observed along the STCC, where baroclinic instability occurs due to the reversal in the potential vorticity gradient. East of 170°W, the offshore North Pacific is largely an eddy desert, except around the Hawaiian Islands.

Being far from the coasts, studies on the impact of eddies on biological fields in Region 4 have largely been limited to from the analysis of satellite observations. The relationship between eddies and the surface Chl-a concentration is spatially variable (Fig. 1). In the KOE and around Hawaii, there is evidence of eddies impacting species in the higher trophic level. In the last two decades, numerical experiments have become a critical tool to study the impact of

eddies on the ecosystem in many parts of Region 4. Table 4 summarizes known/unknown eddy characteristics which have large uncertainties given that in-situ data are scarcer in this Region than in the previous three. Again, knowledge of the eddy impact on zooplankton and higher trophic levels is limited, and targeted field campaigns would help constraining it.

Seasonal to interannual variations of mesoscale activity have been studied mainly by satellite altimetry data as well as numerical modeling, finding that generation mechanisms and variability differ in each subregion in Region 4. Due to the lack of long-term time series of satellite altimetry data and high-resolution model outputs, however, investigations of trends beyond the past two decades are lacking. It is recommended that the variability at longer timescales is studied using long-term high-resolution ocean simulations such as OGCM for the Earth Simulator version 2 (OFES2) (Sasaki et al., 2020). Such studies would also help investigating the relationship between mesoscale and submesoscale activities and climate modes of variability, like the PDO and ENSO. Observations of the submesoscale motions from the forthcoming Surface Water and Ocean Topography (SWOT) altimeter mission (https://swot.jpl.nasa.gov) will be especially valuable in this poorly sampled region.

In addition, there is a strong need to investigate the impact of eddy variability on the biological production and marine ecosystem. Most of Region 4 is far from coasts, and it is difficult to conduct repeated ship observations. The analysis of satellite and biogeochemical Argo data coupled with ecosystem modeling would be especially important to comprehensively quantify the impact of mesoscale processes on the ecosystem. For successful ecosystem modeling, field surveys that target the functional relations between the various components are crucial. Recently, Arostegui et al. (2022) showed a pervasive pattern of increased pelagic predator catch inside anticyclonic eddies relative to cyclones and non-eddy areas using a large-scale fishery dataset. Interdisciplinary comparisons are another key tool to understand the impact of eddies on higher trophic level ecosystem.

Table 4: Characteristics and impact on marine ecosystem of eddies in Region 4. Underlining as in Table 1.

Eddy type	KOE/NPC	STCC	East of 170°W	Near Hawaii
EKE	Very strong and getting	Strong	Weak	Strong
	weaker to the east			

Polarity	Anticyclonic and cyclonic: than anticyclonic eddies (C	Anticyclonic/ Cyclonic (Lumpkin,		
				1998)
Formation mechanism	Instabilities associated	Instabilities	<u>Unknown.</u>	Instabilities
	with strong front/shear	associated with	Numerical	associated with
	(Qiu 2002; Yang and San	meridional	simulations	seamounts (Huppert
	Liang, 2018; Ji et al	potential	could help in	and Bryan, 1976)
	2018)	vorticity	this regard.	
		gradient (e.g.		
		Qiu 1999)		
Diameter	168 ±32 km (anticyclonic	180 ±32 km	150–200 km	~200 km (Fig. 6 in
	eddies), 162 ±28 km	(anticyclonic	(Fig. 4 in	Liu et al., 2012)
	(cyclonic eddies) for	eddies), 174	Cheng et al.,	
	KOE (Cheng et al., 2014)	±30 km	2014)	
		(cyclonic		
		eddies) (Cheng		
		et al., 2014)		
Propagation	Mostly westward but			
	northward/southward at			
	the crests/troughs of	Westward (Cheng	retal 2014)	
	Kuroshio Extension,	westward (Cheng	g et al., 2014)	
	respectively (Itoh and			
	Yasuda, 2010a)			
Lifetime	19 ±21 weeks	17 ±14 weeks	7–21 weeks	Unknown. Analyses
	(anticyclonic eddies), 18	(anticyclonic	(anticyclonic	focusing on eddies
	±16 weeks (cyclonic	eddies), 15 ± 12	eddies), 6–18	near Hawaii are
	eddies) for KOE (Cheng	weeks (cyclonic	weeks	needed.
	et al., 2014)	eddies) for	(cyclonic	
		KOE (Cheng et	eddies) (Figs.	
		al., 2014)	4b and 5b)	
Impact on chlorophyll	Negative (eddy pumping	Weakly positive	Very weak	Positive and
(correlation between	and trapping, e.g.	(eddy-induced		Negative (multiple

SSH anomaly and	Kouketsu et al., 2015,	Ekman		mechanisms, Gaube
chlorophyll-a	Nakano et al., 2013)	pumping,		et al., 2014)
(expected		Gaube et al.,		
mechanisms))		2014)		
Impact on	Zooplankton aggregation	<u>Unknown. Field</u>	<u>Unknown.</u>	Zooplankton were
zoo/ichthyoplankton	at the front of an	or ecosystem	Further studies	concentrated at the
	anticyclonic eddy	modeling	that account for	eddy center (Lobel
	(Yamamoto and	studies are	eddy formation	and Robinson, 1988)
	Nishizawa, 1986)	needed to	area (Region 1	
		characterize	or Region 4)	
		zooplankton	are	
		assemblages.	recommended.	
Impact on higher	Fish (Sugimoto and	Japanese eel		Larval fish (e.g.,
trophic levels	Tameishi, 1992), flying	(Chang et al.,		Lobel and Robinson,
	squid (Alabia et al., 2015)	2018), skipjack		1986), fish
		tuna (Mugo et		recruitment (Fox et
		al., 2010)		al., 2012), fish catch
				(Seki et al., 2002)

4. Concluding remarks

In this work, we have synthesized current knowledge of mesoscale eddies and their impacts on the marine ecosystem across the North Pacific and its marginal Seas, across the CCS region (Region 1), the northeastern North Pacific and the Bering Sea (Region 2), the western boundary of the North Pacific and marginal seas (Region 3), and the extratropical open North Pacific (Region 4) (Figs. 1 and 2).

While not uniformly, eddies form throughout the open North Pacific, more frequently along the eastern boundary (Region 1 and eastern part of Region 2), along island chains between the open North Pacific and marginal seas (Region 2 and 3), and near the Hawaiian Islands (Region 4) and seamounts, and only seldomly in the center of the Alaskan gyre. Correlation analysis between SSH and chlorophyll shows that primary productivity is especially high in cyclonic eddies in Region 1 and in anticyclonic eddies in Region 2, as also indicated by regional studies.

In Region 3 and 4, on the other hand, the correlation coefficient varies from region to region: negative correlations are most prominent along the stream of the Kuroshio Extension, due to the eddy pumping effect (Kouketsu et al., 2015), while north of the KOE slight positive correlations are observed, likely because of cold anticyclonic eddies that originate in the marginal seas and contribute nutrient rich waters (Prants et al., 2016). In the area east of 170°W, the relationship between SSH anomaly and Chl-a is weak everywhere but around Hawaii, due to the overall weaker and sparser eddy activity. Positive coefficients are observed around 18°–23°N, and result from eddy-induced Ekman pumping (Gaube et al., 2014).

Four tables summarize mesoscale characteristics and eddy-ecosystem interactions in each Region, highlighting similarities and differences. For example, both cyclonic and anticyclonic eddies are observed in Region 1 and 4, but specific polarities are predominant in Region 2 and 3, where eddy formation is influenced by topography, or localized currents. Eddies with the longest lifetime (up to 5 years) are observed in Region 2, and quasi-stationary eddies are observed in Region 3. In Region 1 and in the eastern part of Region 2 along the west coast of US and Canada, eddies propagate offshore, where they transport coastal waters via eddy trapping. In Region 3 and 4, on the other hand, upwelling within the eddies and horizontal stirring are key to explain the biogeochemical properties of the mesoscale eddies.

The tables also indicate where more research is needed. In Region 1, the impact of subsurface anticyclones on the marine ecosystem has not been quantified, while in Region 2, the Aleutian eddies are not well characterized. In Region 3, the impact of eddies on the marine ecosystem is better constrained in the southern half of the domain than in the northern part, and in Region 4 eddy formation mechanisms and mesoscale impacts on higher trophic levels ecosystem have received little attention east of 170°W.

Major open questions differ among regions. In Region 1, a better understanding of the relationship between climate forcing and the intrinsic variability of the mesoscale eddy field is urgently needed, in consideration of the increasing frequency in marine heat waves recorded in the last decade (Oliver et al., 2018). In Region 2, it would be important to figure out how climate variability influences mesoscale activity, given recent observations pointing to an increase in the latter between 1993 and 2011 across most of the Northeast Pacific (Ding et al., 2018). Similarly, in Region 3 the impact of climatic changes on mesoscale variability, eddy formation and ecosystem functioning have not been investigated in depth, despite significant

warming in the past three decades. For example, summer marine heatwaves observed during 2010–2016 in the Oyashio region have been correlated with an increase of yellowtail catch in northern Japan (Miyama et al., 2021) and an increase in the detachment of anticyclonic eddies from the Kuroshio Extension, but a mechanistic understanding of the causal relationships among these events is missing. In Region 4, neither altimetry data nor high resolution model outputs provide long enough time series to investigate trends beyond the past two decades. Climate models suggest that under global warming scenarios the circulation in the southern part of the subtropical North Pacific Gyre will weaken while the northern one will intensify and shift northward (Cheon et al., 2012). Whether such a change would be conducive to changes in mesoscale activities has yet to be investigated; current climate models are too coarse to explicitly represent eddy processes.

Although many studies have revealed the impact of mesoscale eddies on phytoplankton, zooplankton and higher trophic level species individually, seamless understanding linking multiscale physics to chemical properties and finally to the marine ecosystem remains an aim. Recently, regional modeling studies have been used to investigate the physical forcing of eddies onto lower trophic level ecosystems (e.g., Chenillat et al., 2016 for an application to Region 1). As detailed in this review, the mechanisms impacting biological production differ from region to region, and sometime within the same region.

In this review we focused on mesoscale processes and their impact on marine ecosystem in the North Pacific, and discussed submesoscale processes when possible. Submesoscale circulations, which are ubiquitous in the world ocean, enhance vertical velocity at fronts and around mesoscale eddies (McWilliams, 2016), and their contribution should be better assessed and accounted. More studies combining high-resolution numerical models and high-resolution in-situ observations, as done for example in Zhong et al. (2017), are needed.

The North Pacific, especially its northwestern portion, is one of the world's major fishing grounds (e.g., FAO, 2019): adaptation to present and anticipated marine ecosystem changes and the development and adoption of policies that allow for a sustainable development and use of marine resources are essential to continue benefitting from these ecosystem services. To achieve these goals, policy makers need reliable information of the current and forecasted status of marine ecosystems. In this review we have argued that a better understanding and consideration of the role of mesoscale and submesoscale variability is needed to attribute the marine

1612 ecosystem responses to natural and/or anthropogenic forcing across a wide spectrum of time and 1613 space scales. As such, investigating biophysical interactions at the ocean mesoscales and 1614 smaller scales should be a scientific priority in the North Pacific. 1615 1616 Acknowledgements 1617 This review is the outcome of the work of the Working Group 38 (Mesoscale and Submesoscale 1618 Processes) of the North Pacific Marine Science Organization (PICES). The authors would like to 1619 thank Dr. Emanuele Di Lorenzo for his support. The authors also thank Dr. Shin-ichi Ito, editor 1620 of this manuscript, and two anonymous reviewers for their constructive and helpful comments. 1621 This is NOAA Pacific Marine Environmental Laboratory (PMEL) contribution number 5037. 1622 1623 Figure captions 1624 Fig. 1. Correlation between SSH anomaly and surface Chl-a anomaly corresponding to eddies 1625 from 1998 to 2012 (after Kouketsu et al. (2015)). SSH anomaly are high-pass-filtered (< 300 1626 days) to remove long-term changes. Chl-a anomalies are logarithmic deviations from the weekly 1627 climatology calculated from 1998 to 2012 data. Gray areas denote correlations that are 1628 insignificant at a 90 % confidence level. Figure courtesy of S. Kouketsu. Adapted by permission 1629 from Springer Nature: Kouketsu et al. (2015). 1630 Fig. 2. Schematic representation for the circulation of the open North Pacific. The thin white 1631 contours, whose contour interval is 0.1 m, indicate the mean dynamic topography produced by 1632 CLS and distributed by Aviso+ with support from Cnes (https://www.aviso.altimetry.fr/), and 1633 downloaded from ftp://ftp-access.aviso.altimetry.fr/auxiliary/mdt/mdt cnes cls2013 global/. 1634 Acronyms used in this figure is as follows: North Pacific Current (NPC), Kuroshio and Oyashio 1635 Extension (KOE), Subtropical Counter Current (STCC), Hawaiian Lee Countercurrent (HLCC), 1636 North Equatorial Current (NEC) and California Current System (CCS). 1637 Fig. 3. Average linear trend over 1980-2018 in °C/decade in the COBE SST2 and Sea-Ice 1638 reanalysis (COBEv2; Hirahara et al., 2014). The COBEv2 data set was developed by the 1639 Japanese Meteorological Agency, covers the period since 1850 and has a spatial resolution of 1° 1640 latitude × 1° longitude. We note that the period considered, for which we have satellite 1641 measurements, is skewed towards a slight predominance of negative PDO conditions.

- Fig. 4. Distribution of anticyclonic eddy (a) formation rate (times year-1), (b) averaged lifetime
- 1643 (day) and (c) yield (sum of lifetime divided by 9149 days (01Jan1993–18Jan2018) for those
- 1644 formed in each $2^{\circ} \times 2^{\circ}$ box over 25 years.
- Fig. 5. Same as Fig. 4 but for cyclonic eddies.
- Fig. 6. Distribution of anticyclonic eddy formation rate (times season-1) in (a) winter, (b)
- spring, (c) summer and (d) fall and cyclonic eddy formation in (e) winter, (f) spring, (g) summer
- and (h) fall at each $2^{\circ}\times2^{\circ}$ grid from January 1, 1993 to January 18, 2018.
- Fig. 7. Schematic representation for the currents of the CCS region (Region 1). Gray arrows
- indicate the direction of mean surface geostrophic velocity with speed greater than 0.05 m s⁻¹.
- 1651 Colors represent bottom topography (see Fig. 2). The mean geostrophic velocity data were
- produced by CLS (Collecte Localisation Satellites), distributed by Aviso+ with support from
- 1653 Cnes data center (https://www.aviso.altimetry.fr/), and downloaded from ftp://ftp-
- access.aviso.altimetry.fr/auxiliary/mdt/mdt cnes cls2013 global/.
- Fig. 8. Sea-surface temperature (right) and chlorophyll (left) measured by satellite along the
- 1656 U.S. west coast on September 26, 1998 (from Barth, 2007).
- Fig. 9. (a) Vertical section of Chl a (mg m⁻³) derived from fluorescence (color) along 37.87°N
- on 30 June 1993 overlaid with contours of density anomaly (kg m⁻³). The locations of each
- SeaSoar up-down cycle are indicated by triangles along the bottom. (b) Geopotential anomaly at
- 1660 100 m, $\Delta \phi 100/200$ (m² s⁻²) (thick curve), and 100 m north-south geostrophic velocity, vg (m s⁻¹)
- (thin curve), both referenced to acoustic Doppler current profiler velocity at 200 m, along
- 1662 37.87°N. From Barth et al. (2002).
- 1663 Fig. 10. The same as Fig. 7 but for the northeastern North Pacific and the Bering Sea (Region
- 1664 2)
- Fig. 11. Map of (a) anticyclonic and (b) cyclonic eddy amplitudes (circle radius), ages (color),
- 1666 from January 2003 to April 2012. From Lyman and Johnson (2015).
- Fig. 12. (a) Trajectories of Kenai 2006 and Kenai 2006a (adapted from Ueno et al., 2012).
- 1668 Colors represent SLA (cm) at the eddy and the radius of each circle in the map mostly
- 1669 corresponds to an Okubo-Weiss radius. (b) Trajectories of long-lived Alaskan Stream eddies
- propagating westward along the Alaskan Stream (after Ueno et al., 2009, © American

- Meteorological Society). Shading represents sea level anomalies (cm) at the eddy center. (c)
- 1672 The track of Aleutian eddies, based on mesoscale altimetry (reprinted from Rogachev et al.,
- 1673 2007, with permission from Elsevier).
- Fig. 13. (a) EKE (cm2 s⁻²) averaged over full years (1993–2009) calculated from AVISO
- altimetry data. Gray shading denotes shelf (< 200 m). Black line shows trajectory of 1997
- 1676 Pribilof Eddy (15 June–27 August 1997) calculated from drifters. Reprinted from Ladd et al.
- 1677 (2012), with permission from Elsevier.
- 1678 Fig. 14. As in Fig. 7 but for the western boundary of the North Pacific and marginal seas
- 1679 (Region 3). In this figure, gray arrows indicate the direction of mean surface geostrophic
- velocity whose speed is stronger than 0.1 m s-1.
- Fig. 15. (a) Snapshot current speed (cm/s) and (b) Lagrangian origin map on August 1, 2010,
- based on AVISO altimetry. Centers of anticyclonic features on this date are marked by
- triangles. Marked in (b) are Kuroshio rings as KR1-3, Hokkaido eddies as HE, Bussol' eddies as
- BE, Kamchatka eddies as KE1-2. (b) Colors mark fluid particles which crossed the sections of
- the same color shown in (a) during two years before the observation date. Isobaths from 7 to 10
- 1686 km are shown by magenta contours. The origin of particles in the white areas could not be
- 1687 determined.
- 1688 Fig. 16. SSH field showing the Bussol' eddy (A) sampled in a cruise in 2012 (white circles,
- Prants et al, 2016) and 'red' anticyclonic eddies with SSH > 45 cm in the Kuril Basin.
- 1690 Up(down)ward oriented triangles indicate the centers of anticyclonic (cyclonic) features on June
- 25, 2012. Reprinted from Prants et al. (2016), with permission from Elsevier.
- 1692 Fig. 17. Schematic of the regional circulation around the Korean Peninsula. Blue, red, purple,
- and orange colors indicate the water temperature of cold, warm, fronts, and riverine waters,
- respectively. Solid and dashed curves denote the persistent and seasonal currents, respectively (s
- and w indicate the directions of currents in summer and winter, respectively). Acronyms of
- primary regional currents are listed in the order of the Yellow Sea Warm Current (YSWC),
- 1697 West Korea Coastal Current (WKCC), Chinese Coastal Current (CCC), Jeju Warm Current
- 1698 (JWC), Jeju Tsushima Front (JTF)/Cheju Tsushima Front (CTF), Jeju Yangtze Front (JYF),
- Yangtze Diluted Water (YDW), Kuroshio Current (KC), North Korea Cold Current (NKCC),
- 1700 Tsushima Warm Current (TWC), Tsushima Warm Current-Nearshore Branch (TWC-NB),

- 1701 Tsushima Warm Current-Offshore Branch (TWC-OB), East Korea Warm Current (EKWC),
- 1702 Subpolar Front (SPF), and Ulleung Warm Eddy (UWE). Adapted from Lee et al. (2019).
- 1703 Fig. 18. EKE distributions in the North Pacific Ocean from the T/P SSH data of October 1992
- 1704 to November 2000 after removing signals longer than the annual period. Contour intervals are
- 1705 0.02 m²s⁻² for solid lines; dashed lines denote the 0.01 m²s⁻² contours. Reprinted by permission
- 1706 from Springer Nature: Qiu (2002).

1707

1708

1709

1710 References

- 1711 Abbott, M.R., Barksdale, B., 1991. Phytoplankton pigment patterns and wind forcing off central
- 1712 California. J. Geophys. Res., 96, 14649–14667. https://doi.org/10.1029/91JC01207.
- 1713 Alabia, I.D., Saitoh, S.-I., Mugo, R., Igarashi, H., Ishikawa, Y., Usui, N., Kamachi, M., Awaji,
- T., Seito, M., 2015. Seasonal potential fishing ground prediction of neon flying squid
- 1715 (Ommastrephes bartramii) in the western and central North Pacific. Fish. Oceanogr., 24:
- 1716 190–203. https://doi.org/10.1111/fog.12102.
- 1717 Alexander, M.A., Bladé, I., Newman, M., Lanzante, J.R., Lau, N.C., Scott, J.D., 2002. The
- atmospheric bridge: The influence of ENSO teleconnections on air—sea interaction over the
- 1719 global oceans. J. Climate, 15, 2205–2231, https://doi.org/10.1175/1520-
- 1720 0442(2002)015<2205:TABTIO>2.0.CO;2.
- Allen, C.B., Kanda, J., Laws, E.A., 1996. New production and photosynthetic rates within and
- outside a cyclonic mesoscale eddy in the North Pacific subtropical gyre. *Deep Sea Res.*
- 1723 *I*, 43(6), 917–936, https://doi.org/10.1016/0967-0637(96)00022-2.
- Amos, C.M., Castelao, R.M., Medeiros P.M., 2019. Offshore transport of particulate organic
- carbon in the California Current System by mesoscale eddies. *Nature Comm.*, 10, 4940,
- 1726 https://doi.org/10.1038/s41467-019-12783-5.

- Andreev, A.G., Budyansky, M.V., Uleysky, M.Y., Prants, S.V., 2018. Mesoscale dynamics and
- walleye pollock catches in the Navarin Canyon area of the Bering Sea. *Ocean Dynamics*, 68,
- 1729 1503–1514. https://doi.org/10.1007/s10236-018-1208-y.
- 1730 Arostegui, M.C., Gaube, P., Woodworth-Jefcoats, P.A. Kobayashi, D.R., Braun, C.D., 2022.
- 1731 Anticyclonic eddies aggregate pelagic predators in a subtropical gyre. Nature 609, 535–540.
- 1732 https://doi.org/10.1038/s41586-022-05162-6.
- 1733 Ascani, F., Richards, K.J., Firing, E., Grant, S., Johnson, K.S., Jia, Y., Lukas, R., Karl, D.M.,
- 1734 2013. Physical and biological controls of nitrate concentrations in the upper subtropical
- North Pacific Ocean. Deep Sea Res. II, 93, 119–134,
- 1736 https://doi.org/10.1016/j.dsr2.2013.01.034.
- 1737 Atwood, E., Duffy-Anderson, J.T., Horne, J.K., Ladd, C., 2010. Influence of mesoscale eddies
- on ichthyoplankton assemblages in the Gulf of Alaska. Fish. Oceanogr., 19, 493–507.
- 1739 http://doi.org/10.1111/j.1365-2419.2010.00559.x.
- Barnston, A.G., Livezey, R.E., 1987. Classification, seasonality and persistence of low-
- frequency atmospheric circulation patterns. *Mon. Weather Rev.*, 115, 1083–1126,
- 1742 https://doi.org/10.1175/1520-0493(1987)115<1083:CSAPOL>2.0.CO;2.
- Barth, J.A., 1994. Short-wavelength instabilities on coastal jets and fronts. J. Geophys. Res.,
- 99, 16095–16115, https://doi.org/10.1029/94JC01270.
- Barth, J.A., Pierce, S.D., Cowles, T.J., 2005. Mesoscale structure and its seasonal evolution in
- the northern California Current System, *Deep Sea Res. II*, 52(1–2), 5–28,
- 1747 https://doi.org/10.1016/j.dsr2.2004.09.026.
- 1748 Barth, J.A., 2007. Upwelling, In "Encyclopedia of Tidepools and Rocky Shores," M. W. Denny
- and S. G. Gaines (eds.), Univ. of Calif. Press, CA, pp. 609–613.
- 1750 Barth, J.A., Cowles, T.J., Kosro, P.M. Shearman, R.K., Huyer, A., Smith, R.L., 2002. Injection
- of carbon from the shelf to offshore beneath the euphotic zone in the California Current. *J.*
- 1752 *Geophys. Res.*, 107(C6), 3057, https://doi.org/10.1029/2001JC000956.

- Batteen, M.L., 1997. Wind-forced modeling studies of currents, meanders, and eddies in the
- 1754 California Current system, J. Geophys. Res., 102(C1), 985–1010,
- 1755 https://doi.org/10.1029/96JC02803.
- Batten, S.D., Crawford, W.R., 2005. The influence of coastal origin eddies on oceanic plankton
- distributions in the eastern Gulf of Alaska. *Deep Sea Res. II*, 52, 991–1009,
- 1758 https://doi.org/10.1016/j.dsr2.2005.02.009.
- 1759 Belkin, I.M., Cornillon, P.C., Sherman, K., 2009. Fronts in large marine ecosystems, *Prog.*
- 1760 Oceanogr., 8(1–4), 223-236, https://doi.org/10.1016/j.pocean.2009.04.015.
- 1761 Bennett, E.B., 1959. Some Oceanographic Features of the Northeast Pacific Ocean during
- 1762 August 1955. J. Fish. Res. Board of Canada. 16(5), 565–633, https://doi.org/10.1139/f59-
- **1763** 047.
- 1764 Bernstein, R.L., 1974. Mesoscale ocean eddies in the North Pacific: Westward
- propagation. *Science*, 183(4120), 71–72, https://doi.org/10.1126/science.183.4120.71.
- Bernstein, R.L., White, W.B., 1977. Zonal variability in the distribution of eddy energy in the
- mid-latitude North Pacific Ocean. J. Phys. Oceanogr., 7(1), 123–126,
- 1768 https://doi.org/10.1175/1520-0485(1977)007<0123:ZVITDO>2.0.CO;2.
- Bishop, S.P., Watts, D.R., Donohue, K.A., 2013. Divergent eddy heat fluxes in the Kuroshio
- 1770 Extension at 144°–148°E. Part I: Mean structure. *J. Phys. Oceanogr.*, 43(8), 1533–1550,
- 1771 https://doi.org/10.1175/JPO-D-12-0221.1.
- 1772 Bishop, S., Watts, D.R., 2014. Rapid eddy-Induced modification of subtropical mode water
- during the Kuroshio Extension System study. *J. Phys, Oceanogr.*, 44, 1941-1953.
- 1774 https://doi.org/10.1175/JPO-D-13-0191.1.
- Bond, N.A., Cronin, M.F., Freeland, H., Mantua, N., 2015. Causes and impacts of the 2014
- warm anomaly in the NE Pacific, Geophys. Res. Lett., 42, 3414–3420,
- 1777 https://doi.org/10.1002/2015GL063306.
- Bower, A.S., Rossby, H.T., Lillibridge, J.L., 1985. The Gulf Stream—Barrier or Blender? J.
- 1779 *Phys. Oceanogr.*, 15(1), 24–32, https://doi.org/10.1175/1520-
- 1780 0485(1985)015<0024:TGSOB>2.0.CO;2.

- Brown, M.T., Lippiatt, S.M., Lohan, M.C., Bruland, K.W., 2012. Trace metal distributions
- within a Sitka eddy in the northern Gulf of Alaska. *Limnol. Oceanogr.*, 57, 503–518,
- 1783 https://doi.org/10.4319/lo.2012.57.2.0503.
- Brown, S.L., Landry, M.R., Selph, K.E., Yang, E.J., Rii, Y.M., Bidigare, R.R., 2008. Diatoms
- in the desert: Plankton community response to a mesoscale eddy in the subtropical North
- 1786 Pacific. Deep Sea Res. II, 55(10–13), 1321–1333, https://doi.org/10.1016/j.dsr2.2008.02.012.
- Budyansky, M.V., Goryachev, V.A., Kaplunenko, D.D., Lobanov, V.B., Prants, S.V., Sergeev,
- 1788 A.F., Shlyk, N.V., Uleysky, M.Yu., 2015. Role of mesoscale eddies in transport of
- Fukushima-derived cesium isotopes in the ocean, *Deep Sea Res. I*, 96, 15–27,
- 1790 https://doi.org/10.1016/j.dsr.2014.09.007.
- 1791 Budyansky, M.V. Prants, S.V., Uleysky, M.Yu., 2022. Odyssey of Aleutian eddies, *Ocean*
- 1792 *Dynamics*, 72, 455–476, https://doi.org/10.1007/s10236-022-01508-w.
- 1793 Bulatov, N.V. Lobanov V.B., 1983. Investigation of mesoscale eddies to the east of the Kuril
- 1794 Islands on the base of meteorological satellites data. *Issled. Zemli iz kosmosa (Earth*
- 1795 Research from Space), 3, 40–47 (in Russian, with English Abstr.).
- 1796 Bulatov, N.V., Kurennaya, L.A., Muktepavel, L.S., Aleksanina, M.G., Herbeck, F.F., 1999.
- 1797 Eddy water structure in the southern Okhotsk Sea and its seasonal variability (results of
- 1798 satellite monitoring). *Oceanology*, 1999, 39(1), 29–37.
- Burkholder, K., Lozier, M., 2011. Subtropical to subpolar pathways in the North Atlantic:
- Deductions from Lagrangian trajectories. J. Geophys. Res., 116, C07017,
- 1801 https://doi.org/10.1029/2010JC006697.
- Burkholder, K.C., Lozier, M.S., 2014. Tracing the pathways of the upper limb of the North
- 1803 Atlantic Meridional Overturning Circulation. Geophys. Res, Lett., 41(12), 4254–4260,
- 1804 https://doi.org/10.1002/2014GL060226.
- 1805 Calil, P.H.R., Richards, K.J., Jia, Y., Bidigare, R.R., 2008. Eddy activity in the lee of the
- 1806 Hawaiian islands, *Deep Sea Res. II*, 55(10–13), 1179–1194,
- 1807 https://doi.org/10.1016/j.dsr2.2008.01.008.

- 1808 Calil, P.H.R., Richards, K.J., 2010. Transient upwelling hot spots in the oligotrophic North
- Pacific. J. Geophys, Res., 115, C02003, https://doi.org/10.1029/2009JC005360.
- 1810 Capone, D.G., Hutchins, D.A., 2013. Microbial biogeochemistry of coastal upwelling regimes
- in a changing ocean. *Nature Geosci.*, 6, 711–717, https://doi.org/10.1038/ngeo1916.
- 1812 Cedarholm, E., Rypina, I. I., Macdonald A., Yoshida, S., 2019. Investigating subsurface
- pathways of Fukushima-derived Cesium in the Northwest Pacific. *Geophys. Res. Letters*, 46,
- 1814 6821–6829, https://doi.org/10.1029/2019GL082500.
- 1815 Chaigneau, A., Eldin, G., Dewitte B., 2009. Eddy activity in the four major upwrelling systems
- 1816 from satellite altimetry (1992-2007), *Prog. Oceanogr.*, 83(1–4), 117–123,
- 1817 https://doi.org/10.1016/j.pocean.2009.07.012.
- 1818 Chan, F., Barth, J.A., Blanchette, C.A., Byrne, R.H., Chavez, F., Cheriton, O., Feely, R.A.,
- Friederich, G., Gaylord, B., Gouhier, T., Hacker, S., Hill, T., Hofmann, G., McManus, M.A.,
- Menge, B.A., Nielsen, K.J., Russell, A., Sanford, E., Sevadjian, J., Washburn, L., 2017.
- Persistent spatial structuring of coastal ocean acidification in the California Current
- 1822 System. Sci. Rep., 7, 2526, https://doi.org/10.1038/s41598-017-02777-y.
- 1823 Chang, K.-I., Teague, W.J., Lyu, S.J., Perkins, H.T., Lee, D.-K., Watts, D.R., Kim, Y.-B.,
- Mitchell, D.A., Lee, C.M., Kim, K., 2004. Circulation and currents in the southwestern
- East/Japan Sea: Overview and review. *Prog. Oceanogr.*, 61, 105–156,
- 1826 https://doi.org/10.1016/j.pocean.2004.06.005.
- 1827 Chang, Y.-L., Oey, L.-Y., 2014. Instability of the North Pacific Subtropical Countercurrent. J.
- 1828 *Phys. Oceanogr.*, 44, 818–833, https://doi.org/10.1175/JPO-D-13-0162.1.
- 1829 Chang, Y.-L., Miyazawa, Y., Guo, X., 2015. Effects of the STCC eddies on the Kuroshio based
- on the 20-year JCOPE2 reanalysis results, *Prog. Oceanogr.*, 135, 64–76,
- 1831 https://doi.org/10.1016/j.pocean.2015.04.006.
- 1832 Chang, Y.-L., Miyazawa, Y., Oey, L.-Y., Kodaira, T., Huang S., 2017. The formation processes
- of phytoplankton growth and decline in mesoscale eddies in the western North Pacific
- 1834 Ocean, J. Geophys. Res., 122, 4444–4455, https://doi.org/10.1002/2017JC012722.

- 1835 Chang, Y.-L., Miyazawa, Y., Béguer-Pon, M., Han, Y.-S., Ohashi, K., Sheng, J., 2018. Physical
- and biological roles of mesoscale eddies in Japanese eel larvae dispersal in the western
- North Pacific Ocean. Sci. Rep., 8, 5013. https://doi.org/10.1038/s41598-018-23392-5
- 1838 Checkley, D.M., Dotson, R.C., Griffith D.A., 2000. Continuous, underway sampling of eggs of
- Pacific sardine (Sardinops sagax) and northern anchovy (Engraulis mordax) in spring 1996
- and 1997 off southern and central California. Deep Sea Res. II, 47, 1139–1155,
- 1841 https://doi.org/10.1016/S0967-0645(99)00139-3.
- 1842 Checkley, D., Barth J.A., 2009. Patterns and processes in the California Current System. *Prog.*
- 1843 *Oceanogr.*, 83, 49–64, https://doi.org/10.1016/j.pocean.2009.07.028.
- 1844 Chelton, D.B., Schlax, M.G., Samelson, R.M., de Szoeke, R.A., 2007. Global observations of
- large oceanic eddies. Geophys. Res. Lett. 34, L15606,
- 1846 https://doi.org/10.1029/2007GL030812.
- 1847 Chelton, D.B., Gaube, P., Schlax, M.G., Early, J.J., Samelson, R.M., 2011a. The influence of
- nonlinear mesoscale eddies on near-surface oceanic chlorophyll. *Science* 334, 328–332,
- 1849 https://doi.org/10.1126/science.1208897.
- 1850 Chelton, D.B., Schlax, M.G., Samelson, R.M., 2011b. Global observations of nonlinear
- mesoscale eddies. *Prog. Oceanogr.*, 91, 167–216.
- https://doi.org/10.1016/j.pocean.2011.01.002
- 1853 Chen, R., McClean, J.L., Gille, S.T., Griesel, A., 2014. Isopycnal Eddy Diffusivities and
- 1854 Critical Layers in the Kuroshio Extension from an Eddying Ocean Model. *J. Phys.*
- 1855 Oceanogr., 44(8), 2191–2211, https://doi.org/10.1175/JPO-D-13-0258.1.
- 1856 Cheng, Y., Ho, C., Zheng, Q., Kuo, N., 2014. Statistical Characteristics of Mesoscale Eddies in
- the North Pacific Derived from Satellite Altimetry. *Remote Sensing*, 6, 5164-5183,
- 1858 https://doi.org/10.3390/rs6065164.
- 1859 Chenillat, F., Rivière, P., Capet, X., Franks, P.J.S., B. Blanke, 2013. California coastal
- upwelling onset variability: Cross-shore and bottom-up propagation in the planktonic
- ecosystem, *PLoS One*, 8(5), e62281, https://doi.org/10.1371/journal.pone.0062281.

- 1862 Chenillat, F., Franks, P.J.S., Combes, V., 2016. Biogeochemical properties of eddies in the
- 1863 California Current System. *Geophys. Res. Lett.*, 43, 5812–5820,
- https://doi.org/10.1002/2016GL068945.
- 1865 Chenillat, F., Franks, P.J.S., Capet, X., Rivière, P., Grima, N., Blanke, B., Combes, V., 2018.
- Eddy properties in the Southern California Current System. *Ocean Dynamics*, 68, 761–777,
- 1867 https://doi.org/10.1007/s10236-018-1158-4.
- 1868 Cheon, W.G., Park, Y.-G. Yeh, S.-W., Kim, B.-M., 2012. Atmospheric impact on the
- northwestern Pacific under a global warming scenario, *Geophys. Res. Lett.*, 39, L16709,
- 1870 https://doi.org/10.1029/2012GL052364.
- 1871 Chereskin, T.K., Morris, M.Y., Niiler, P.P., Kosro, P.M., Smith, R.L., Ramp, S.R. Collins, C.A.
- Musgrave D.L., 2000. Spatial and temporal characteristics of the mesoscale circulation of
- the California Current from eddy-resolving moored and shipboard measurements, *J.*
- 1874 *Geophys. Res.*, 105(C1), 1245–1269, https://doi.org/10.1029/1999jc900252.
- 1875 Chhak, K., Di Lorenzo, E., 2007. Decadal variations in the California Current upwelling cells.
- 1876 Geophys. Res. Lett., 34, L14604, https://doi.org/10.1029/2007GL030203
- 1877 Chhak, K.C., Di Lorenzo, E., Schneider, N., Cummins, P.F., 2009. Forcing of Low-Frequency
- Ocean Variability in the Northeast Pacific. *J. Climate*, 22(5) 1255–1276,
- 1879 https://doi.org/10.1175/2008jcli2639.1.
- 1880 Chuang, W.-S., Li, H.-W., Tang, T., Wu, C.-K., 1993. Observations of the countercurrent on the
- inshore side of the Kuroshio northeast of Taiwan. *J. Oceanogr.* 49(5), 581–592.
- 1882 https://doi.org/10.1007/BF02237464.
- 1883 Collins, C.A., Margolina, T., Rago, T.A., Ivanov, L., 2013. Looping RAFOS floats in the
- California Current System, Deep Sea Res. II, 85, 42–61,
- 1885 https://doi.org/10.1016/j.dsr2.2012.07.027.
- 1886 Combes, V., Chenillat, F., Di Lorenzo, E., Rivière, P., Ohman M.D., Bograd, S.J., 2013. Cross-
- shore transport variability in the California Current: Ekman upwelling vs. eddy dynamics.
- 1888 *Prog. Oceanogr.*, 109, 78–89, https://doi.org/10.1016/j.pocean.2012.10.001.

- 1889 Combes, V., Di Lorenzo, E., Curchitser, E., 2009. Interannual and decadal variations in cross-
- shelf transport in the Gulf of Alaska. J. Phys. Oceanogr., 39(4), 1050–1059,
- 1891 https://doi.org/10.1175/2008JPO4014.1.
- 1892 Cotté, C., Park, Y-H., Guinet, C., Bost, C-A., 2007. Movements of foraging king penguins
- through marine mesoscale eddies. *Proc. R. Soc. B*, 274, 2385–2391,
- http://doi.org/10.1098/rspb.2007.0775.
- 1895 Cotté, C., d'Ovidio, F., Dragon, A.-C., Guinet, C., Lévy, M., 2015. Flexible preference of
- southern elephant seals for distinct mesoscale features within the antarctic circumpolar
- current. *Prog. Oceanogr.*, 131, 46–58. https://doi.org/10.1016/j.pocean.2014.11.011.
- 1898 Crawford, W.R., Thomson, R.E., 1991. Physical oceanography of the western Canadian
- 1899 continental shelf. Cont. Shelf Res., 11(8–10), 669–683, https://doi.org/10.1016/0278-
- 1900 4343(91)90073-F.
- 1901 Crawford, W.R., Cherniawsky, J.Y., Foreman, M.G.G., 2000. Multi-year meanders and eddies
- in Alaskan Stream as observed by TOPEX/Poseidon altimeter. *Geophys. Res. Lett.* 27, 1025–
- 1903 1028, https://doi.org/10.1029/1999GL002399.
- 1904 Crawford, W.R., 2002. Physical characteristics of Haida Eddies. J. Oceanogr., 58, 703–713,
- 1905 https://doi.org/10.1023/A:1022898424333.
- 1906 Crawford, W.R., Cherniawsky, J.Y., Foreman, M.G.G., Gower, J.F.R., 2002. Formation of the
- Haida-1998 oceanic eddy. J. Geophysical Research 107, C7, 3069,
- 1908 https://doi.org/10.1029/2001JC000876.
- 1909 Crawford, W.R., 2005. Heat and fresh water transport by eddies into the Gulf of Alaska. Deep-
- 1910 *Sea Res. II* 52(7–8), 893–908, https://doi.org/10.1016/j.dsr2.2005.02.003.
- 1911 Crawford, W.R., Brickley, P.J., Peterson, T.D., Thomas, A.C., 2005. Impact of Haida Eddies on
- chlorophyll distribution in the Eastern Gulf of Alaska. *Deep Sea Res. II*, 52(7–8), 975–989,
- 1913 https://doi.org/10.1016/j.dsr2.2005.02.011.
- 1914 Crawford, W.R., Brickley, P.J., Thomas, A.C., 2007. Mesoscale eddies dominate surface
- 1915 phytoplankton in northern Gulf of Alaska. *Prog. Oceanogr.*, 75(2), 287–303,
- 1916 https://doi.org/10.1016/j.pocean.2007.08.016.

- 1917 Crusius, J., Schroth, A.W., Resing, J.A., Cullen, J., Campbell, R.W., 2017. Seasonal and spatial
- variabilities in northern Gulf of Alaska surface water iron concentrations driven by shelf
- sediment resuspension, glacial meltwater, a Yakutat eddy, and dust. Global Biogeochem.
- 1920 *Cycles*, 31, 942–960, https://doi.org/10.1002/2016GB005493.
- 1921 Cullen, J.T., Chong, M., Ianson D., 2009. British Columbian continental shelf as a source of
- dissolved iron to the subarctic northeast Pacific Ocean. *Global Biogeochem. Cycles*, 23,
- 1923 GB4012, https://doi.org/10.1029/2008GB003326.
- 1924 Danchenkov, M.A., Lobanov, V.B., Riser, S.C., Kim, K., Takematsu, M., Yoon, J.-H., 2006. A
- history of physical oceanographic research in the Japan/East Sea. *Oceanogr.*, 19(3), 18–31,
- 1926 https://doi.org/10.5670/oceanog.2006.41.
- 1927 Dantzler, H.L., 1976.. Geographic variations in intensity of the North Atlantic and North Pacific
- oceanic eddy fields. In Deep Sea Res. Oceanogr. Abst., 23(9), 783–794,
- 1929 https://doi.org/10.1016/0011-7471(76)90846-9.
- 1930 Davis, A., Di Lorenzo, E., 2015. Interannual forcing mechanisms of California Current
- transports I: Meridional Currents. *Deep Sea Res. II*, 112, 18–30,
- 1932 https://doi.org/10.1016/j.dsr2.2014.02.005.
- 1933 Denman, K.L., Mackas, D.L., Freeland, H.J., Austin, M.J. and Hill, S.H., 1981. Persistent
- upwelling and mesoscale zones of high productivity off the west coast of Vancouver Island,
- 1935 Canada. *Coastal upwelling*, 1, pp.514–521, https://doi.org/10.1029/CO001p0514.
- 1936 Deutsch, C., Ferrel, A., Seibel, B., Pörtner, H.-O., Huey, R.B., 2015. Climate change tightens a
- metabolic constraint on marine habitats. *Science*, 348, 1132–1135,
- 1938 https://doi.org/10.1126/science.aaa1605.
- 1939 Di Lorenzo, E., Foreman, M.G.G., Crawford, W.R., 2005. Modelling the generation of Haida
- 1940 Eddies. *Deep Sea Res.t II* 52(7–8), 853–873, https://doi.org/10.1016/j.dsr2.2005.02.007.
- 1941 Di Lorenzo, E., Schneider, N., Cobb, K.M., Franks, P.J.S., Chhak, K., Miller, A.J., McWilliams,
- 1942 A.C., Bograd, S.J., Arango, H., Curchitser, E., Powell T.M., Riviere P., 2008. North Pacific
- 1943 Gyre Oscillation links ocean climate and ecosystem change. *Geophys. Res. Lett.*, 35,
- 1944 L08607, https://doi.org/10.1029/2007gl032838

- 1945 Di Lorenzo, E., Fiechter, J., Schneider, N., Bracco, A., Miller, A.J., Franks, P.J.S., Bograd, S.J.,
- Moore, A.M., Thomas, A.C., Crawford, W., Pena A., Hermann A.J., 2009. Nutrient and
- salinity decadal variations in the central and eastern North Pacific. *Geophys. Res. Lett.*, 36,
- 1948 L14601, https://doi.org/10.1029/2009gl038261.
- 1949 Di Lorenzo, E., Mountain, D., Batchelder, H.P., Bond N., Hofmann E.E., 2013a. Advances in
- 1950 Marine Ecosystem Dynamics from US GLOBEC The Horizontal-Advection Bottom-up
- Forcing Paradigm. *Oceanogr.*, 26(4) 22–33, https://doi.org/10.5670/oceanog.2013.73.
- 1952 Di Lorenzo, E., Combes, V., Keister, J.E., Strub, P.T., Tomas, A.C., Franks, P.J.S., Ohman,
- 1953 M.D., Furtado, J.C., Bracco, A., Bograd, S.J., Peterson, W.T., Schwing, F.B., Chiba, S.,
- Taguchi, B., Hormazabal, S. Parada C., 2013b. Synthesis of Pacific Ocean climate and
- 1955 ecosystem dynamics. *Oceanogr.* 26(4), 68–81, https://doi.org/10.5670/oceanog.2013.76.
- 1956 Di Lorenzo, E., Mantua, N., 2016. Multi-year persistence of the 2014/15 North Pacific marine
- heatwave, *Nat. Clim. Change*, 6, 1042–1047, https://doi.org/10.1038/NCLIMATE3082
- Ding, M., Lin, P., Liu, H., Chai, F., 2018, Increased Eddy Activity in the Northeastern Pacific
- during 1993–2011. J. Climate, 31, 387–399, https://doi.org/10.1175/JCLI-D-17-0309.1
- 1960 Dobashi, R., Ueno, H., Okada, Y., Tanaka, T., Nishioka, J., Hirawake, T., Ooki, A., Itoh, S.,
- Hasegawa, D., Sasai, Y., Sasaki, H., Yasuda, I., 2021. Observations of anticyclonic eddies in
- the western subarctic North Pacific. J. Oceanogr., 77, 229–242,
- 1963 https://doi.org/10.1007/s10872-020-00586-y.
- Dong, D., Brandt, P., Chang, P., Schütte, F., Yang, X., Yan, J., Zeng, J., 2017. Mesoscale eddies
- in the Northwestern Pacific Ocean: Three-dimensional eddy structures and heat/salt
- 1966 transports. J. *Geophys. Res.*, 122, 9795–9813. https://doi.org/10.1002/2017JC013303.
- Ducet, N., Le Traon, P.-Y., 2001. A comparison of surface eddy kinetic energy and Reynolds
- stresses in the Gulf Stream and the Kuroshio Current Systems from merged
- 1969 TOPEX/Poseidon and ERS-1/2 altimetric data. *J. Geophys. Res.*, 106(C8), 16603–16622,
- 1970 https://doi.org/10.1029/2000JC000205.
- 1971 Ebuchi, N. Hanawa, K., 2000. Mesoscale eddies observed by TOLEX-ADCP and
- TOPEX/POSEIDON altimeter in the Kuroshio recirculation region south of Japan, J.
- 1973 *Oceanogr.*, 56, 43–57, https://doi.org/10.1023/A:1011110507628.

- 1974 Emery, W.J., 1983. On the geographical variability of the upper level mean and eddy fields in
- the North Atlantic and North Pacific. J. Phys. Oceanogr., 13(2), 269–291,
- 1976 https://doi.org/10.1175/1520-0485(1983)013<0269:OTGVOT>2.0.CO;2.
- 1977 Falkowski, P., Ziemann, D., Kolber, Z., Bienfang, P., 1991. Role of eddy pumping in enhancing
- primary production in the ocean, *Nature*, 352, 55–58, https://doi.org/10.1038/352055a0.
- 1979 FAO. 2019. FAO yearbook. Fishery and Aquaculture Statistics 2017/FAO annuaire. Statistiques
- des pêches et de l'aquaculture 2017/FAO anuario. Estadísticas de pesca y acuicultura 2017.
- 1981 Rome/Roma.
- Fayman, P., Ostrovskii, A., Lobanov, V., Park, J.-H., Park, Y.-G., Sergeev, A., 2019a.
- Submesoscale eddies in Peter the Great Bay of the Japan/East Sea in winter. *Ocean*
- 1984 *Dynamics*, 69, 443–462, https://doi.org/10.1007/s10236-019-01252-8.
- 1985 Fayman, P.A., Prants, S.V., Budyansky, M.V., Uleysky, M.Y., 2019b. Coastal summer eddies
- in the Peter the Great Bay of the Japan Sea: *In situ* data, numerical modeling and Lagrangian
- analysis. Cont. Shelf Res., 181, 143–155. https://doi.org/10.1016/j.csr.2019.05.002.
- 1988 Ferrari, R., Nikurashin, M., 2010. Suppression of Eddy Diffusivity across Jets in the Southern
- 1989 Ocean. J. Phys. Oceanogr., 40, 1501–1519, https://doi.org/10.1175/2010JPO4278.1.
- 1990 Fiechter, J. Moore, A.M., 2012. Iron limitation impact on eddy-induced ecosystem variability in
- 1991 the coastal Gulf of Alaska. J. Mar. Sys., 92(1), 1–15,
- 1992 https://doi.org/10.1016/j.jmarsys.2011.09.012.
- Fong, A.A., Karl, D.M., Lukas, R., Letelier, R.M., Zehr, J.P., Church, M.J., 2008. Nitrogen
- fixation in an anticyclonic eddy in the oligotrophic North Pacific Ocean. ISME J., 2, 663–
- 1995 676, https://doi.org/10.1038/ismej.2008.22.
- 1996 Fox, H.E., Haisfield, K.M., Brown, M.S., Stevenson, T.C., Tissot, B.N., Walsh, W.J., Williams,
- 1997 I.D., 2012. Influences of oceanographic and meteorological features on reef fish recruitment
- in Hawai'i. *Mar. Ecol. Prog. Ser.*, 463, 259–272, http://www.jstor.org/stable/24876050.
- 1999 Freeland, H.J., 1993. Intense currents in the deep northeast Pacific Ocean. J. Physical
- 2000 Oceanogr., 23(8), 1872–1876, https://doi.org/10.1175/1520-
- 2001 0485(1993)023<1872:ICITDN>2.0.CO;2.

- Frischknecht, M., Münnich, M., Gruber N., 2015. Remote versus local influence of ENSO on
- the California Current System, J. Geophys. Res., 120, 1353–1374,
- 2004 https://doi.org/10.1002/2014JC010531
- 2005 Garfield, N., Collins, C.A., Paquette, R.G., Carter E., 1999. Lagrangian Exploration of the
- 2006 California Undercurrent, 1992–95, *J. Phys. Oceanogr.*, 29(4), 560–583,
- 2007 https://doi.org/10.1175/1520-0485(1999)029<0560:Leotcu>2.0.Co;2.
- 2008 Garraffo, Z.D., Kim, H.-C., Mehra, A., Spindler, T., Rivin, I., Tolman, H.L., 2014. Modeling of
- 2009 137Cs as a Tracer in a Regional Model for the Western Pacific, after the Fukushima–Daiichi
- Nuclear Power Plant Accident of March 2011. Weather and Forecasting, 31(2), 553–579,
- 2011 https://doi.org/10.1175/WAF-D-13-00101.1.
- Gaube, P., McGillicuddy, D.J., Chelton, D.B., Behrenfeld, M.J., Strutton P.G., 2014. Regional
- variations in the influence of mesoscale eddies on near-surface chlorophyll, *J. Geophys*.
- **2014** *Res.*, 119, https://doi.org/10.1002/2014JC010111.
- Gaube, P., Chelton D.B., Samelson, R.M., Schlax, M.G., O'Neill, L.W., 2015. Satellite
- observations of mesoscale eddy-induced Ekman pumping. J. Phys. Oceanogr. 45, 104–32,
- 2017 https://doi.org/10.1175/JPO-D-14-0032.1.
- 2018 Gaughan, D.J., 2007. Potential mechanisms of influence of the Leeuwin Current eddy system on
- teleost recruitment to the Western Australian continental shelf, *Deep Sea Res. II*, 54(8-10),
- 2020 1129–1140, https://doi.org/10.1016/j.dsr2.2006.06.005.
- Gill, A.E., Green, J.S.A., Simmons, A.J., 1974. Energy partition in the large-scale ocean
- circulation and the production of mid-ocean eddies. *Deep Sea Res. Oceanogr. Abst.*, 21,
- 2023 499–528, https://doi.org/10.1016/0011-7471(74)90010-2.
- Gong, G.-C., Shiah, F.-K., Liu, K.-K., Chuang, W.-S., Chang, J., 1997. Effect of the Kuroshio
- intrusion on the chlorophyll distribution in the southern East China Sea during spring 1993,
- 2026 Cont. Shelf Res., 17, 79–94, https://doi.org/10.1016/0278-4343(96)00022-2.
- Gower, J.F.R., 1989, Geosat altimeter observations of the distribution and movement of sea-
- surface height anomalies in the north-east Pacific. Oceans 89: the global ocean. Institute of
- Electrical and Electronics Engineers, Seattle, Washington, pp. 977–981.

- 2030 Gower, J.F.R., S. Tabata, S., 1993. Measurement of eddy motion in the north-east Pacific using
- the Geosat altimeter. p. 375–382. In Satellite Remote Sensing of the Oceanic Environment,
- ed. by I.S.F. Jones, Y. Sugimori and R. W. Stewart, Seibutsu Kenkyusha, Tokyo.
- 2033 Gruber, N., Frenzel, H., Doney, S.C., Marchesiello, P., McWilliams, J.C., Moisan, J.R., Oram,
- J., Plattner, G.-K., Stolzenbach, K.D., 2006. Eddy-resolving simulation of plankton
- ecosystem dynamics in the California Current System. *Deep Sea Res. I* 53(9), 1483–1516,
- 2036 https://doi.org/10.1016/j.dsr.2006.06.005
- 2037 Gruber, N., Hauri, C., Lachkar, Z., Loher, D., Frölicher, T.L., Plattner, G.-K., 2012. Rapid
- progression of ocean acidification in the California Current System. *Science*, 337, 6091,
- 2039 220–223, https://doi.org/10.1126/science.1216773.
- 2040 Gruber, N., Lachkar, Z., Frenzel, H., Marchesiello, P., Münnich, M., McWilliams, J.C., Nagai,
- T., Plattner, G.-K., 2011. Eddy-induced reduction of biological production in eastern
- boundary upwelling systems, *Nature Geosci.*, 4, 787–792, https://doi.org/10.1038/ngeo1273.
- Guidi, L., Calil, P.H., Duhamel, S., Björkman, K.M., Doney, S.C., Jackson, G.A., Li, B.,
- Church, M.J., Tozzi, S., Kolber, Z.S., Richards, K.J., Fong, A.A., Letelier, R.M., Gorsky, G.,
- Stemmann, L., Karl, D.M., 2012. Does eddy-eddy interaction control surface phytoplankton
- distribution and carbon export in the North Pacific Subtropical Gyre? J. Geophys. Res., 117,
- 2047 G02024, https://doi.org/10.1029/2012JG001984.
- Hasegawa, D., Matsuno, T., Tsutsumi, E., Senjyu, T., Endoh, T., Tanaka, T., Yoshie, N.,
- Nakamura, H., Nishina, A., Kobari, T., Nagai, T, Guo, X., 2021. How a small reef in the
- Kuroshio cultivates the ocean. *Geophys. Res. Lett.*, 48, e2020GL092063.
- 2051 https://doi.org/10.1029/2020GL092063.
- 2052 Hayward, T.L., Venrick, E.L., 1998. Nearsurface pattern in the California Current: coupling
- between physical and biological structures. Deep Sea Res. II, 45, 1617–1638,
- 2054 https://doi.org/10.1016/S0967-0645(98)80010-6.
- Healey, M.C, Thomson, K.A, Leblond, P.H, Huato, L., Hinch, S.G. and Walters C.J., 2000.
- 2056 Computer simulations of the effects of the Sitka eddy on the migration of sockeye salmon
- returning to British Columbia. Fish. Oceanogr., 9: 271–281, https://doi.org/10.1046/j.1365-
- **2058** 2419.2000.00135.x.

- Henson, S.A., Thomas, A.C., 2008. A census of oceanic anticyclonic eddies in the Gulf of
- 2060 Alaska. *Deep-Sea Res. I*, 55, 163–176. http://doi.org/10.1016/j.dsr.2007.11.005.
- Hirahara, S., Ishii, M., Fukuda, Y., 2014. Centennial-scale sea surface temperature analysis and
- its uncertainty, *J. Clim.*, 27, 57–75, https://doi.org/10.1175/JCLI-D-12-00837.1.
- Holloway, G., 1986. Estimation of oceanic eddy transports from satellite altimetry. *Nature*, 323,
- 2064 243–244, https://doi.org/10.1038/323243a0.
- Honda, M.C., Sasai, Y., Siswanto, E., Kuwano-Yoshida, A., Aiki, H., Cronin, M.F., 2018.
- Impact of cyclonic eddies and typhoons on biogeochemistry in the oligotrophic ocean based
- on biogeochemical/physical/meteorological time-series at station KEO. *Prog. Earth Planet.*
- 2068 Sci. 5, 42, https://doi.org/10.1186/s40645-018-0196-3.
- Hsu, S.-C., Lin, F.-J., Jeng, W.-L., Tang, T.-Y., 1998. The effect of a cyclonic eddy on the
- distribution of lithogenic particles in the southern East China Sea, J. Marine Res., 56, 813–
- 2071 832, https://doi.org/10.1357/002224098321667387.
- Huntley, M.E., González, A., Zhu1, Y., Zhou, M., Irigoien, X., 2000. Zooplankton dynamics in
- a mesoscale eddy-jet system off California. Mar. Ecol. Prog. Ser. 201, 165–178,
- 2074 https://doi.org/10.3354/meps201165.
- Huppert, H. E., Bryan, K., 1976. Topographically generated eddies. *Deep Sea Res. Oceanogr.*
- 2076 Abst., 23(8), 655–679, https://doi.org/10.1016/S0011-7471(76)80013-7.
- Hurst, M.P., Aguilar-Islas, A.M., Bruland, K.W., 2010. Iron in the southeastern Bering Sea:
- Elevated leachable particulate Fe in shelf bottom waters as an important source for surface
- 2079 waters. Cont. Shelf Res. 30, 467–480, http://doi.org/10.1016/j.csr.2010.01.001.
- Huyer, A., Barth, J.A., Kosro, P. M., Shearman, R. K., Smith R.L., 1998. Upper-ocean water
- 2081 mass characteristics of the California current, Summer 1993, *Deep Sea Res. II*, 45(8–9),
- 2082 1411–1442, https://doi.org/10.1016/s0967-0645(98)80002-7.
- Hwang, J.H., Van, S.P., Choi, B.-J., Chang, Y.S., Kim, Y.H., 2014. The physical processes in
- 2084 the Yellow Sea. *Ocean Coast. Manag.* 102, 449–457.
- 2085 https://doi.org/10.1016/j.ocecoaman.2014.03.026.

- 2086 Ishi, Y., Hanawa, K., 2005. Large-scale variabilities of wintertime wind stress curl field in the
- North Pacific and their relation to atmospheric teleconnection patterns. *Geophys. Res. Lett.*,
- 2088 32, L10607, http://doi.org/10.1029/2004gl022330.
- 2089 Isoguchi, O., Kawamura, H., 2003. Eddies advected by time-dependent Sverdrup circulation in
- the western boundary of the subarctic North Pacific. Geophys. Res. Lett. 30(15), 1794,
- 2091 https://doi.org/10.1029/2003gl017652.
- 2092 Itoh, S., Rudnick, D.L., 2017. Fine-scale variability of isopycnal salinity in the California
- 2093 Current System, *J. Geophys. Res.*, 122, 7066-7081, https://doi.org/10.1002/2017jc013080.
- 2094 Itoh, S., Yasuda, I., 2010a. Characteristics of mesoscale eddies in the Kuroshio Oyashio
- Extension region detected from the distribution of the sea surface height anomaly. *J. Phys.*
- 2096 Oceanogr., 40, 1018–1034. https://doi.org/10.1175/2009JPO4265.1.
- 2097 Itoh, S., Yasuda, I., 2010b. Water mass structure of warm and cold anticyclonic eddies in the
- western boundary region of the Subarctic North Pacific. J. Phys. Oceanogr., 40, 2624–2642.
- 2099 https://doi.org/10.1175/2010jpo4475.1.
- 2100 Itoh, S., Shimizu, Y., Ito, S., Yasuda, I., 2011. Evolution and decay of a warm-core ring within
- 2101 the western subarctic gyre of the North Pacific, as observed by profiling floats. *J Oceanogr.*,
- 2102 67, 281–293, https://doi.org/10.1007/s10872-011-0027-2
- 2103 Jacox, M.G., Bograd, S.J.. Hazen, E.L., Fiechter, J., 2015. Sensitivity of the California Current
- nutrient supply to wind, heat, and remote ocean forcing. *Geophys. Res. Lett.*, 42, 5950–5957,
- 2105 https://doi.org/10.1002/2015GL065147
- 2106 Jacox, M.G., Hazen, E.L., Zaba, K.D., Rudnick, D.L., Edwards, C.A., Moore, A.M., Bograd,
- 2107 S.J., 2016. Impacts of the 2015–2016 El Niño on the California Current System: Early
- assessment and comparison to past events, *Geophys. Res. Lett.*, 43, 7072–7080,
- 2109 https://doi.org/10.1002/2016GL069716.
- 2110 Jacox, M.G., Edwards, C.A., Hazen, E.L., Bograd S.J., 2018. Coastal Upwelling Revisited:
- Ekman, Bakun, and Improved Upwelling Indices for the U.S. West Coast. J. Geophys. Res,
- 2112 123, 7332–7350, https://doi.org/10.1029/2018JC014187.

- 2113 Janout, M.A., Weingartner, T.J., Okkonen, S.R., Whitledge, T.E. and Musgrave, D.L., 2009.
- Some characteristics of Yakutat Eddies propagating along the continental slope of the
- 2115 northern Gulf of Alaska. *Deep Sea Res. II*, 56(24), 2444–2459,
- 2116 https://doi.org/10.1016/j.dsr2.2009.02.006.
- 2117 Jeong, H.-D., Kwoun, C.-H., Kim, S.-W., Cho, K.-D., 2009. Fluctuation of tidal front and
- expansion of cold water region in the Southwestern Sea of Korea. J. Korean Soc. Mar.
- 2119 Environ. Saf. 15, 289–296 (in Korean, with English Abstr.).
- 2120 Ji, J., Dong, C., Zhang, B., Liu, Y., Zou, B., King, G. P., Xu, G., Chen, D., 2018. Oceanic eddy
- characteristics and generation mechanisms in the Kuroshio Extension region. *J. Geophys.*
- 2122 Res., 123, 8548–8567. https://doi.org/10.1029/2018JC014196.
- Jo, Y-H., Choi, J-G., Park, J., 2017. Physical boundaries of Intrathermocline Ulleung Eddies in
- 2124 the East/Japan Sea, *Deep Sea Res. II*, 143, 15–23, https://doi.org/10.1016/j.dsr2.2016.09.004.
- 2125 Johns, W. E., Lee, T. N., Zhang, D. X., Zantopp, R., Liu, C. T., Yang, Y., 2001. The Kuroshio
- east of Taiwan: Moored transport observations from the WOCE PCM-1 array, *J. Phys.*
- 2127 Oceanogr., 31(4), 1031–1053, https://doi.org/10.1175/1520-
- 2128 0485(2001)031<1031:TKEOTM>2.0.CO;2.
- Johnson, K.W., Miller, L.A., Sutherland, N.E., Wong, C.S., 2005. Iron transport by mesoscale
- 2130 Haida eddies in the Gulf of Alaska. *Deep Sea Res. II*, 52 (7–8), 933–953,
- 2131 https://doi.org/10.1016/j.dsr2.2004.08.017.
- 2132 Kahru, M., Kudela, R.M., Manzano-Sarabia, M., Mitchell B.G., 2012. Trends in the surface
- 2133 chlorophyll of the California Current: Merging data from multiple ocean color satellites.
- 2134 Deep Sea Res. II, 77–80, 89–98, https://doi.org/10.1016/j.dsr2.2012.04.007.
- 2135 Kamidaira, Y., Uchiyama, Y., Mitarai, S., 2017. Eddy-induced transport of the Kuroshio warm
- water around the Ryukyu Islands in the East China Sea. Cont. Shelf Res., 143, 206–218,
- 2137 https://doi.org/10.1016/j.csr.2016.07.004.
- 2138 Kaneko, H., Itoh, S., Kouketsu, S., Okunishi, T., Hosoda, S., Suga, T., 2015. Evolution and
- 2139 modulation of a poleward- propagating anticyclonic eddy along the Japan and Kuril-
- **2140** Kamchatka trenches. *J. Geophys. Res.*, 120, 4418–4440.
- 2141 https://doi.org/10.1002/2014jc010693.

- Kang, J-H., Kim, W-S., Chang, K-I., Noh, J-H., 2004, Distribution of plankton related to the
- 2143 mesoscale physical structure within the surface mixed layer in the southwestern East Sea,
- 2144 Korea, J. Plankton Res., 26(12), 1515–1528, https://doi.org/10.1093/plankt/fbh140.
- 2145 Kasai, A., Kimura, S., Nakata, H., Okazaki, Y., 2002. Entrainment of coastal water into a
- frontal eddy of the Kuroshio and its biological significance. J. Mar. Sys., 37(1–3), 185–198,
- 2147 https://doi.org/10.1016/S0924-7963(02)00201-4.
- 2148 Katsura, S., Ueno, H., Mitsudera, H., Kouketsu, S., 2020. Spatial distribution and seasonality of
- halocline structures in the sub- arctic North Pacific. J. Phys. Oceanogr., 50, 95–109,
- 2150 https://doi. org/10.1175/JPO-D-19-0133.1.
- 2151 Kawabe, M., 1995. Variations of current path, velocity, and volume transport of the Kuroshio in
- relation with the large meander, *J. Phys. Oceanogr.*, 25, 3103–3117,
- 2153 https://doi.org/10.1175/1520-0485(1995)025<3103:VOCPVA>2.0.CO;2.
- Kim, C.K., Chang, K.I., Park, K., Suk, M.S., 2000a. The South Sea circulation of Korea: two-
- dimensional barotropic model. Sea J. Korean Soc. Oceanogr. 5, 226–257. (in Korean, with
- 2156 English Abstr.)
- 2157 Kim, S-W., Saito, S., Ishizaka, J., Isoda, Y., Kishino, M., 2000b. Temporal and Spatial
- Variability of Phytoplankton Pigment Concentrations in the Japan Sea Derived from CZCS
- 2159 Images, J. Oceanogr., 56, 527–538, https://doi.org/10.1023/A:1011148910779.
- 2160 Kim, K.-R., Kim, G., Kim, K., Lobanov, V., Ponomarev, V., Salyuk, A., 2002. A sudden
- bottom-water formation during the severe winter 2000–2001: The case of the East/Japan
- 2162 Sea. Geophys. Res. Lett., 29(8), 1234–1237, https://doi.org/10.1029/2001GL014498.
- Kim, H., Yoo, S., Oh, I.S., 2007. Relationship between phytoplankton bloom and wind stress in
- the sub-polar frontal area of the Japan/East Sea, *J. Mar. Sys.*, 67, 205–216,
- 2165 https://doi.org/10.1016/j.jmarsys.2006.05.016.
- 2166 Kim, D., Yang, E. J., Kim, K. H., Shin, C-W., Park, J., Yoo, S., Hyun, J-H., 2012. Impact of an
- anticyclonic eddy on the summer nutrient and chlorophyll a distributions in the Ulleung
- 2168 Basin, East Sea (Japan Sea). *ICES J. Mar. Sci.*, 69, 23–29,
- 2169 https://doi.org/10.1093/icesjms/fsr178.

- 2170 Kimura, S, Nakata, H, Okazaki, 2000. Biological production in meso-scale eddies caused by
- frontal disturbances of the Kuroshio Extension, *ICES J. Mar. Sci.*, 57, 133–142,
- 2172 https://doi.org/10.1006/jmsc.1999.0564.
- Kinney, J.C., Maslowski, W., Okkonen, S., 2009. On the processes controlling shelf-basin
- exchange and outer shelf dynamics in the Bering Sea. *Deep Sea Res. II*, 56, 1351–1362,
- 2175 http://doi.org/10.1016/j.dsr2.2008.10.023.
- 2176 Kinder, T.H., Coachman, L.K., Galt, J.A., 1975. The Bering Slope Current system. J. Phys.
- 2177 Oceanogr. 5, 231–244, https://doi.org/10.1175/1520-
- 2178 0485(1975)005<0231:TBSCS>2.0.CO;2.
- 2179 Kirwan, A.D., McNally, G.J., Reyna, E., Merrell, W.J., 1978. Near-surface circulation of
- 2180 eastern North Pacific. J. Phys. Oceanogr. 8(6), 937–945, https://doi.org/10.1175/1520-
- 2181 0485(1978)008<0937:TNSCOT>2.0.CO;2.
- 2182 Kishi, M.J., Kashiwai, M., Ware, D.M., Megrey, B.A., Eslinger, D.L., Werner, F.E., Aita, M.N.,
- Azumaya, T., Fujii, M., Hashimoto, S., Huang, D., Iizumi, H., Ishida, Y., Kang, S.,
- Kantakov, G.A., Kim, H., Komatsu, K., Navrotsky, V.V., Smith, S.L., Tadokoro, K., Tsuda,
- A., Yamamura, O., Yamanaka, Y., Yokouchi, K., Yoshie, N., Zhang, J., Zuenko, Y.I.,
- Zvalinsky, V.I., 2007. NEMURO—A lower trophic level model for the North Pacific marine
- 2187 ecosystem, *Ecol. Modell.*, 202, 12–25, https://doi.org/10.1016/j.ecolmodel.2006.08.021.
- 2188 Kitano, K., 1975. Some properties of the warm eddies generated in the confluence zone of the
- 2189 Kuroshio and Oyashio currents. *J. Phys. Oceanogr.* 5, 245–252.
- 2190 https://doi.org/10.1175/1520-0485(1975)005<0245:SPOTWE>2.0.CO;2.
- Kline, T.C., 2010. Stable carbon and nitrogen isotope variation in the northern lampfish and
- Neocalanus, marine survival rates of pink salmon, and meso-scale eddies in the Gulf of
- 2193 Alaska. *Prog. Oceanogr.*, 87, 49–60, https://doi.org/10.1016/j.pocean.2010.09.024.
- 2194 Kobashi, F., Kawamura, H., 2001. Variation of sea surface height at periods of 65–220 days in
- the subtropical gyre of the North Pacific, J. Geophys. Res., 106, 26,817–26,831,
- 2196 https://doi.org/10.1029/2000JC000361.

- 2197 Kobashi, F., Kawamura, H., 2002. Seasonal variation and instability nature of the North Pacific
- Subtropical Countercurrent and the Hawaiian Lee Countercurrent. J. Geophys. Res., 107,
- 2199 3185, https://doi.org/10.1029/2001JC001225.
- 2200 Kobashi, F., and A. Kubokawa, 2012. Review on North Pacific Subtropical Countercurrents and
- Subtropical Fronts: Role of mode waters in ocean circulation and climate. J. Oceanogr., 68,
- 2202 21–43, https://doi.org/10.1007/s10872-011-0083-7.
- 2203 Komatsu, K., Hiroe, Y., Yasuda, I., Kawasaki, K., Joyce, T.M., Bahr, F., Kawasaki, Y., 2004.
- 2204 Hydrographic structure and transport of intermediate water south of Japan. J. Oceanogr.,
- 2205 60(2), 487–503, https://doi.org/10.1023/B:JOCE.0000038062.00146.6c.
- 2206 Kouketsu, S., Yasuda, I., Hiroe, Y., 2005. Observation of frontal waves and associated salinity
- minimum formation along the Kuroshio Extension. J. Geophys. Res., 110, C08011,
- 2208 https://doi.org/10.1029/2004JC002862.
- 2209 Kouketsu, S., Yasuda, I., Hiroe, Y., 2007. Three-dimensional structure of frontal waves and
- associated salinity minimum formation along the Kuroshio Extension. J. Phys.
- 2211 *Oceanogr.*, 37, 644–656, https://doi.org/10.1175/JPO3026.1.
- 2212 Kouketsu, S., Yasuda, I., 2008. Unstable frontal waves along the Kuroshio Extension with low-
- potential vorticity intermediate Oyashio water. J. Phys. Oceanogr., 38, 2308–2321.
- 2214 https://doi.org/10.1175/2008JPO3814.1.
- 2215 Kouketsu, S., Kaneko, H., Okunishi, T., Sasaoka, K., Itoh, S., Inoue, R., Ueno, H., 2015.
- Mesoscale eddy effects on temporal variability of surface chlorophyll a in the Kuroshio
- 2217 Extension, J. Oceanogr., 72, 439–451. https://doi.org/10.1007/s10872-015-0286-4.
- 2218 Kurian, J., Colas, F., Capet, X., McWilliams, J.C., Chelton, D.B., 2011. Eddy properties in the
- 2219 California Current System. J. Geophys. Res., 116, C08027,
- 2220 https://doi.org/10.1029/2010JC006895
- 2221 Kuroda, H., Hirota, Y., Setou, T., Aoki, K., Takahashi, D., Watanabe, T., 2014. Properties of
- winter mixed layer variability on the shelf-slope region facing the Kuroshio—study of Tosa
- Bay, southern Japan. *Ocean Dyn.* 64(1), 47–60. http://doi.org/10.1007/s10236-013-0670-9.

- 2224 Kuroda, H., Yokouchi, K. 2017. Interdecadal decrease in potential fishing areas for Pacific
- saury off the southeastern coast of Hokkaido, Japan. Fish. Oceanogr. 26, 439–454.
- **2226** https://doi.org/10.1111/fog.12207.
- 2227 Kuroda, H., Takasuka, A., Hirota, Y., Kodama, T., Ichikawa, T., Takahashi, D., Aoki, K, Setou,
- T., 2018. Numerical experiments based on a coupled physical-biochemical ocean model to
- study the Kuroshio-induced nutrient supply on the shelf-slope region off the southwestern
- 2230 coast of Japan, *J. Mar. Sys.*, 179, 38–54, https://doi.org/10.1016/j.jmarsys.2017.11.002.
- 2231 Kusakabe, M., Andreev, A., Lobanov, V., Zhabin, I., Kumamoto, Y., Murata, A., 2002. Effects
- of the anticyclonic eddies on water masses, chemical parameters and chlorophyll
- distributions in the Oyashio current region. J. Oceanogr., 58, 691–701,
- 2234 https://doi.org/10.1023/a:1022846407495.
- 2235 Ladd, C., Kachel, N.B., Mordy, C.W., Stabeno, P.J., 2005a. Observations from a Yakutat eddy
- in the northern Gulf of Alaska. J. Geophys. Res., 110, C03003,
- 2237 http://doi.org/10.1029/2004JC002710.
- 2238 Ladd, C., Stabeno, P., Cokelet, E.D., 2005b. A note on cross-shelf exchange in the northern
- **2239** Gulf of Alaska. *Deep-Sea Res. II* 52, 667–679.
- 2240 Ladd, C., 2007. Interannual variability of the Gulf of Alaska eddy field. Geophys. Res. Lett., 34,
- 2241 L11605.
- 2242 Ladd, C., Mordy, C.W., Kachel, N.B., Stabeno, P.J., 2007. Northern Gulf of Alaska eddies and
- associated anomalies. Deep Sea Res. I, 54, 487–509. http://doi.
- **2244** org/10.1016/j.dsr.2007.01.006.
- Ladd, C., Crawford, W.R., Harpold, C.E., Johnson, W.K., Kachel, N.B., Stabeno, P.J., Whitney,
- F., 2009. A synoptic survey of young mesoscale eddies in the Eastern Gulf of Alaska. *Deep*
- 2247 Sea Res. II, 56, 2460–2473. http://doi.org/10.1016/j.dsr2.2009.02.007.
- 2248 Ladd, C., Stabeno, P.J., O'Hern, J.E., 2012. Observations of a Pribilof eddy. Deep Sea Res. I,
- 2249 66, 67–76. https://doi.org/10.1016/j.dsr.2012.04.003.
- 2250 Ladd, C., Cheng W., 2016. Gap winds and their effects on regional oceanography Part I: Cross
- 2251 Sound, Alaska. *Deep Sea Res. II*, 132, 41–53, https://doi.org/10.1016/j.dsr2.2015.08.006.

- 2252 Ladd, C., Cheng, W., Salo, S., 2016. Gap winds and their effects on regional oceanography Part
- 2253 II: Kodiak Island, Alaska. Deep Sea Res. II, 132, 54–67,
- 2254 https://doi.org/10.1016/j.dsr2.2015.08.005.
- 2255 Ladychenko, S.Y., Lobanov, V.B., 2013. Mesoscale eddies in the area of Peter the Great Bay
- according to satellite data. *Izv. Atmos. Ocean. Phys.* 49, 939–951.
- 2257 https://doi.org/10.1134/S0001433813090193.
- 2258 Landry, M.R., Decima, M., Simmons, M.P., Hannides, C.C., Daniels, E., 2008.
- Mesozooplankton biomass and grazing responses to Cyclone Opal, a subtropical mesoscale
- 2260 eddy. *Deep Sea Res. II*, 55(10–13), 1378–1388, https://doi.org/10.1016/j.dsr2.2008.01.005.
- Lee, E.A. Kim, S.Y., 2018. Regional variability and turbulent characteristics of the satellite-
- sensed submesoscale surface chlorophyll concentrations, J. Geophys. Res., 123(6), 4250–
- **2263** 4279, https://doi.org/10.1029/2017JC013732.
- 2264 Lee, E.A., Kim, S.Y., Min, H.S., 2019. Climatological descriptions on regional circulation
- around the Korean Peninsula, *Tellus A Dyn. Meteorol. Oceanogr.*, 71:1, 1–22
- 2266 https://doi.org/10.1080/16000870.2019.1604058.
- Lee, K., Nam, S., Kim, Y.G., 2019. Statistical characteristics of East Sea mesoscale eddies
- detected, tracked, and grouped using satellite altimeter data from 1993 to 2017. J. Korean
- 2269 Soc. Oceanogr., 24(2), 267–281. (in Korean, with English Abstr.)
- 2270 L'Her, A., Reinert, M., Prants, S., Carton, X., Morvan, M., 2021. Eddy formation in the bays of
- Kamchatka and fluxes to the open ocean. *Ocean Dyn.*, 71, 601–612.
- 2272 https://doi.org/10.1007/s10236-021-01449-w.
- Lie, H.-J., 1989. Tidal fronts in the southeastern Hwanghae (Yellow Sea). Cont. Shelf Res. 9,
- 2274 527–546. https://doi.org/10.1016/0278-4343(89)90019-8.
- Lie, H.-J., Cho, C.-H., Jung, K.T., 2015. Occurrence of large temperature inversion in the
- thermohaline frontal zone at the Yellow Sea entrance in winter and its relation to advection.
- 2277 J. Geophys. Res., 120, 417–435. https://doi.org/10.1002/2014JC010653.

- 2278 Liguori, G., Di Lorenzo, E., 2018 Meridional Modes and Increasing Pacific Decadal Variability
- 2279 Under Anthropogenic Forcing. Geophys. Res. Lett., 45(2) 983–991,
- 2280 https://doi.org/10.1002/2017g1076548.
- Lippiatt, S.M., Lohan, M.C., Bruland, K.W., 2010. The distribution of reactive iron in northern
- Gulf of Alaska coastal waters. Marine Chemistry 121 (1–4), 187–199,
- 2283 https://doi.org/10.1016/j.marchem.2010.04.007.
- Lippiatt, S.M., Brown, M.T., Lohan, M.C., Bruland, K.W., 2011. Reactive iron delivery to the
- 2285 Gulf of Alaska via a Kenai eddy, *Deep Sea Res. I*, 58(11), 1091–1102,
- 2286 https://doi.org/10.1016/j.dsr.2011.08.005.
- Liu, G., Bracco, A., Sitar, A., 2021. Submesoscale mixing across the mixed layer in the Gulf of
- 2288 Mexico. Front. Mar. Sci., 8:615066. https://doi.org/10.3389/fmars.2021.615066
- 2289 Liu, K.-K., Gong, G.-C., Shyu, C.-Z., Pai, S.-C., Wei, C.-L., Chao, S.-Y. 1992. Response of
- 2290 Kuroshio upwelling to the onset of the northeast monsoon in the sea north of Taiwan:
- Observations and a numerical simulation, J. Geophys. Res., 97, 12511–12526, C12014,
- 2292 https://doi.org/10.1029/92JC01179.
- 2293 Liu, K.-K., Chao, S.-Y., Lee, H.-G., Gong, G.-C., Teng, Y.-C., 2010. Seasonal variation of
- primary productivity in the East China Sea: A numerical study based on coupled physical-
- biogeochemical model, Deep Sea Res. II, 57, 1762–1782,
- 2296 https://doi.org/10.1016/j.dsr2.2010.04.003.
- Liu, Y., Dong, C., Guan, Y., Chen, D., McWilliams, J., Nencioli, F., 2012. Eddy analysis in the
- subtropical zonal band of the North Pacific Ocean. *Deep-Sea Res.*, 68, 54–67,
- 2299 https://doi.org/10.1016/j.dsr.2012.06.001.
- 2300 Lobel, P.S., Robinson, A.R., 1986. Transport and entrapment of fish larvae by ocean mesoscale
- eddies and currents in Hawaiian waters. *Deep Sea Res. As*, 33(4), 483–500,
- 2302 https://doi.org/10.1016/0198-0149(86)90127-5.
- 2303 Lobel, P.S., Robinson, A.R., 1988. Larval fishes and zooplankton in a cyclonic eddy in
- 2304 Hawaiian waters. J. Plankton Res., 10(6), 1209–1223,
- 2305 https://doi.org/10.1093/plankt/10.6.1209.

- 2306 Lobel, P.S., 2011. Transport of reef lizardfish larvae by an ocean eddy in Hawaiian waters. *Dyn.*
- 2307 Atmos. Oceans, 52(1–2), 119–130, https://doi.org/10.1016/j.dynatmoce.2011.01.001.
- 2308 Logerwell, E.A., Lavaniegos, B., Smith, P.E., 2001. Spatially-explicit bioenergetics of Pacific
- sardine in the Southern California Bight: are mesoscale eddies areas of exceptional
- 2310 prerecruit production? *Prog. Oceanogr.*, 49, 391–406, https://doi.org/10.1016/S0079-
- **2311** 6611(01)00032-5
- 2312 Logerwell, E., Smith, P., 2001. Mesoscale eddies and survival of late stage Pacific sardine
- 2313 (Sardinops sagax) larvae. Fisheries Oceanography, 10, 13–25,
- 2314 https://doi.org/10.1046/j.1365-2419.2001.00152.x.
- 2315 Lumpkin, C. F., 1998. Eddies and currents in the Hawaii islands, Ph.D. Thesis, University of
- Hawaii, Hawaii, USA, ftp://ftp.aoml.noaa.gov/phod/pub/lumpkin/hawaiiR2.pdf.
- Lyman, J.M., Johnson, G.C., 2015. Anomalous eddy heat and freshwater transport in the Gulf
- 2318 of Alaska, J. Geophys. Res., 120, 1397–1408, https://doi.org/10.1002/2014JC010252.
- 2319 Lynn, R. J., Simpson J.J., 1987. The California Current system: The seasonal variability of its
- physical characteristics, J. Geophys. Res., 92(C12), 12947,
- 2321 https://doi.org/10.1029/JC092iC12p12947.
- Mackas, D.L., Galbraith, M.D., 2002. Zooplankton distribution and dynamics in a North Pacific
- eddy of coastal origin: 1. Transport and loss of continental margin species. J. Oceanogr., 58,
- 2324 725–738, https://doi.org/10.1023/A:1022802625242.
- Mackas, D.L., Tsurumi, M., Galbraith, M.D. and Yelland, D.R., 2005. Zooplankton distribution
- and dynamics in a North Pacific Eddy of coastal origin: II. Mechanisms of eddy colonization
- by and retention of offshore species. *Deep Sea Res. II*, 52(7–8), 1011–1035,
- 2328 https://doi.org/10.1016/j.dsr2.2005.02.008.
- Mantua, N. J., Hare, S.R., Zhang, Y., Wallace J. M., Francis, R.C., 1997. A Pacific interdecadal
- climate oscillation with impacts on salmon production. Bull. Amer. Meteor. Soc., 78, 1069–
- 2331 1079, https://doi.org/10.1175/1520-0477(1997)078<1069:APICOW>2.0.CO;2.
- 2332 Mantua, N. J., Hare, S.R., 2002. The Pacific Decadal Oscillation. J. Oceanogr. 58, 35-44,
- 2333 https://doi.org/10.1023/A:1015820616384.

- 2334 Marchesiello, P., McWilliams, J.C., Shchepetkin, A., 2003. Equilibrium structure and dynamics
- of the California Current System, J. Phys. Oceanogr., 33, 753–783,
- 2336 https://doi.org/10.1175/1520-0485(2003)33<753:ESADOT>2.0.CO;2.
- Martin, J.H., Gordon, R.M., Fitzwater, S., Broenkow, W.W., 1989. Vertex: phytoplankton/iron
- 2338 studies in the Gulf of Alaska. *Deep Sea Res. A* 36(5), 649–680, https://doi.org/10.1016/0198-
- 2339 0149(89)90144-1.
- 2340 Matsuno, T., Lee, J.-S., Yanao, S., 2009. The Kuroshio exchange with the South and East China
- 2341 Seas, *Ocean Sci.*, 5, 303–312, https://doi.org/10.5194/os-5-303-2009_
- Maximenko, N.A., Koshlyakov, M.N., Ivanov, Y.A., Yaremchuk, M.I., Panteleev, G.G., 2001.
- 2343 Hydrophysical experiment "Megapolygon-87" in the northwestern Pacific subarctic frontal
- zone. J. Geophys. Res., 106(C7) 14143–14163, https://doi.org/10.1029/2000JC000436.
- 2345 McCabe, R. M., Hickey, B.M., Kudela, R.M., Lefebvre, K.A., Adams, N.G., Bill, B.D.,
- Gulland, F.M.D., Thomson, R.E., Cochlan, W.P., Trainer V.L., 2016. An unprecedented
- coastwide toxic algal bloom linked to anomalous ocean conditions. *Geophys. Res. Lett.*, 43,
- 2348 10,366–10,376, https://doi.org/10.1002/2016GL070023.
- 2349 McEwen, G.F., Thompson, T.G., van Cleve, R., 1930. Hydrographic sections and calculated
- currents in the Gulf of Alaska, 1927 and 1928, Rep. Inst. Fish. Comm., No. 4, 5–36.
- 2351 McGillicuddy, D.J. Jr, Robinson, A.R., McCarthy, J.J., 1995. Coupled physical and biological
- 2352 modeling of the spring bloom in the North Atlantic (II): three dimensional bloom and post-
- 2353 bloom processes. *Deep Sea Res. I*, 42, 1359–1398, https://doi.org/10.1016/0967-
- **2354** 0637(95)00035-5.
- 2355 McGillicuddy, D.J., 2016. Mechanisms of physical-biological-biogeochemical interaction at the
- oceanic mesoscale. Ann. Rev. Mar. Sci., 8, 125–159, https://doi.org/10.1146/annurev-
- 2357 marine-010814-015606
- 2358 McWilliams, J.C., 2016. Submesoscale currents in the ocean. *Proc. R. Soc. A*, 472, 20160117,
- 2359 https://doi.org/10.1098/rspa.2016.0117

- Melsom, A., Meyers, S.D., Hurlburt, H.E., Metzger, J.E., O'Brien, J.J., 1999. ENSO effects on
- Gulf of Alaska eddies. Earth Interactions 3, 1–3, https://doi.org/10.1175/1087-
- 2362 3562(1999)003<0001:EEOGOA>2.3.CO;2.
- 2363 Miller, A.J., DiLorenzo, E., Neilson, D.J., Kim, H.J., Capotondi, A., Alexander, M.A., Bograd,
- S.J., Schwing, F.B., Mendelssohn, R., Hedstrom, K., Musgrave, D.L., 2005. Interdecadal
- changes in mesoscale eddy variance in the Gulf of Alaska circulation: Possible implications
- for the Steller sea lion decline. *Atmos.-Ocean*, 43(3), pp.231–240,
- 2367 https://doi.org/10.3137/ao.430303.
- 2368 Miller, J.M., Otake, T., Minagawa, G., Inagaki, T., Tsukamoto, K., 2002. Distribution of
- leptocephali in the Kuroshio Current and East China Sea, Mar. Ecol. Prog. Ser., 235, 279–
- 2370 288, https://doi.org/10.3354/meps235279.
- 2371 Mitnik, L.M., Dubina V.A., 2019. The Sea of Okhotsk: scientific applications of remote
- sensing. In: Barale, V., Gade, M. (Eds), Remote Sensing of the Asian Seas, Springer, pp.
- 2373 159–175, https://doi.org/10.1007/978-3-319-94067-0 8.
- 2374 Miyama T, Minobe S and Goto H., 2021, Marine Heatwave of Sea Surface Temperature of the
- 2375 Oyashio Region in Summer in 2010–2016. *Front. Mar. Sci.* 7:576240.
- 2376 https://doi.org/10.3389/fmars.2020.576240
- 2377 Mizobata, K., Saitoh, S., 2004. Variability of Bering Sea eddies and primary productivity along
- the shelf edge during 1998–2000 using satellite multi- sensor remote sensing. *J. Mar. Sys.*
- 2379 50, 101–111, https://doi.org/10.1016/j.jmarsys.2003.09.014.
- 2380 Mizobata, K., Saitoh, S.I., Shiomoto, A., Miyamura, T., Shiga, N., Imai, K., Toratani, M.,
- Kajiwara, Y., Sasaoka, K., 2002. Bering Sea cyclonic and anticyclonic eddies observed
- during summer 2000 and 2001. *Prog. Oceanogr.* 55, 65–75, https://doi.org/10.1016/S0079-
- **2383** 6611(02)00070-8.
- 2384 Mizobata, K., Wang, J., Saito, S.-I., 2006. Eddy-induced cross-slope exchange maintaining
- summer high productivity of the Bering Sea shelf break. J. Geophys. Res., 111, C10017,
- 2386 https://doi.org/10.1029/2005JC003335.
- 2387 Mizobata, K., Saitoh, S.-I., Wang, J., 2008. Interannual variability of summer biochemical
- enhancement in relation to mesoscale eddies at the shelf break in the vicinity of the Pribilof

- 2389 Islands. Bering Sea. *Deep Sea Res. II*, 55, 1717–1728,
- 2390 https://doi.org/10.1016/j.dsr2.2008.03.002.
- Mizuno, K., White, W.B., 1983. Annual and interannual variability in the Kuroshio Current
- 2392 system. J. Phys. Oceanogr., 13, 1848–1869, https://doi.org/10.1175/1520-
- 2393 0485(1983)013<1847:AAIVIT>2.0.CO;2.
- Molemaker, M.J., McWilliams, J.C., Dewar, W.K., 2015. Submesoscale Instability and
- Generation of Mesoscale Anticyclones near a Separation of the California Undercurrent, J.
- 2396 *Phys. Oceanogr.*, 45(3), 613–629, https://doi.org/10.1175/Jpo-D-13-0225.1.
- Mugo, R., Saitoh, S.-I., Nihira, A., Kuroyama, T., 2010. Habitat characteristics of skipjack tuna
- 2398 (Katsuwonus pelamis) in the western North Pacific: a remote sensing perspective. Fish.
- 2399 Oceanogr., 19, 382–396. https://doi.org/10.1111/j.1365-2419.2010.00552.x
- 2400 Murray, C.P., Morey, S.L., O'Brien, J.J., 2001. Interannual variability of upper ocean vorticity
- 2401 balances in the Gulf of Alaska. *J. Geophys. Res.* 106(C3), 4479–4491,
- 2402 https://doi.org/10.1029/1999JC000071.
- Nagai, T., Gruber, N., Frenzel, H., Lachkar, Z., McWilliams, J. C., Plattner, G.-K., 2015.
- Dominant role of eddies and filaments in the offshore transport of carbon and nutrients in the
- 2405 California Current System, J. Geophys. Res., 120, 5318–5341,
- 2406 https://doi.org/10.1002/2015JC010889.
- Nagai, T., Hasegawa, D., Tsutsumi, E., Nakamura, H., Nishina, A., Senjyu, T., Endoh, T.,
- Matsuno, T., Inoue, R., Tandon, A., 2021. The Kuroshio flowing over seamounts and
- associated submesoscale flows drive 100-km-wide 100-1000-fold enhancement of
- 2410 turbulence. Commun. Earth Environ., 2, 170, https://doi.org/10.1038/s43247-021-00230-7.
- 2411 Nagano, A., Kawabe, M., 2004. Monitoring of Generation and Propagation of the Kuroshio
- Small Meander Using Sea Level Data along the Southern Coast of Japan. J. Oceanogr., 60,
- 2413 879–892, https://doi.org/10.1007/s10872-005-5780-7.
- 2414 Nakamura, T., Matthews, J. P., Awaji, T., Mitsudera, H., 2012. Submesoscale eddies near the
- 2415 Kuril Straits: Asymmetric generation of clockwise and counterclockwise eddies by
- 2416 barotropic tidal flow. J. Geophys. Res., 117, C12014, https://doi.org/10.1029/2011JC007754.

- 2417 Nakata, H, Kimura, S, Okazaki, Y, Kasai, A, 2000. Implications of meso-scale eddies caused by
- frontal disturbances of the Kuroshio Current for anchovy recruitment, ICES J. Mar. Sci., 57,
- 2419 143–152, https://doi.org/10.1006/jmsc.1999.0565.
- Nakano, H., Tsujino, H., Sakamoto, K., 2013. Tracer transport in cold-core rings pinched off
- from the Kuroshio Extension in an eddy-resolving ocean general circulation model, *J.*
- **2422** *Geophys. Res.*, 118, 5461–5488, https://doi.org/10.1002/jgrc.20375.
- Niiler, P.P., Hall, M.M., 1988. Low-frequency eddy variability at 28° N, 152°W in the eastern
- North Pacific subtropical gyre. J. Phys. Oceanogr., 18(11), 1670–1685,
- 2425 https://doi.org/10.1175/1520-0485(1988)018<1670:LFEVAI>2.0.CO;2.
- Nishioka, J., Takeda, S., Wong, C.S., Johnson, W.K., 2001. Size-fractionated iron
- concentrations in the Northeast Pacific Ocean: distribution of soluble and small colloidal
- 2428 iron. Mar. Chem., 74, 157–179, https://doi.org/10.1016/S0304-4203(01)00013-5.
- 2429 Nonaka M, Nakamura H, Tanimoto Y, Kagimoto T, Sasaki H., 2008. Interannual-to-decadal
- variability in the Oyashio Current and its influence on temperature in the subarctic frontal
- zone: an eddy-resolving OGCM simulation. *J Clim.*, 21, 6283–6303,
- 2432 https://doi.org/10.1175/2008JCLI2294.1.
- 2433 Nordstrom, C.A., Battaile, B.C., Cotte', C., Trites, A.W., 2013. Foraging habitats of lactating
- northern fur seals are structured by thermocline depths and submesoscale fronts in the
- 2435 eastern Bering Sea. *Deep Sea Res. II*, 88–89, 78–96,
- 2436 https://doi.org/10.1016/j.dsr2.2012.07.010.
- 2437 Ohshima, K. I., Wakatsuchi, M., Fukamachi, Y., Mizuta G., 2002. Near-surface circulation and
- tidal currents of the Okhotsk Sea observed with satellite-tracked drifters. J. Geophys. Res.,
- 2439 107, 3195, https://doi.org/10.1029/2001JC001005.
- 2440 Ohshima, K.I., Fukamachi, Y., Mutoh, T., Wakatsuchi, M., 2005. A generation mechanism for
- mesoscale eddies in the Kuril Basin of the Okhotsk Sea: Baroclinic instability caused by
- enhanced tidal mixing. J. Oceanogr., 61(2), 247–260. https://doi.org/10.1007/s10872-005-
- **2443** 0035-1.

- Okkonen, S.R., 1992. The shedding of an anticyclonic eddy from the Alaskan Stream as
- observed by the Geosat altimeter. *Geophys. Res. Lett.*, 19, 2397–2400,
- 2446 https://doi.org/10.1029/92GL01882.
- Okkonen, S.R., 1993. Observations of topographic planetary waves in the Bering Slope Current
- using the Geosat altimeter. J. Geophys. Res. 98, 22603–22613,
- 2449 https://doi.org/10.1029/93JC02344.
- Okkonen, S.R., 2001. Altimeter observations of the Bering Slope Current eddy field. J.
- 2451 Geophys. Res., 106, 2465–2476, https://doi.org/10.1029/2000JC000285.
- Okkonen, S.R., Weingartner, T.J., Danielson, S.L., Musgrave, D.L., Schmidt, G.M., 2003.
- Satellite and hydrographic observations of eddy-induced shelf-slope exchange in the
- northwestern Gulf of Alaska. Journal of Geophysical Research: Oceans, 108(C2), 3033,
- 2455 https://doi.org/10.1029/2002JC001342.
- 2456 Okubo, A., 1970. Horizontal dispersion of floatable particles in the vicinity of velocity
- singularity such as convergences. Deep Sea Res., 17, 445–454, https://doi.org/10.1016/0011-
- **2458** 7471(70)90059-8.
- Okuda, K., Yasuda, I., Hiroe, Y., Shimizu, Y., 2001. Structure of subsurface intrusion of the
- Oyashio water into the Kuroshio Extension and formation process of the North Pacific
- 2461 Intermediate Water. J. Oceanogr., 57, 121–140, https://doi.org/10.1023/A:1011135006278.
- Oliver, E.C., Donat, M.G., Burrows, M.T., Moore, P.J., Smale, D.A., Alexander, L.V.,
- Benthuysen, J.A., Feng, M., Gupta, A.S., Hobday, A.J., Holbrook, N.J., Perkins-Kirkpatrick,
- S.E., Scannell, H.A., Straub S.C., Wernberg, T., 2018. Longer and more frequent marine
- heatwaves over the past century. *Nature Commun.* 9, 1324, https://doi.org/10.1038/s41467-
- **2466** 018-03732-9.
- Owen, R.W., 1980. Eddies of the California Current System: physical and ecological
- characteristics. In: Power, D. (Ed.), The California Islands: Proceedings of a
- Multidisciplinary Symposium, Santa Barbara Mus. of Nat. Hist., Santa Barbara, CA, pp.
- **2470** 237–263.
- 2471 Paluszkiewicz, T., Niebauer, H.J., 1984. Satellite observations of circulation in the Eastern
- 2472 Bering Sea. J. Geophys. Res. 89, 3663–3678, http://dx.doi.org/10.1029/ JC089iC03p03663.

- Paredes, R., Orben, R.A., Suryan, R.M., Irons, D.B., Roby, D.D., Harding, A.M.A., Young,
- 2474 R.C., Benoit-Bird, K., Ladd, C., Renner, H., Heppell, S., Phillips, R.A., Kitaysky A., 2014.
- Foraging responses of black-legged kittiwakes to prolonged food shortages around colonies
- in the Bering Sea shelf. PLoS ONE, 9(3), e92520,
- 2477 https://doi.org/10.1371/journal.pone.0092520.
- Park, Y.-H., Yoon, J.-H., Youn, Y.-H., Vivier, F., 2012a. Recent warming in the western North
- Pacific in relation to rapid changes in the atmospheric circulation of the Siberian High and
- 2480 Aleutian Low systems, *J. Clim.*, 25, 3476–3493, https://doi.org/10.1175/2011JCLI4142.1.
- 2481 Park, K-A., Woo, H-J., Ryu, J-H., 2012b. Spatial Scales of Mesoscale Eddies from GOCI
- 2482 Chlorophyll-a Concentration Images in the East/Japan Sea, *Ocean Sci. J.* 47, 347–358
- 2483 https://doi.org/10.1007/s12601-012-0033-3.
- 2484 Pelland, N.A., Eriksen, C.C., Lee, C.M., 2013. Subthermocline Eddies over the Washington
- 2485 Continental Slope as Observed by Seagliders, 2003-09, J. Phys. Oceanongr., 43(10), 2025–
- 2486 2053, https://doi.org/10.1175/Jpo-D-12-086.1.
- Pelland, N.A., Sterling, J.T., Lea, M-A, Bond, N.A., Ream, R.R., Lee, C.M., Eriksen, C.C.,
- 2488 2014. Fortuitous Encounters between Seagliders and Adult Female Northern Fur Seals
- (Callorhinus ursinus) off the Washington (USA) Coast: Upper Ocean Variability and Links
- to Top Predator Behavior. *PLoS ONE* 9(8): e101268.
- 2491 https://doi.org/10.1371/journal.pone.0101268.
- 2492 PICES, 2004. North Pacific Marine Science Organization (PICES) Annual Report, PICES,
- Sidney, BC, Canada. https://meetings.pices.int/publications/annual-
- reports/2004/AnnRep2004.pdf.
- 2495 Pinsky, M.L., Worm, B., Fogarty, M.J., Sarmiento, J.L., Levin S.A., 2013. Marine Taxa Track
- Local Climate Velocities. Science, 341, 1239–1242,
- 2497 https://doi.org/10.1126/science.1239352.
- 2498 Plattner, G.-K., Gruber, N., Frenzel, H., McWilliams. J.C., 2005. Decoupling marine export
- production from new production, *Geophys. Res. Lett.*, 32, L11612,
- 2500 https://doi.org/10.1029/2005GL022660.

- Prants, S.V., Budyansky, M.V., Ponomarev, V.I., Uleysky, M.Y., 2011. Lagrangian study of
- transport and mixing in a mesoscale eddy street. *Ocean Model.*, 38, 114–125.
- 2503 https://doi.org/10.1016/j.ocemod.2011.02.008.
- Prants, S.V., Andreev, A.G., Budyansky, M.V., Uleysky, M.Y., 2013. Impact of mesoscale
- eddies on surface flow between the Pacific Ocean and the Bering Sea across the near strait.
- 2506 Ocean Model., 72, 143–152. https://doi.org/10.1016/j.ocemod.2013.09.003.
- 2507 Prants, S.V., Budyansky, M.V., Uleysky, M.Y., 2014a. Identifying Lagrangian fronts with
- favorable fishery conditions. *Deep Sea Res. I*, 90, 27–35.
- 2509 https://doi.org/10.1016/j.dsr.2014.04.012.
- Prants, S.V., Budyansky, M.V., Uleysky, M.Y., 2014b. Lagrangian study of surface transport in
- 2511 the Kuroshio Extension area based on simulation of propagation of Fukushima- derived
- radionuclides. Nonlin. Processes Geophys., 21, 279–289. https://doi.org/10.5194/npg-21-
- **2513** 279-2014.
- Prants, S.V., Budyansky, M.V., Ponomarev, V.I., Uleysky, M.Y., Fayman, P.A., 2015.
- 2515 Lagrangian analysis of the vertical structure of eddies simulated in the Japan Basin of the
- 2516 Japan/East Sea. *Ocean Model.*, 86, 128–140, https://doi.org/10.1016/j.ocemod.2014.12.010.
- Prants, S.V., Lobanov, V.B., Budyansky, M.V., Uleysky, M.Y., 2016. Lagrangian analysis of
- formation, structure, evolution and splitting of anticyclonic Kuril eddies. *Deep Sea Res. I*,
- 2519 109, 61–75, https://doi.org/10.1016/j.dsr.2016.01.003.
- 2520 Prants, S.V., Budyansky, M.V., Uleysky, M.Y., 2017a. Lagrangian simulation and tracking of
- 2521 the mesoscale eddies contaminated by Fukushima-derived radionuclides. *Ocean Sci.*, 13,
- 2522 453–463. https://doi.org/10.5194/os-13-453-2017.
- 2523 Prants, S.V., Budyansky, M.V., Uleysky, M.Y., 2017b. Statistical analysis of Lagrangian
- transport of subtropical waters in the Japan Sea based on AVISO altimetry data. *Nonlin*.
- **2525** *Processes Geophys.*, 24, 89–99. https://doi.org/10.5194/npg-24-89-2017.
- 2526 Prants, S.V., Andreev, A.G., Uleysky, M.Y., Budyansky, M.V., 2017c. Mesoscale circulation
- along the Sakhalin Island eastern coast. *Ocean Dyn.*, 67, 345–356.
- 2528 https://doi.org/10.1007/s10236-017-1031-x.

- 2529 Prants, S.V., Uleysky, M.Y., Budyansky, M.V., 2017d. Lagrangian oceanography: large-scale
- transport and mixing in the ocean. Berlin, New York. Springer Verlag. pp. 271.
- 2531 https://doi.org/10.1007/978-3-319-53022-2.
- 2532 Prants, S.V., Budyansky, M.V., Uleysky, M.Y., 2018. How eddies gain, retain and release
- water: A case study of a Hokkaido anticyclone. J. Geophys. Res., 123, 2081–2096,
- 2534 https://doi.org/10.1002/2017jc013610.
- 2535 Prants, S.V., Andreev, A.G., Uleysky, M.Y., Budyansky, M.V., 2019. Lagrangian study of
- mesoscale circulation in the Alaskan Stream area and the eastern Bering Sea. *Deep Sea Res.*
- 2537 *II*, 169–179, 104560, https://doi.org/10.1016/j.dsr2.2019.03.005.
- 2538 Prants S.V., Budyansky, M.V., Lobanov V.B., Sergeev A.F., Uleysky, M.Y., 2020. Observation
- and Lagrangian analysis of quasi-stationary Kamchatka trench eddies. J. Geophys. Res., 125,
- 2540 e2020JC016187, https://doi.org/10.1029/2020JC016187
- Prants, S.V., Budyansky, M.V., Uleysky, M.Y., Kulik V.V., 2021. Lagrangian fronts and saury
- catch locations in the Northwestern Pacific in 2004–2019. J. Mar. Sys., 222, 103605,
- 2543 https://doi.org/10.1016/j.jmarsys.2021.103605.
- 2544 Qiu, B., 1999. Seasonal eddy field modulation of the North Pacific subtropical countercurrent:
- TOPEX/Poseidon observations and theory. J. Phy. Oceanogr., 29, 2471–2486,
- 2546 https://doi.org/10.1175/1520-0485(1999)029<2471:SEFMOT>2.0.CO;2.
- 2547 Qiu, B., 2002. The Kuroshio Extension System: Its Large-Scale Variability and Role in the
- 2548 Midlatitude Ocean-Atmosphere Interaction. J. Oceanogr., 58, 57–75,
- 2549 https://doi.org/10.1023/A:1015824717293.
- 2550 Qiu, B., Chen, S., 2005. Variability of the Kuroshio Extension jet, recirculation gyre and
- mesoscale eddies on decadal timescales. J. Phys. Oceanogr., 35, 2090–2103,
- 2552 https://doi.org/10.1175/JPO2807.1.
- 2553 Qiu, B., Hacker, P., Chen, S., Donohue, K.A., Watts, D.R., Mitsudera, H., Hogg N.G., Jayne,
- S.R., 2006. Observations of the Subtropical Mode Water evolution from the Kuroshio
- Extension System Study. J. Phys. Oceanogr., 36, 457–473,
- 2556 https://doi.org/10.1175/JPO2849.1.

- 2557 Qiu, B., Scott, R., Chen, S., 2008. Length scales of eddy generation and nonlinear evolution of
- 2558 the seasonally modulated South Pacific Subtropical Countercurrent. J. Phys. Oceanogr., 38,
- 2559 1515–1528, https://doi.org/10.1175/2007JPO3856.1.
- 2560 Qiu, B., Chen, S., 2010. Interannual variability of the North Pacific Subtropical Countercurrent
- and its associated mesoscale eddy field. J. Phys. Oceanogr., 40, 213–225,
- 2562 https://doi.org/10.1175/2009JPO4285.1.
- 2563 Qiu, B., Chen, S., Klein, P., Sasaki, H., Sasai, Y., 2014. Seasonal mesoscale and submesoscale
- eddy variability along the North Pacific Subtropical Countercurrent. J. Phys. Oceanogr., 44,
- 2565 3079–3098, https://doi.org/10.1175/JPO-D-14-0071.1.
- 2566 Qiu, B., Chen, S.M., Schneider, N. 2017. Dynamical links between the decadal variability of the
- Oyashio and Kuroshio extensions. J. Clim. 30, 9591–9605. https://doi.org/10.1175/JCLI-D-
- **2568** 17-0397.1.
- 2569 Qiu, B., Chen, S., Klein, P., Wang, J., Torres, H., Fu, L.-L., Menemenlis, D., 2018. Seasonality
- in transition scale from balanced to unbalanced motions in the world ocean. J. Phys.
- 2571 *Oceanogr.*, 48, 591–605, https://doi.org/10.1175/JPO-D-17-0169.1.
- 2572 Rabinovich, A.B., Thomson, R.E., Bograd, S.J., 2002. Drifter observations of anticyclonic
- eddies near Bussol' Strait, the Kuril Islands. J. Oceanogr., 58, 661–671.
- 2574 https://doi.org/10.1023/a:1022890222516.
- Ream, R.R., Sterling, J.T., Loughlin, T.R., 2005. Oceanographic features related to northern fur
- seal migratory movements. *Deep Sea Res. II*, 52, 823–843,
- 2577 https://doi.org/10.1016/j.dsr2.2004.12.021.
- 2578 Reid J.L. Jr., Roden, G.I., Wyllie, J.G., 1958. Studies of the California Current system. Prog.
- Rep. Calif. Coop. Ocean. Fish. Invest, pp. 28-56
- 2580 Robinson, A.R., McWilliams, J.C., 1974. The baroclinic instability of the open ocean. *J. Phys.*
- 2581 Oceanogr. 4, 281–294, https://doi.org/10.1175/1520-
- **2582** 0485(1974)004<0281:TBIOTO>2.0.CO;2.
- 2583 Robinson, A. R. (Ed.), 1983. Eddies in Marine Science, 609 pp., Springer-Verlag, Berlin,
- 2584 https://doi.org/10.1007/978-3-642-69003-7.

- 2585 Roden, G.I., 1995. Aleutian Basin of the Bering Sea: Thermohaline, oxygen, nutrient, and
- 2586 current structure in July 1993. *J. Geophys. Res.*, 100, 13539–13554,
- 2587 https://doi.org/10.1029/95JC01291.
- Roemmich, D., Gilson, J., 2001. Eddy transport of heat and thermocline waters in the North
- Pacific: A key to interannual/decadal climate variability? J. Phys. Oceanogr., 31, 675–687,
- 2590 https://doi.org/10.1175/1520-0485(2001)031<0675:ETOHAT>2.0.CO;2.
- 2591 Rogachev, K.A., 2000a. Rapid thermohaline transition in the Pacific western subarctic and
- 2592 Oyashio fresh core eddies. *J. Geophys. Res.*, 105, 8513–8526.
- 2593 https://doi.org/10.1029/1999jc900330.
- Rogachev, K.A., 2000b. Recent variability in the Pacific western subarctic boundary currents
- and Sea of Okhotsk. *Prog. Oceanogr.*, 47, 299–336, https://doi.org/10.1016/S0079-
- **2596** 6611(00)00040-9.
- 2597 Rogachev, K., Shlyk, N., Carmack, E., 2007. The shedding of mesoscale anticyclonic eddies
- from the Alaskan Stream and westward transport of warm water. Deep Sea Res. II, 54,
- 2599 2643–2656, https://doi.org/10.1016/j.dsr2.2007.08.017.
- 2600 Rogachev, K.A., Carmack, E.C., Foreman, M.G.G. 2008. Bowhead whales feed on plankton
- concentrated by estuarine and tidal currents in Academy Bay, Sea of Okhotsk. *Cont. Shelf*
- 2602 Res., 28, 1811–1826., https://doi.org/10.1016/j.csr.2008.04.014.
- 2603 Rogachev, K.A., Shlyk N.V., 2019. Characteristics of the Kamchatka Current Eddies. *Russ*.
- 2604 *Meteorol. Hydrol.*, 44, 416–423. https://doi.org/10.3103/S1068373919060062.
- 2605 Rovegno, P.S., Edwards, C.A., Bruland, K.W., 2009. Observations of a Kenai Eddy and a Sitka
- Eddy in the Northern Gulf of Alaska. J. Geophys. Res., 114, C11012.
- 2607 https://doi.org/10.1029/2009JC005451.
- Royer, T.C., 1978. Ocean eddies generated by seamounts in the North
- 2609 Pacific. Science, 199(4333), 1063–1064, https://doi.org/10.1126/science.199.4333.1063.
- 2610 Rypina, I.I., Brown, M.G., Beron-Vera, F. J., Kocak, H., Olascoaga, M. J., Udovydchenkov,
- 2611 I.A., 2007. Robust transport barriers resulting from strong Kolmogorov-Arnold-Moser
- 2612 stability. *Phys. Rev. Lett.*, 98, 104102, https://doi.org/10.1103/PhysRevLett.98.104102.

- Rypina, I.I., Pratt, L.J., Lozier, M.S., 2011. Near-Surface Transport Pathways in the North
- 2614 Atlantic Ocean: Looking for Throughput from the Subtropical to the Subpolar Gyre. J. Phys.
- 2615 *Oceanogr.*, 41(5), 911–925, https://doi.org/10.1175/2011JPO4498.1.
- 2616 Rypina, I.I., Jayne, S.R., Yoshida, S., Macdonald, A.M., Douglass, E.M., Buesseler, K.O., 2013.
- Short-term dispersal of Fukushima-derived radionuclides off Japan: modeling efforts and
- 2618 model-data intercomparison, *Biogeosci.*, 10, 4973–4990, https://doi.org/10.5194/bg-10-
- **2619** 4973-2013.
- 2620 Rypina, I.I., Llopiz, J.K., Pratt, L.J., Lozier, M.S., 2014. Dispersal pathways of American eel
- larvae from the Sargasso Sea. Limnol. Oceanogr., 59(5), 1704–1714,
- 2622 https://doi.org/10.4319/lo.2014.59.5.1704.
- Rypina, I.I., Pratt, L.J., Lozier, M.S., 2016. Influence of ocean circulation changes on the inter-
- annual variability of American eel larvae dispersal. Limnol. Oceanogr., 61(5), 1574–1588,
- 2625 https://doi.org/10.1002/lno.10297.
- Rypina, I.I., Llewellyn Smith, S.G., Pratt, L.J., 2018. Connection between encounter volume
- and diffusivity in geophysical flows. *Nonlin. Processes Geophys.*, 25(2), 267–278,
- 2628 https://doi.org/10.5194/npg-25-267-2018.
- Rypina, I.I., Hernandez, C., Chen., K., Pratt, L., Llopiz, J., 2019. Investigating the Suitability of
- the Slope Sea for Atlantic Bluefin Tuna Spawning using a high-resolution ocean circulation
- 2631 model. ICES J. Mar. Sci., 76, 1666–1677, https://doi.org/10.1093/icesjms/fsz079.
- 2632 Saito, R., Yamaguchi, A., Yasuda, I., Ueno, H., Ishiyama, H., Onishi, H., Imai, I., 2014.
- 2633 Influences of mesoscale anticyclonic eddies on zooplankton community south of the western
- Aleutian Islands during the summer of 2010. *J Plankton Res* 36(1), 117–128.
- **2635** https://doi.org/10.1093/plankt/fbt087.
- 2636 Saito, R., Yasuda, I., Komatsu, K., Ishiyama, H., Ueno, H., Onishi H, Setou, T., Shimizu, M.,
- 2016. Subsurface hydrographic structures and the temporal variations of Aleutian eddies.
- 2638 Ocean Dyn. 66, 605–621. https://doi.org/10.1007/s10236-016-0936-0.
- 2639 Saitoh, S., Kosaka, S., Iisaka, J., 1986. Satellite infrared observations of Kuroshio warm-core
- rings and their application to study of Pacific saury migration. Deep Sea Res. A. 33, 1601–
- 2641 1615. https://doi.org/10.1016/0198-0149(86)90069-5.

- 2642 Santora, J.A., Eisner, L.B., Kuletz, K.J., Ladd, C., Renner, M., Hunt, G.L., Jr., 2018,
- Biogeography of seabirds within a high-latitude ecosystem: Use of a data-assimilative ocean
- model to assess impacts of mesoscale oceanography. J. Mar. Sys., 178, 38–51,
- 2645 https://doi.org/10.1016/j.jmarsys.2017.10.006.
- Sasai, Y., Richards, K., Ishida, A., Sasaki, H., 2010. Effects of cyclonic mesoscale eddies on the
- marine ecosystem in the Kuroshio Extension region using an eddy-resolving coupled
- 2648 physical-biological model, *Ocean Dyn.*, 60, 693–704, https://doi.org/10.1007/s10236-010-
- **2649** 0264-8.
- 2650 Sasaki, H., Klein, P., Qiu, B., Sasai, Y., 2014, Impact of oceanic scale-interactions on the
- seasonal modulation of ocean dynamics by the atmosphere. *Nature Commun.* 5, 5636.
- 2652 https://doi.org/10.1038/ncomms6636.
- 2653 Sasaki, H., Klein, P., Sasai, Y., Qiu, B., 2017. Reginality and seasonality of submesoscale and
- mesoscale turbulence in the North Pacific Ocean. Ocean Dyn., 67, 1195–1216,
- 2655 https://doi.org/10.1007/s10236-017-1083-y.
- 2656 Sasaki, H., Kida, S., Furue, R., Aiki, H. Komori, N., Masumoto, Y., Miyama, T., Nonaka, M.,
- Sasai, Y., Taguchi, B., 2020. A global eddying hindcast ocean simulation with OFES2.
- 2658 Geosci. Model Dev. Discuss., 13, 3319–3336, https://doi.org/10.5194/gmd-13-3319-2020.
- Sasaki, H., B. Qiu, P. Klein, Y. Sasai, and M. Nonaka., 2020. Interannual to decadal variations
- of submesoscale motions around the North Pacific subtropical countercurrent, Fluid.
- 2661 2020, 5(3), 116, https://doi.org/10.3390/fluids5030116.
- Sasaki, H., B. Qiu, P. Klein, M. Nonaka, and Y. Sasai., 2022. Interannual variations of
- submesoscale circulations in the subtropical Northeastern Pacific, Geophysical Research
- 2664 Letters, 49, e2021GL097664, https://doi.org/10.1029/2021GL097664.
- 2665 Sasaki, Y. N., and S. Minobe, 2015: Climatological mean features and interannual to decadal
- variability of ring formations in the Kuroshio Extension region. J. Oceanogr., 71, 499–509,
- 2667 https://doi.org/10.1007/s10872-014-0270-4Sassa, C., Tsukamoto, Y., Nishiuchi, K. Konishi,
- Y., 2008. Spawning ground and larval transport processes of jack mackerel *Trachurus*
- japonicus in the shelf-break region of the southern East China Sea. Cont. Shelf Res., 28,
- 2670 2574–2583, https://doi.org/10.1016/j.csr.2008.08.002.

- Sassa, C., Tsukamoto, Y., 2010. Distribution and growth of Scomber japonicus and S.
- australasicus larvae in the southern East China Sea in response to oceanographic conditions.
- 2673 *Mar. Ecol. Prog. Ser.*, 419, 185–199, https://doi.org/10.3354/meps08832.
- 2674 Scharffenberg, M.G., Stammer, D., 2010. Seasonal variations of the large-scale geostrophic
- flow field and eddy kinetic energy inferred from the TOPEX/Poseidon and Jason-1 tandem
- 2676 mission data. J. Geophys. Res., 115, C02008, https://doi.org/10.1029/2008JC005242.
- 2677 Schmitz Jr, W.J., 1988. Exploration of the eddy field in the midlatitude North Pacific. J. Phys.
- 2678 Oceanogr., 18(3), 459–468, https://doi.org/10.1175/1520-
- 2679 0485(1988)018<0459:EOTEFI>2.0.CO;2.
- 2680 Schumacher, J.D., Stabeno, P.J., 1994. Ubiquitous eddies of the eastern Bering Sea and their
- coincidence with concentrations of larval pollock. Fish. Oceanogr. 3, 182–190,
- 2682 https://doi.org/10.1111/j.1365-2419.1994.tb00095.x.
- Seki, M.P., Lumpkin, R., Flament, P., 2002. Hawaii cyclonic eddies and blue marlin catches:
- the case study of the 1995 Hawaiian International Billfish Tournament. J. Oceanogr., 58(5),
- 2685 739–745, https://doi.org/10.1023/A:1022854609312.
- Shen, M., Tseng, Y., Jan, S. 2011. The formation and dynamics of the cold-dome off
- 2687 northeastern Taiwan. J. Mar. Sys., 86, 10–27, https://doi.org/10.1016/j.jmarsys.2011.01.002.
- Shi, W., Wang, M., 2012. Satellite views of the Bohai Sea, Yellow Sea, and East China Sea,
- 2689 *Prog. Oceanogr.*, 104, 30–45, https://doi.org/10.1016/j.pocean.2012.05.001.
- Shimode, S., Takahashi, K., Shimizu, Y., Nonomura, T., Tsuda, A., 2012. Distribution and life
- 2691 history of the planktonic copepod, *Eucalanus californic*us, in the northwestern Pacific:
- Mechanisms for population maintenance within a high primary production area. *Prog.*
- 2693 Oceanogr., 96(1), 1–13, https://doi.org/10.1016/j.pocean.2011.08.002.
- Shore, J., Stacey, M.W. and Wright, D.G., 2008. Sources of eddy energy simulated by a model
- of the northeast Pacific Ocean. J. Phys. Oceanogr., 38(10), 2283–2293,
- 2696 https://doi.org/10.1175/2008JPO3800.1.

- 2697 Shotwell, S.K., Hanselman, D.H., Belkin, I.M., 2014. Toward biophysical synergy:
- 2698 Investigating advection along the Polar Front to identify factors influencing Alaska sablefish
- 2699 recruitment. *Deep Sea Res. II*, 107, 40–53. https://doi.org/10.1016/j.dsr2.2012.08.024.
- Shulman, I., Penta, B., Richman, J., Jacobs, G., Anderson, S., Sakalaukus, P., 2015. Impact of
- submesoscale processes on dynamics of phytoplankton filaments, *J. Geophys.*
- 2702 Res., 120, 2050–2062, https://doi.org/10.1002/2014JC010326
- Solomon, H., Ahlnäs, K., 1978. Eddies in the Kamchatka Current. Deep Sea Res. 25, 403–410.
- 2704 https://doi.org/10.1016/0146-6291(78)90566-0.
- Smith, K.S., 2007a. Eddy amplitudes in baroclinic turbulence driven by nonzonal mean flow:
- Shear dispersion of potential vorticity. *J. Phys. Oceanogr.* 37, 1037–1050,
- 2707 https://doi.org/10.1175/JPO3030.1.
- 2708 Smith, K.S., 2007b. The geography of linear baroclinic instability in Earth's oceans. *J. Mar.*
- 2709 Res. 65, 655–683, https://doi.org/10.1357/002224007783649484.
- 2710 Son, Y.T., Lee, S.H., Choi, B.J., Lee, J.C., 2010. Frontal structure and thermohaline intrusions
- in the South Sea of Korea from observed data and a relocation method. J. Geophys. Res. 115,
- 2712 C02011, https://doi.org/10.1029/2009JC005266.
- 2713 Song, H., Miller, A.J., Cornuelle, B.D., Di Lorenzo, E., 2011. Changes in upwelling and its
- water sources in the California Current System driven by different wind forcing. *Dyn.*
- 2715 Atmos. Oceans, 52(1–2) 170–191, https://doi.org/10.1016/j.dynatmoce.2011.03.001
- 2716 Song, H., Long, M.C., Gaube, P., Frenger, I., Marshall, J., McGillicuddy, D.J. Jr., 2018.
- Seasonal variation in the correlation between anomalies of sea level and chlorophyll in the
- 2718 Antarctic Circumpolar Current. *Geophys. Res. Lett.*, 45, 5011–5019.
- 2719 https://doi.org/10.1029/2017GL076246
- 2720 Spall, M.A., 2000. Generation of strong mesoscale eddies by weak ocean gyres. J. Mar. Res. 58,
- **2721** 97–116, https://doi.org/10.1357/002224000321511214.
- 2722 Springer, A.M., McRoy, C.P., Flint, M.V., 1996. The Bering Sea Green Belt: shelf edge
- processes and ecosystem production. Fish. Oceanogr., 5, 205–223,
- 2724 https://doi.org/10.1111/j.1365-2419.1996.tb00118.x.

- 2725 Stabeno, P.J., Reed, R.K., Overland, J.E., 1994. Lagrangian measurements in the Kamchatka
- 2726 Current and Oyashio. *J. Oceanogr.*, 50, 653–662. https://doi.org/10.1007/bf02270498.
- 2727 Stabeno, P.J., Shumacher, J.D., Ohtani, K., 1999. Physical oceanography of the Bering Sea. In:
- Loughlin, T.R., Ohtani, K. (Eds.), Dynamics of the Bering Sea, Alaska Sea Grant, University
- of Alaska Fairbanks, pp. 1–28.
- 2730 Stammer, D., 1998. On eddy characteristics, eddy transports, and mean flow properties. *J. Phys.*
- **2731** *Oceanogr.* 28, 727–739, https://doi.org/10.1175/1520-
- **2732** 0485(1998)028<0727:OECETA>2.0.CO;2.
- 2733 Stammer, D., Wunsch, C., 1999. Temporal changes in eddy energy of the oceans. *Deep Sea Res*.
- 2734 *II*, 46, 77–108, https://doi.org/10.1016/S0967-0645(98)00106-4.
- 2735 Stegmann, P.M., Schwing, F., 2007. Demographics of mesoscale eddies in the California
- 2736 Current. *Geophys. Res. Lett.*, 34, L14602, https://doi.org/10.1029/2007GL029504.
- 2737 Sterling, J.T., Springer, A.M., Iverson, S.J., Johnson, S.P., Pelland, N.A., Johnson, D.S., Lea,
- 2738 M.-A., Bond, N.A., 2014, The Sun, Moon, Wind, and Biological Imperative-Shaping
- 2739 Contrasting Wintertime Migration and Foraging Strategies of Adult Male and Female
- Northern Fur Seals (*Callorhinus ursinus*). *PLoS ONE* 9(4), e93068,
- 2741 https://doi.org/10.1371/journal.pone.0093068.
- 2742 Stockhausen, W.T., Coyle, K.O., Hermann, A.J., Doyle, M., Gibson, G., Hinckley, S., Ladd, C.,
- Parada, C., 2019. Running the Gauntlet: Connectivity between natal and nursery areas for
- Pacific ocean perch (*Sebastes alutus*) in the Gulf of Alaska, as inferred from a biophysical
- 2745 Individual-based Model. Deep Sea Res. II., 165, 74–88,
- 2746 https://doi.org/10.1016/j.dsr2.2018.05.016.
- 2747 Strub, P.T., James, C., 2000. Altimeter-derived variability of surface velocities in the California
- 2748 Current System: 2. Seasonal circulation and eddy statistics. *Deep-Sea Res. II*, 47, 831–870,
- 2749 https://doi.org/10.1016/S0967-0645(99)00129-0.
- 2750 Strub, P.T., James, C., Thomas, A.C., Abbott, M.R., 1990. Seasonal and nonseasonal variability
- of satellite-derived surface pigment concentration in the California Current. J. Geophys.
- 2752 *Res.*, 95, 11501–11530, https://doi.org/10.1029/JC095iC07p11501.

- 2753 Stukel, M.R., Aluwihare, L.I., Barbeau, K.A., Chekalyuk, A.M., Goericke, R., Miller, A.J.,
- Ohman, M.D., Ruacho, A., Song, H., Stephens, B.M., Landry, M.R., 2017. Mesoscale ocean
- fronts enhance carbon export due to gravitational sinking and subduction. *Proc. Natl. Acad.*
- 2756 *Sci.*, 114, 1252–1257, https://doi.org/10.1073/pnas.1609435114.
- 2757 Sugimoto, T., Kawasaki, Y., Li, J., 1992. A description of the time-dependent hydrographic
- structure of the warm streamer around the Kuroshio warm-core ring 86B. *Deep Sea Res. A*,
- 2759 39, S77–S96. https://doi.org/10.1016/s0198-0149(11)80006-3.
- 2760 Sugimoto, T., Tameishi, H., 1992. Warm-core rings, streamers and their role on the fishing
- ground formation around Japan. *Deep Sea Res. A*, 39, S183–S201.
- 2762 https://doi.org/10.1016/S0198-0149(11)80011-7.
- Sugimoto, S., Hanawa, K., 2012. Relationship between the path of the Kuroshio in the south of
- Japan and the path of the Kuroshio Extension in the east. J. Oceanogr., 68, 219–225.
- 2765 https://doi.org/10.1007/s10872-011-0089-1.
- 2766 Swaters, G.E., Mysak, L.A., 1985. Topographically-induced baroclinic eddies near a coastline,
- with application to the Northeast Pacific. J. Phys. Oceanogr., 15 (11), 1470–1485,
- 2768 https://doi.org/10.1175/1520-0485(1985)015<1470:TIBENA>2.0.CO;2.
- 2769 Syah, A.F., Saitoh, S., Alabia, I., Hirawake, T., 2016. Predicting potential fishing zones for
- Pacific saury (*Cololabis saira*) with maximum entropy models and remotely sensed data.
- 2771 Fish. Bull., 114, 330–342, https://doi.org/10.7755/FB.114.3.6.
- Tabata, S., 1982. The anticyclonic, baroclinic eddy off Sitka, Alaska in the Northeast Pacific
- 2773 Ocean. J. Phys, Oceanogr., 12(11), 1260–1282, https://doi.org/10.1175/1520-
- 2774 0485(1982)012<1260:TABEOS>2.0.CO;2.
- Tai, C.-T., White, W.B., 1990. Eddy variability in the Kuroshio Extension as revealed by
- 2776 GEOSAT altimetry: Energy propagation away from the jet, Reynolds stress, and seasonal
- 2777 cycle. J. Phys. Oceanogr., 20, 1761–1777, https://doi.org/10.1175/1520-
- **2778** 0485(1990)020<1761:EVITKE>2.0.CO;2.
- 2779 Takematsu, M., Ostrovskii, A.G., Nagano, Z, 1999. Observations of eddies in the Japan Basin
- 2780 interior. J. Oceanogr., 55(2), 237–246, https://doi.org/10.1023/A:1007846114165.

- Talley, L.D., Lobanov, V., Ponomarev, V., Salyuk, A., Tishchenko, P., Zhabin, I., Riser, S.,
- 2782 2003. Deep convection and brine rejection in the Japan Sea. *Geophys. Res. Lett.*, 30(4),
- 2783 1159–1162. https://doi.org/10.1029/2002GL016451.
- Tanaka, T., Yasuda, I., Kuma K., Nishioka J., 2012. Turbulent iron flux sustains Green Belt
- along the shelf break in the southeastern Bering Sea. *Geophys. Res. Lett.*, 39, L08603,
- 2786 https://doi.org/10.1029/2012GL051164.
- 2787 Tanaka, T., Yasuda, I., Onishi, H., Ueno, H., Masujima M., 2015. Observations of current and
- mixing around the shelf break in Pribilof Canyon in the Bering Sea, J. Oceanogr., 71, 1–
- 2789 17, https://doi.org/10.1007/s10872-014-0256-2.
- 2790 Tanaka, T., Yasuda, I., Kuma K., Nishioka J., 2017. Evaluation of the biogeochemical impact of
- iron-rich shelf water to the Green Belt in the southeastern Bering Sea. Cont. Shelf Res.,
- 2792 143, 130–138, http://dx.doi.org/10.1016/j.csr.2016.11.008.
- 2793 Teo, S.L.H., Block, B.A., 2010. Comparative influence of ocean conditions on yellowfin and
- Atlantic bluefin tuna catch from longlines in the Gulf of Mexico. *PLoS ONE*, 5, e10756,
- 2795 https://doi.org/10.1371/journal.pone.0010756
- 2796 Terazaki, M.,1992. Horizontal and vertical distribution of chaetograths in a Kuroshio warm-
- 2797 core ring. *Deep Sea Res. A*, 39, S231–S245, https://doi.org/10.1016/S0198-0149(11)80014-
- **2798** 2.
- Thomson, R.E., Gower, J.F.R., 1998. A basin-scale oceanic instability event in the Gulf of
- 2800 Alaska. J. Geophys. Res., 103(C2), 3033–3040, https://doi.org/10.1029/97JC03220.
- Tomosada, A., 1986. Generation and decay of Kuroshio warm-core rings. *Deep Sea Res. A*, 33,
- 2802 1475–1486, https://doi.org/10.1016/0198-0149(86)90063-4.
- Trenberth, K.E., Hurrell, J.W., 1994. Decadal atmosphere-ocean variations in the Pacific. Clim.
- 2804 *Dyn.* 9, 303–319, https://doi.org/10.1007/BF00204745.
- 2805 Trusenkova, O.O., Kaplunenko, D.D., 2022. Intra-Annual Sea Level Fluctuations and
- Variability of Mesoscale Processes in the Northern Japan/East Sea From Satellite Altimetry
- 2807 Data. Front. Mar. Sci. 9:866328, https://doi.org/10.3389/fmars.2022.866328.

- 2808 Trusenkova, O.O., Nikitin, A.A., Lobanov, V.B., 2009. Circulation features in the Japan/East
- Sea related to statistically obtained wind patterns in the warm season. J. Mar. Sys., 78(2),
- 2810 214–225, https://doi.org/10.1016/j.jmarsys.2009.02.019.
- Tsuda, A., Nemoto T., 1992. Distribution and growth of salps in a Kuroshio warm-core ring
- during summer 1987. *Deep Sea. Res. A*, 39, S219–S229, https://doi.org/10.1016/S0198-
- 2813 0149(11)80013-0.
- 2814 Uchimoto, K., Mitsudera, H., Ebuchi, N., Miyazawa, Y., 2007. Anticyclonic Eddy Caused by
- the Soya Warm Current in an Okhotsk OGCM. J. Oceanogr., 63, 379–391,
- 2816 https://doi.org/10.1007/s10872-007-0036-3.
- Ueno, H., Freeland, H.J., Crawford, W.R., Onishi, H., Oka, E., Sato, K., Suga, T., 2009.
- Anticyclonic eddies in the Alaskan Stream. J. Phys. Oceanogr. 39, 934–951,
- 2819 https://doi.org/10.1175/2008JPO3948.1.
- 2820 Ueno, H., Crawford, W.R., Onishi, H., 2010. Impact of Alaskan Stream eddies on chlorophyll a
- distribution in the western and central subarctic North Pacific, *J. Oceanogr.*, 66, 319–328,
- 2822 https://doi.org/10.1007/s10872-010-0028-6
- Ueno, H., Yasuda, I., Itoh, S., Onishi, H., Hiroe, Y., Suga, T., Oka E., 2012. Modification of a
- Kenai eddy along the Alaskan Stream, J. Geophys. Res., 117, C08032,
- 2825 https://doi.org/10.1029/2011JC007506.
- Ueno, H., Oda, M., Yasui, K., Dobashi, R., Mitsudera, H., 2022. Global distribution and
- interannual variation in the winter halocline, J. Phys. Oceanogra., 52(4), 665-676,
- 2828 https://doi.org/10.1175/JPO-D-21-0056.1.
- Usui, N., Tsujino, H., Fujii, Y., Kamachi M., 2008. Generation of a trigger meander for the
- 2830 2004 Kuroshio large meander, *J. Geophys. Res.*, 113, C01012,
- 2831 https://doi.org/10.1029/2007JC004266.
- Vaillancourt, R.D., Marra, J., Seki, M.P., Parsons, M.L., Bidigare, R.R., 2003. Impact of a
- 2833 cyclonic eddy on phytoplankton community structure and photosynthetic competency in the
- subtropical North Pacific Ocean. Deep Sea Res. I, 50(7), 829–847,
- 2835 https://doi.org/10.1016/S0967-0637(03)00059-1.

- Vaz, A.C., Richards, K.J., Jia, Y., Paris, C.B., 2013. Mesoscale flow variability and its impact
- on connectivity for the island of Hawaii. *Geophys. Res. Lett.*, 40(2), 332–337,
- 2838 https://doi.org/10.1029/2012GL054519.
- Venrick, E.L., 1990. Mesoscale patterns of chlorophyll a in the central North Pacific. Deep Sea
- 2840 Res. A., 37(6), 1017–1031, https://doi.org/10.1016/0198-0149(90)90108-8.
- Vélez-Belchí, P., Centurioni, L.R., Lee, D.-K., Jan, S., Niiler, P.P., 2013. Eddy induced
- 2842 Kuroshio intrusions onto the continental shelf of the East China Sea. J. Mar. Res., 71(1–2),
- 2843 83–107, https://doi.org/10.1357/002224013807343470.
- Wakatsuchi, M., Martin, S., 1990. Satellite Observations of the Ice Cover of the Kuril Basin
- Region of the Okhotsk Sea and Its Relation to the Regional Oceanography. J. Geophys. Res.,
- 2846 95, 13393–13410, https://doi.org/10.1029/JC095iC08p13393.
- Wakatsuchi, M., Ohshima, K.I., 1990. Observations of ice-ocean eddy streets in the Sea of
- Okhotsk off the Hokkaido coast using radar images. J. Phys. Oceanogr., 20, 585–594,
- 2849 https://doi.org/10.1175/1520-0485(1990)020<0585:OOIOES>2.0.CO;2.
- Wakatsuchi, M., Martin, S., 1991. Water circulation in the Kuril basin of the Okhotsk Sea and
- its relation to eddy formation. J. Oceanogr. Soc. Japan., 47, 152–168.
- 2852 https://doi.org/10.1007/BF02301064.
- Wang, S., Liu, Z., Pang, C., Liu, H., 2016. The decadally modulating eddy field in the upstream
- 2854 Kuroshio Extension and its related mechanisms. *Acta Oceanol. Sin.* 35, 9–17,
- 2855 https://doi.org/10.1007/s13131-015-0741-5
- Weiss, J., 1991. The dynamics of enstrophy transfer in two dimensional hydrodynamics,
- 2857 *Physica D*, 48, 273–294, https://doi.org/10.1016/0167-2789(91)90088-Q.
- 2858 Whitney, F., Robert, M., 2002. Structure of Haida eddies and their transport of nutrient from
- coastal margins into the NE Pacific Ocean. J. Oceanogr., 58(5), pp.715–723,
- 2860 https://doi.org/10.1023/A:1022850508403.
- Wiebe, P.H., Hulburt, E.M., Carpenter, E.J., Jahn, A.E., Knapp, G.P. III, Boyd, S.H., Ortner,
- P.B., Cox, J.L., 1976. Gulf Stream cold core rings: large-scale interaction sites for open

- ocean plankton communities. Deep Sea Res. Oceanogr. Abst., 23, 695–710,
- 2864 https://doi.org/10.1016/S0011-7471(76)80015-0
- Wong, G.T.F., Zhang, L.S., 2003. Geochemical dynamics of iodine in marginal seas: the
- 2866 southern East China Sea. *Deep Sea Res. II*, 50, 1147–1162. https://doi.org/10.1016/s0967-
- 2867 0645(03)00015-8
- 2868 Wyllie, J., 1966. Geostrophic flow of the California Current at the surface and at 200 meters,
- 2869 Calif. Coop. Ocean. Fish. Invest, Atlas 4.
- 2870 https://www.calcofi.org/publications/atlases/CalCOFI Atlas 04.pdf
- Xiu, P., Palacz, A.P., Chai, F., Roy, E.G., Wells, M.L., 2011. Iron flux induced by Haida eddies
- in the Gulf of Alaska. Geophys. Res. Lett., 38(13), L13607,
- 2873 https://doi.org/10.1029/2011GL047946.
- Yamada, K., Ishizaka, J., Yoo, S., Kim, H., Chiba, S., 2004. Seasonal and interannual variability
- of sea surface chlorophyll a concentration in the Japan/East Sea (JES), *Prog. Oceanogr.*, 61,
- 2876 193–211, https://doi.org/10.1016/j.pocean.2004.06.001.
- 2877 Yamada, K., Ishizaka, J., Nagata, H., 2005. Spatial and Temporal Variability of Satellite
- 2878 Primary Production in the Japan Sea from 1998 to 2002, *J. Ocenogr.*, 61(5), 857–869,
- 2879 https://doi.org/10.1007/s10872-006-0005-2.
- 2880 Yamamoto, T., Nishizawa S., 1986. Small-scale zooplankton aggregations at the front of a
- 2881 Kuroshio warm-core ring, *Deep Sea Res. A*, 33(11–12), 1729–1740,
- 2882 https://doi.org/10.1016/0198-0149(86)90076-2.
- Yang, G., Wang, F., Li, Y., Lin P., 2013. Mesoscale eddies in the northwestern subtropical
- Pacific Ocean: Statistical characteristics and three-dimensional structures, *J. Geophys. Res.*,
- 2885 118, 1906–1925, https://doi.org/10.1002/jgrc.20164.
- Yang, Y.J., Kim, S.H., Rho, H.K. 1998. A study on the temperature fronts observed in the
- South-West Sea of Korea and the northern area of the East China Sea. *Korean J. Fish Aquat*.
- 2888 *Sci.* 31, 695–706. (in Korean, with English Abstr.)
- Yang, Y., San Liang, X., 2018. On the Seasonal Eddy Variability in the Kuroshio Extension. J.
- 2890 *Phys. Oceanogr.* 48, 1675–1689, https://doi.org/10.1175/JPO-D-18-0058.1.

- 2891 Yasuda, I., Okuda, K., Hirai, M., 1992. Evolution of a Kuroshio Warm-Core Ring.- Variability
- of the Hydrographic Structure, *Deep Sea Res. A*, 39, S131–S161,
- 2893 https://doi.org/10.1016/S0198-0149(11)80009-9
- Yasuda, I., Watanabe, Y., 1994. On the relationship between the Oyashio front and saury
- fishing grounds in the north-western Pacific, Fish. Oceanogr., 3, 172–181,
- 2896 https://doi.org/10.1111/j.1365-2419.1994.tb00094.x.
- Yasuda, I., Kitagawa, D., 1996. Locations of early fishing grounds of saury in the North-
- 2898 western Pacific, Fish. Oceanogr., 5, 63–69, https://doi.org/10.1111/j.1365-
- **2899** 2419.1996.tb00018.x
- 2900 Yasuda, I., Okuda, K., Shimizu, Y., 1996. Distribution and modification of the North Pacific
- Intermediate Water in the Kuroshio-Oyashio Interfrontal zone., J. Phys. Oceanogr. 26, 448–
- 2902 465, https://doi.org/10.1175/1520-0485(1996)026<0448:DAMONP>2.0.CO;2.
- 2903 Yasuda, I., Ito, S., Shimizu, Y., Ichikawa, K., Ueda, K., Honma, T., Uchiyama, M., Watanabe,
- K., Suno, T., Tanaka K., Koizumi, K., 2000. Cold-core anti-cyclonic eddies south of the
- Bussol' Strait in the north-western Subarctic Pacific. J. Phys. Oceanogr., 30, 1137–1157,
- 2906 https://doi.org/10.1175/1520-0485(2000)030<1137:CCAESO>2.0.CO;2.
- 2907 Yasuda, I., 2003. Hydrographic structure and variability in the Kuroshio-Oyashio transition
- 2908 area. J. Oceanogr, 59, 389–402, https://doi.org/10.1023/A:1025580313836.
- 2909 Yin, Y., Lin, X., He, R., Hou, Y. 2017. Impact of mesoscale eddies on Kuroshio intrusion
- variability northeast of Taiwan, J. Geophys. Res., 122, 3021–3040,
- 2911 https://doi.org/10.1002/2016JC012263.
- 2912 Yin, Y., Lin, X., Hou, Y., 2019. Seasonality of the Kuroshio intensity east of Taiwan modulated
- 2913 by mesoscale eddies, *J. Mar. Sys.*, 193, 84–93,
- 2914 https://doi.org/10.1016/j.jmarsys.2019.02.001.
- 2915 Yoo, J. G., Kim, S.Y., Kim, H.S., 2018. Spectral descriptions of submesoscale surface
- circulation in a coastal region, J. Geophys. Res. Oceans 123(6), 4224–4249,
- 2917 https://doi.org/10.1029/2016JC012517

- Yoo, S., Park, J., 2009. Why is the southwest the most productive region of the East Sea/Sea of
- 2919 Japan? J. Mar. Sys., 78(2), 301–315, https://doi.org/10.1016/j.jmarsys.2009.02.014.
- Yoon, J.-H., Kim, Y.-J., 2009. Review on the seasonal variation of the surface circulation in the
- 2921 Japan/East Sea. J. Mar. Sys., 78(2), 226–236, https://doi.org/10.1016/j.jmarsys.2009.03.003.
- Yoshida, S., Qiu, B., Hacker, P., 2010. Wind-generated eddy characteristics in the lee of the
- island of Hawaii. *J. Geophys. Res.*, 115, C03019, https://doi.org/10.1029/2009JC005417.
- Yoshida, S., Qiu, B., Hacker P., 2011. Low-frequency eddy modulations in the Hawaiian Lee
- 2925 Countercurrent: Observations and connection to the Pacific Decadal Oscillation, *J. Geophys.*
- **2926** *Res.*, 116, C12009, https://doi.org/10.1029/2011JC007286.
- Yoshikawa, Y., Lee, C.M., Thomas, L.N., 2012. The subpolar front of the Japan/East Sea. Part
- 2928 III: Competing roles of frontal dynamics and atmospheric forcing in driving ageostrophic
- vertical circulation and subduction, *J. Phys. Oceanogr.*, 42(6), 991–1011,
- 2930 https://doi.org/10.1175/JPO-D-11-0154.1.
- Yuan, X., Talley, L.D., 1996. The subarctic frontal zone in the North Pacific: Characteristics of
- frontal structure from climatological data and synoptic surveys, *J. Geophys. Res.*, 101(C7),
- 2933 16491–16508, https://doi.org/10.1029/96JC01249.
- 2934 Zhabin, I.A., Abrosimova, A.A., Dubina, V.A., Nekrasov, D.A., 2010. Influence of the Amur
- River runoff on the hydrological conditions of the Amur Liman and Sakhalin Bay (Sea of
- Okhotsk) during the spring-summer flood. *Russ. Meteorol. Hydrol.*, 4, 295–300,
- 2937 https://doi.org/10.3103/S1068373910040084.
- 2938 Zhabin, I.A., Andreev, A.G., 2019. Interaction of Mesoscale and Submesoscale Eddies in the
- Sea of Okhotsk Based on Satellite Data. Izv. Atmos. Ocean. Phys., 55(9), 1114–1124,
- 2940 https://doi.org/10.1134/S0001433819090573.
- 2941 Zhai X., 2017. The annual cycle of surface eddy kinetic energy and its influence on eddy
- momentum fluxes as inferred from altimeter data. Satellite Oceanogr. Meteorol., 2(2), 299,
- 2943 http://dx.doi.org/10.18063/SOM.v2i2.299
- Zhang, D.X., Lee, T.N., Johns, W.E., Liu, C.T., Zantopp R., 2001. The Kuroshio east of
- Taiwan: Modes of variability and relationship to interior ocean mesoscale eddies, *J. Phys.*

2946 Oceanogr., 31(4), 1054–1074, https://doi.org/10.1175/1520 2947 0485(2001)031<1054:TKEOTM>2.0.CO;2.

Zhong, Y., Bracco, A., Tian, J., Dong, J., Zhao, W., Zhang, Z., 2017. Observed and simulated submesoscale vertical pump of an anticyclonic eddy in the South China Sea. *Sci. Rep.* 7, 44011, https://doi.org/10.1038/srep44011.

2955 Figures

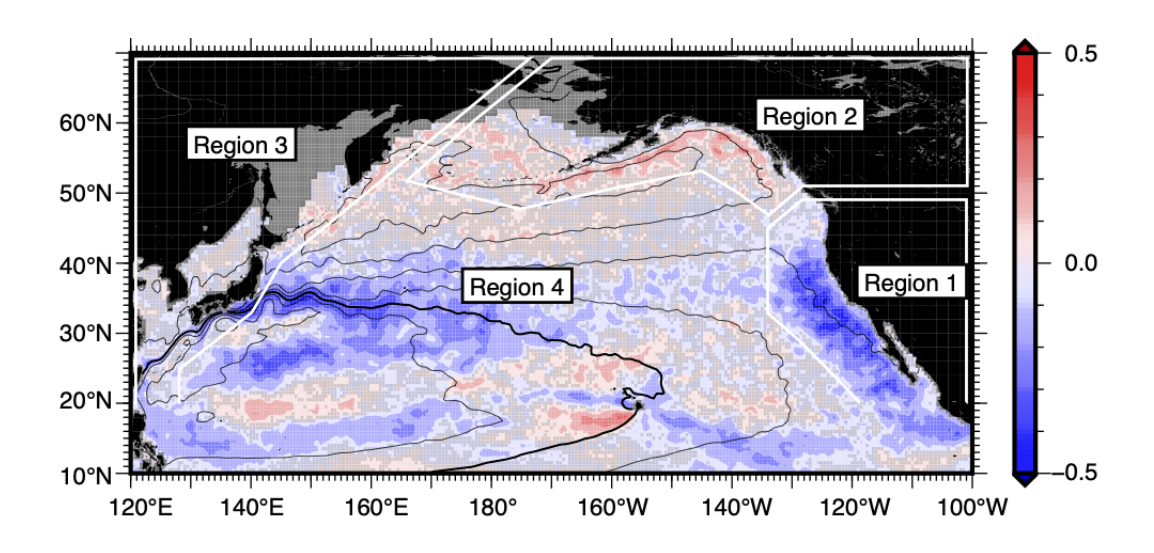


Fig. 1. Correlation between SSH anomaly and surface Chl-a anomaly corresponding to eddies from 1998 to 2012 (after Kouketsu et al. (2015)). SSH anomaly are high-pass-filtered (< 300 days) to remove long-term changes. Chl-a anomalies are logarithmic deviations from the weekly climatology calculated from 1998 to 2012 data. Gray areas denote insignificant correlations at a 90 % confidence level. Figure courtesy of S. Kouketsu. Adapted by permission from Springer Nature: Kouketsu et al. (2015).

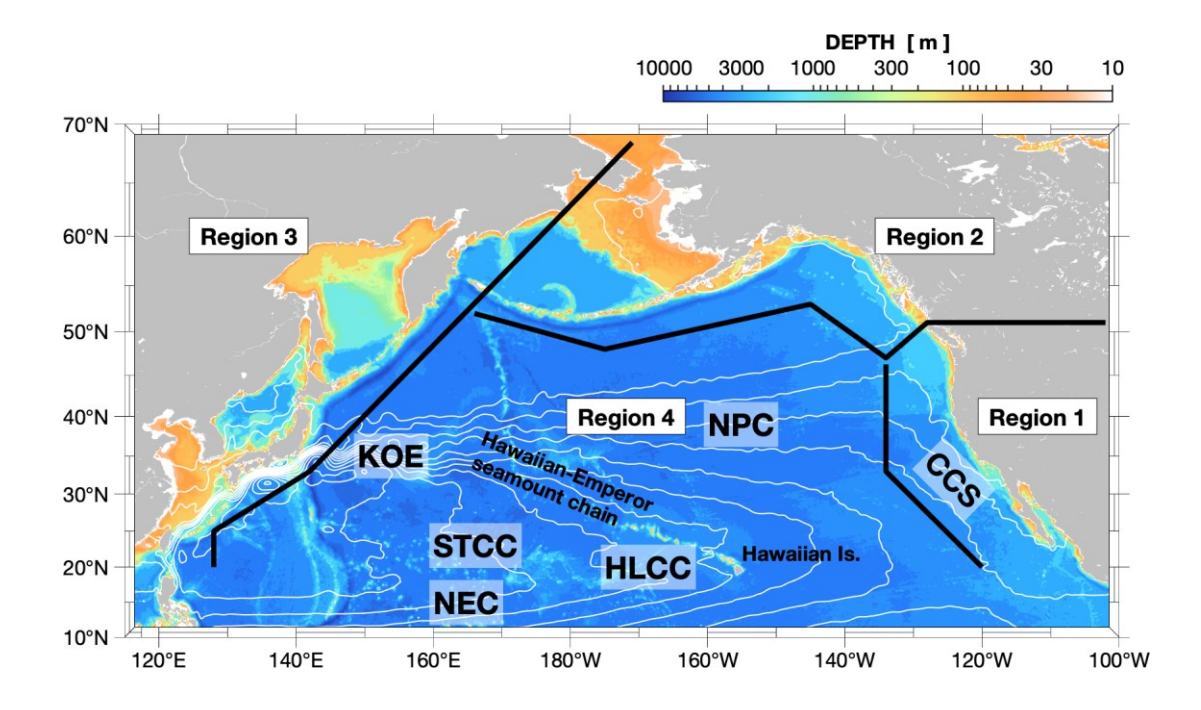


Fig. 2. Schematic representation for the circulation of the open North Pacific. The thin white contours, whose contour interval is 0.1 m, indicate the mean dynamic topography produced by CLS and distributed by Aviso+ with support from Cnes (https://www.aviso.altimetry.fr/), and downloaded from ftp://ftp-access.aviso.altimetry.fr/auxiliary/mdt/mdt_cnes_cls2013_global/. Acronyms used in this figure is as follows: North Pacific Current (NPC), Kuroshio and Oyashio Extension (KOE), Subtropical Counter Current (STCC), Hawaiian Lee Countercurrent (HLCC), North Equatorial Current (NEC) and California Current System (CCS).

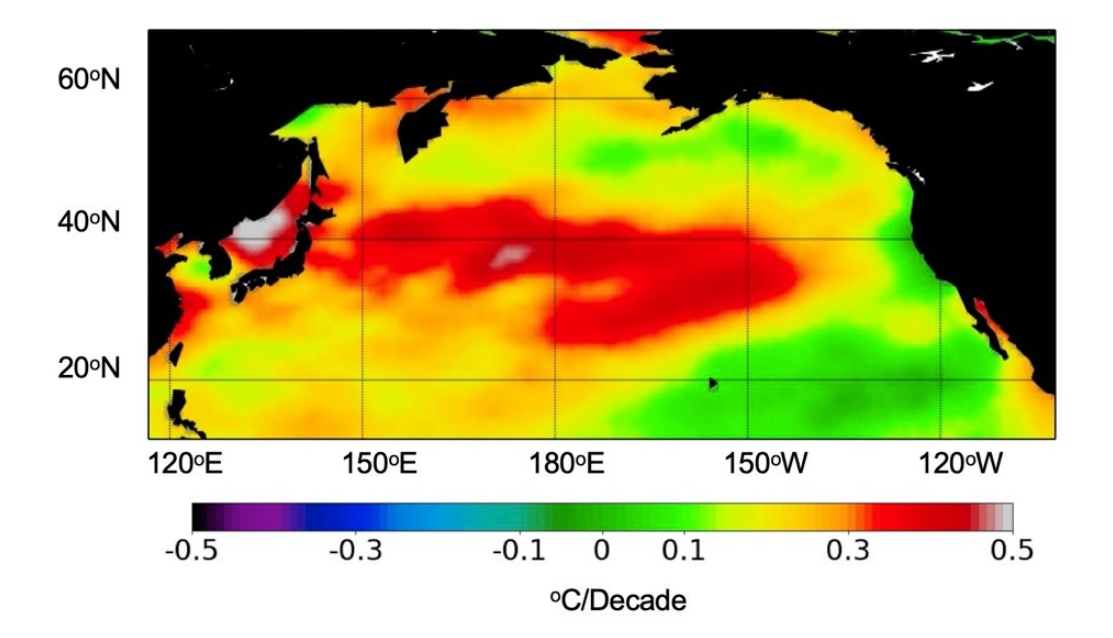
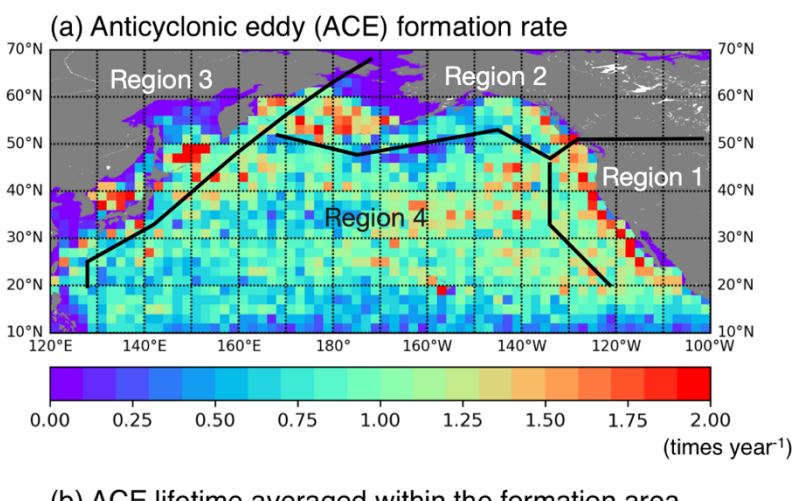
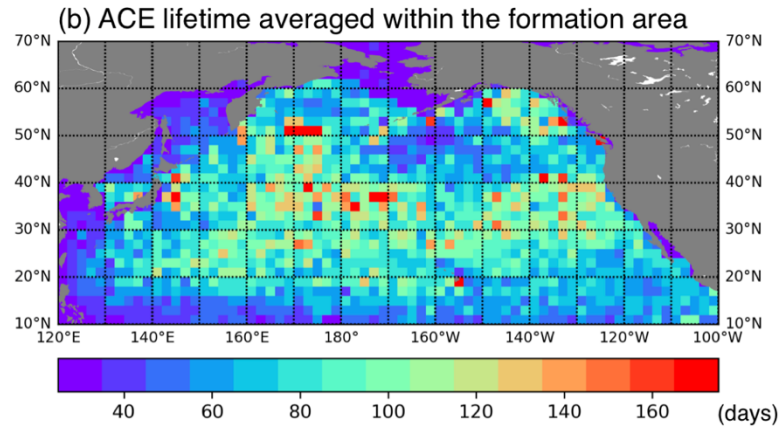


Fig. 3. Average linear trend over 1980-2018 in °C/decade in the COBE SST2 and Sea-Ice reanalysis (COBEv2; Hirahara et al., 2014). The COBEv2 data set was developed by the Japanese Meteorological Agency, covers the period since 1850 and has a spatial resolution of 1° latitude × 1° longitude. We note that the period considered, for which we have satellite measurements, is skewed towards a slight predominance of negative PDO conditions.





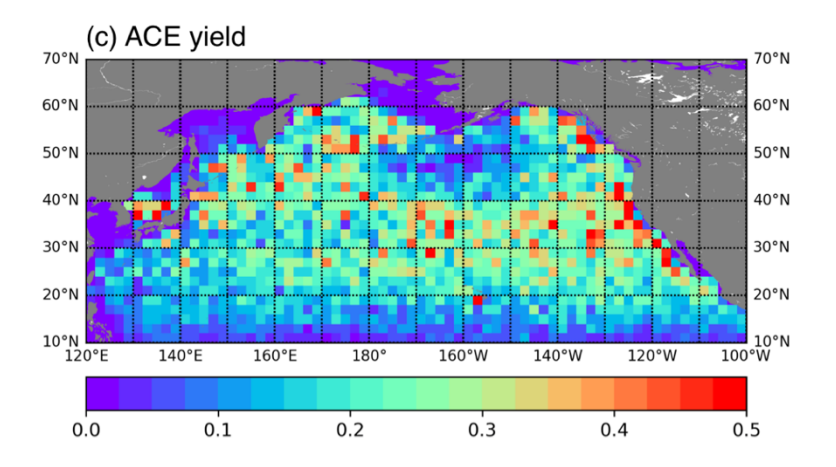
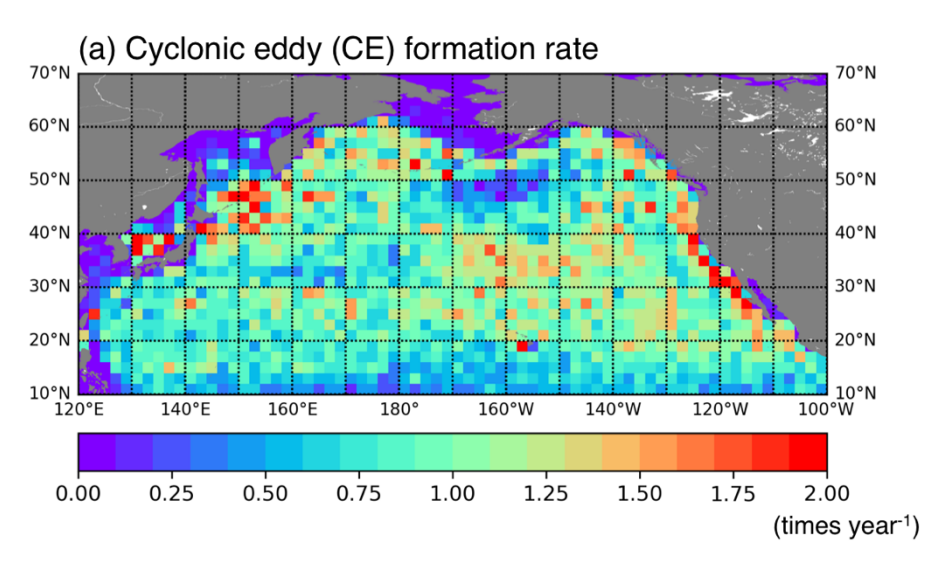
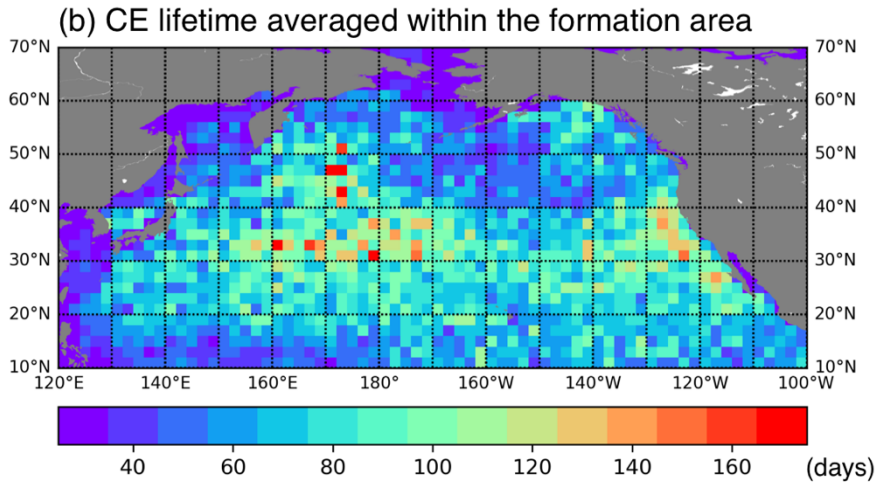


Fig. 4. Distribution of anticyclonic eddy (a) formation rate (times year⁻¹), (b) averaged lifetime (day) and (c) yield (sum of lifetime divided by 9149 days (01Jan1993–18Jan2018) for those formed in each 2°×2° box over 25 years.





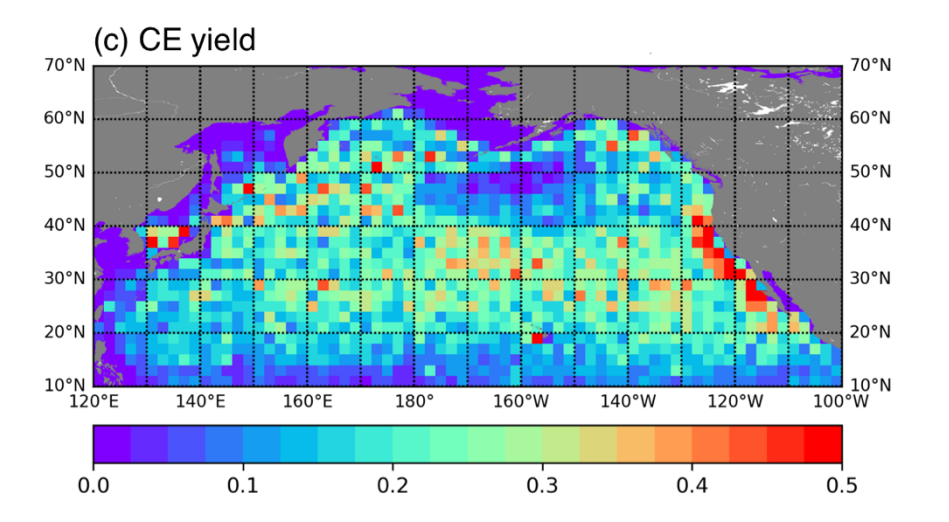


Fig. 5. Same as Fig. 4 but for cyclonic eddies.

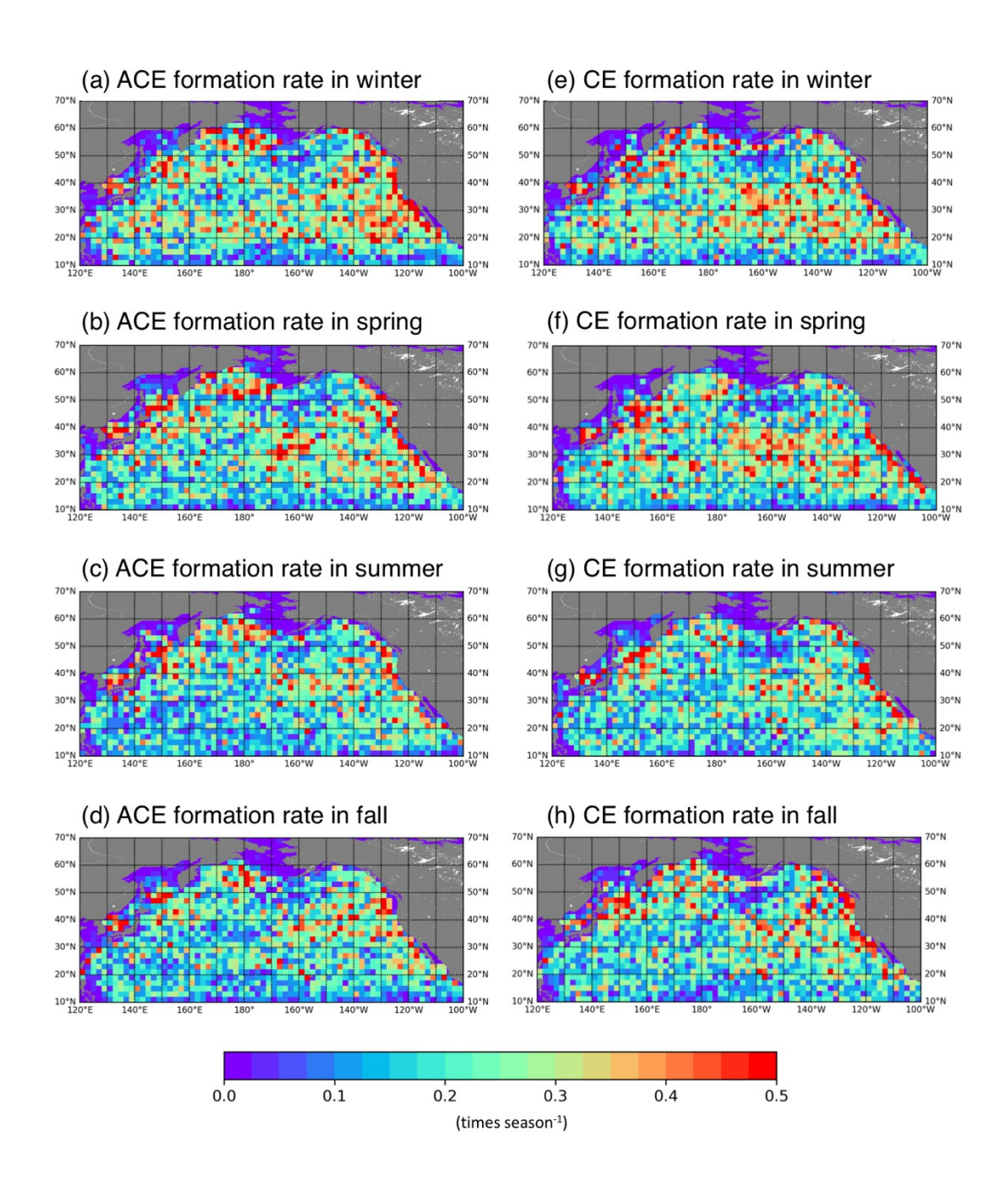


Fig. 6. Distribution of anticyclonic eddy formation rate (times season⁻¹) in (a) winter, (b) spring, (c) summer and (d) fall and cyclonic eddy formation in (e) winter, (f) spring, (g) summer and (h) fall at each 2°×2° grid from January 1, 1993 to January 18, 2018.

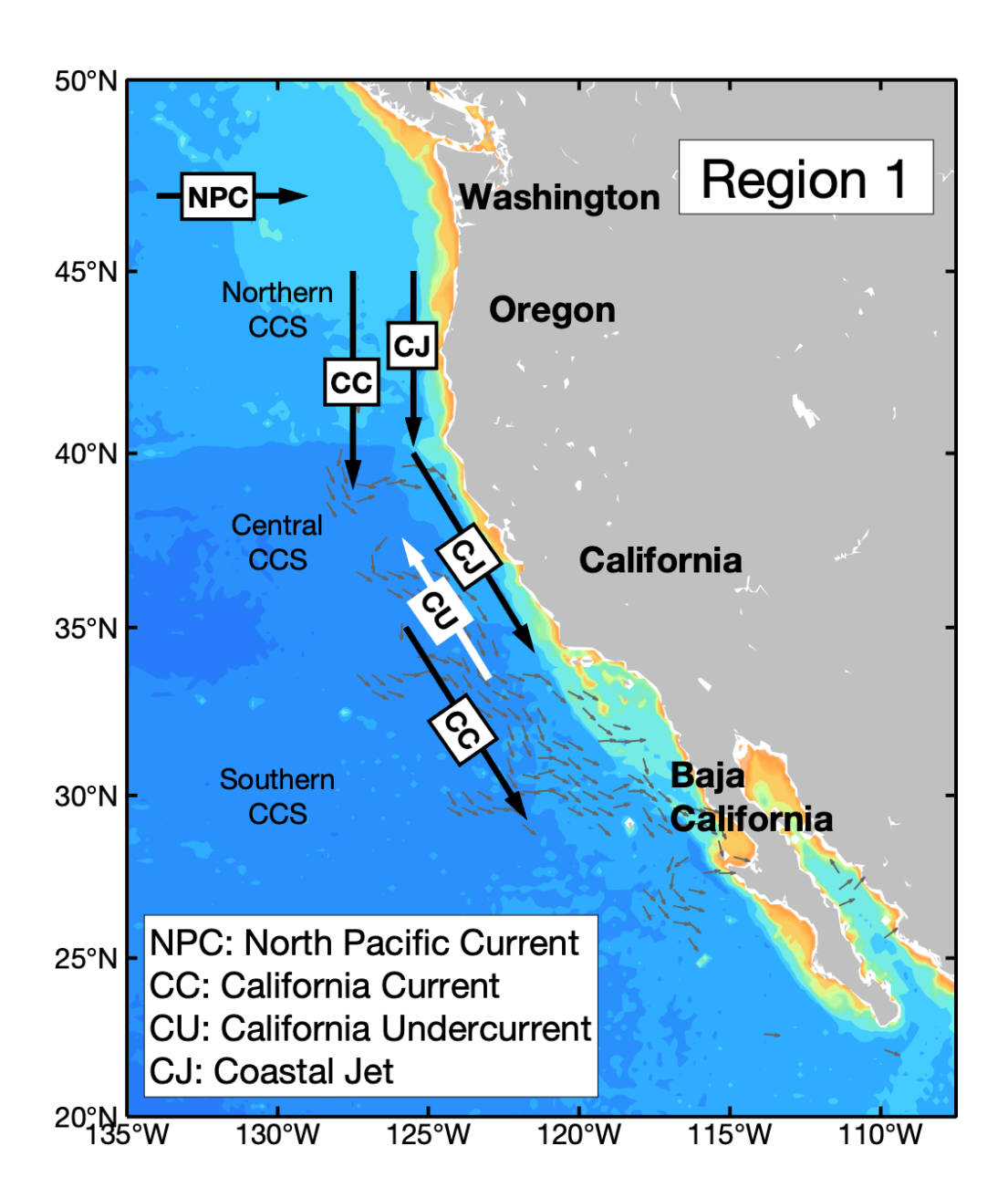


Fig. 7. Schematic representation for the currents of the CCS region (Region 1). Gray arrows indicate the direction of mean surface geostrophic velocity with speed greater than 0.05 m s⁻¹. Colors represent bottom topography (see Fig. 2). The mean geostrophic velocity data were produced by CLS (Collecte Localisation Satellites), distributed by Aviso+ with support from Cnes data center (https://www.aviso.altimetry.fr/), and downloaded from ftp://ftp-access.aviso.altimetry.fr/auxiliary/mdt/mdt cnes cls2013 global/.

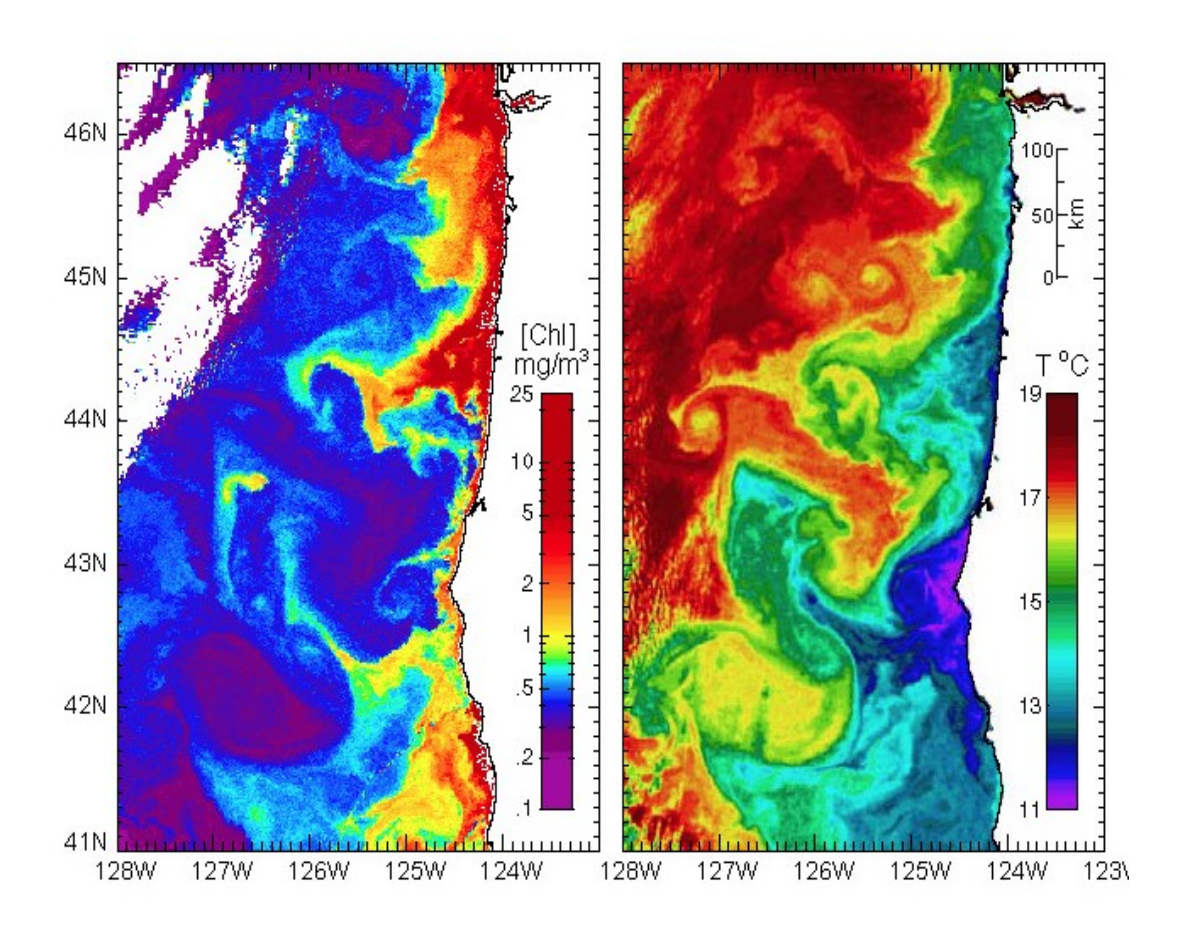


Fig. 8. Sea-surface temperature (right) and chlorophyll (left) measured by satellite along the U.S. west coast on September 26, 1998 (from Barth, 2007).

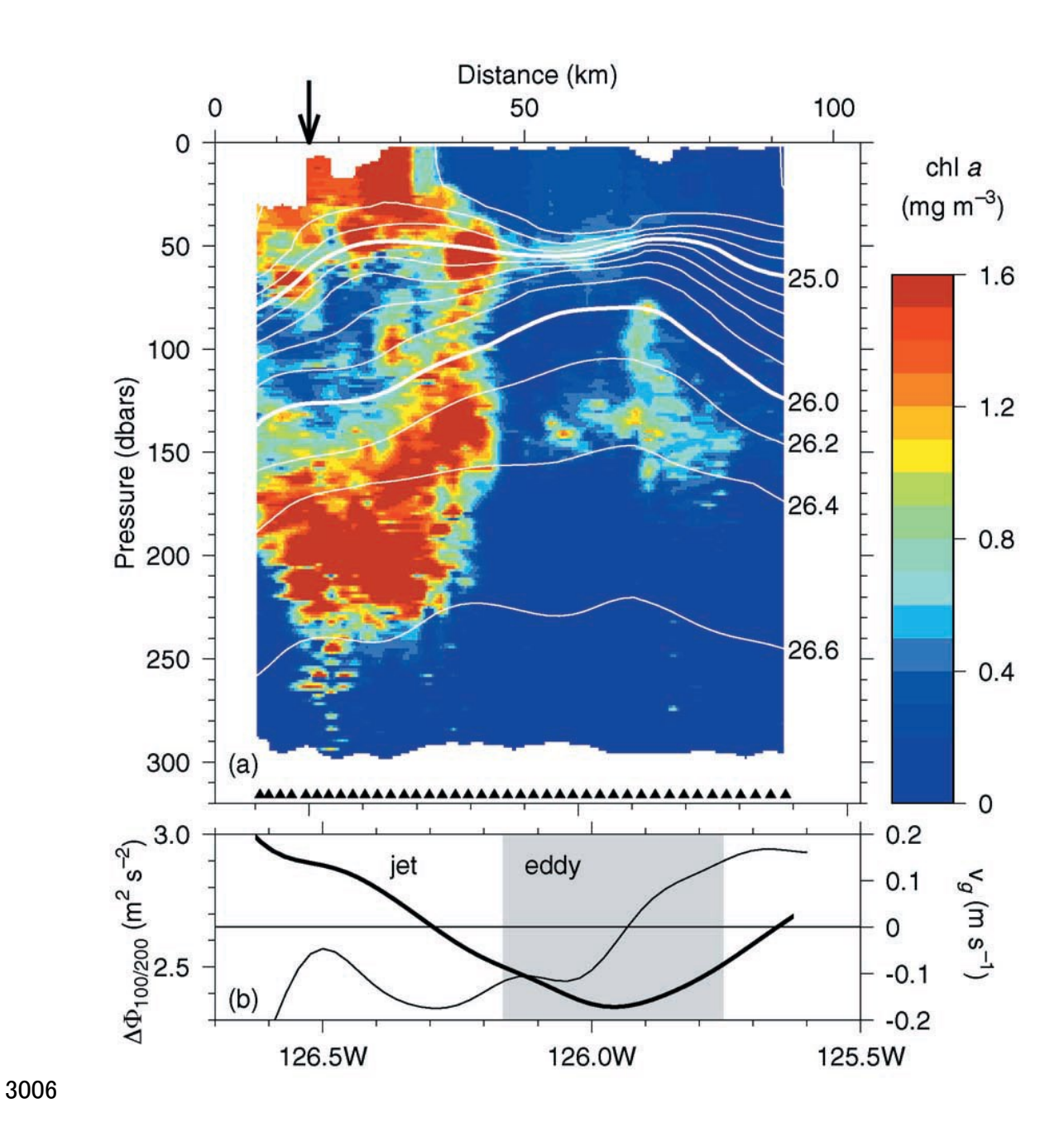


Fig. 9. (a) Vertical section of Chl a (mg m⁻³) derived from fluorescence (color) along 37.87°N on 30 June 1993 overlaid with contours of density anomaly (kg m⁻³). The locations of each SeaSoar up-down cycle are indicated by triangles along the bottom. (b) Geopotential anomaly at 100 m, $\Delta \phi_{100/200}$ (m² s⁻²) (thick curve), and 100 m north-south geostrophic velocity, v_g (m s⁻¹) (thin curve), both referenced to acoustic Doppler current profiler velocity at 200 m, along 37.87°N. From Barth et al. (2002).

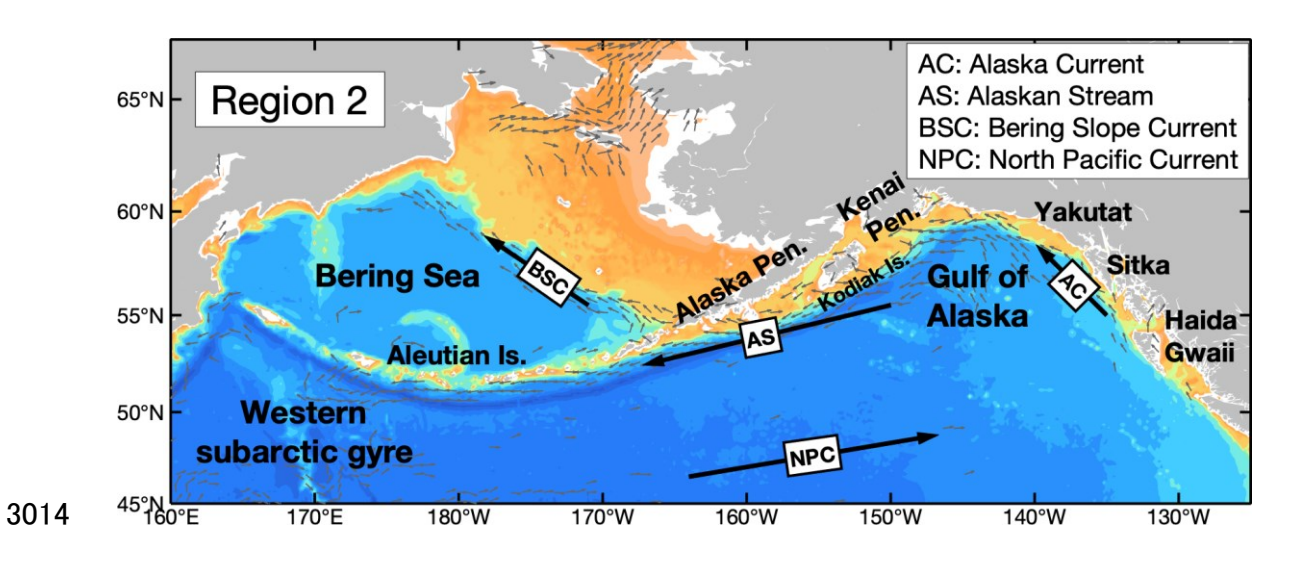


Fig. 10. The same as Fig. 7 but for the northeastern North Pacific and the Bering Sea (Region 2)

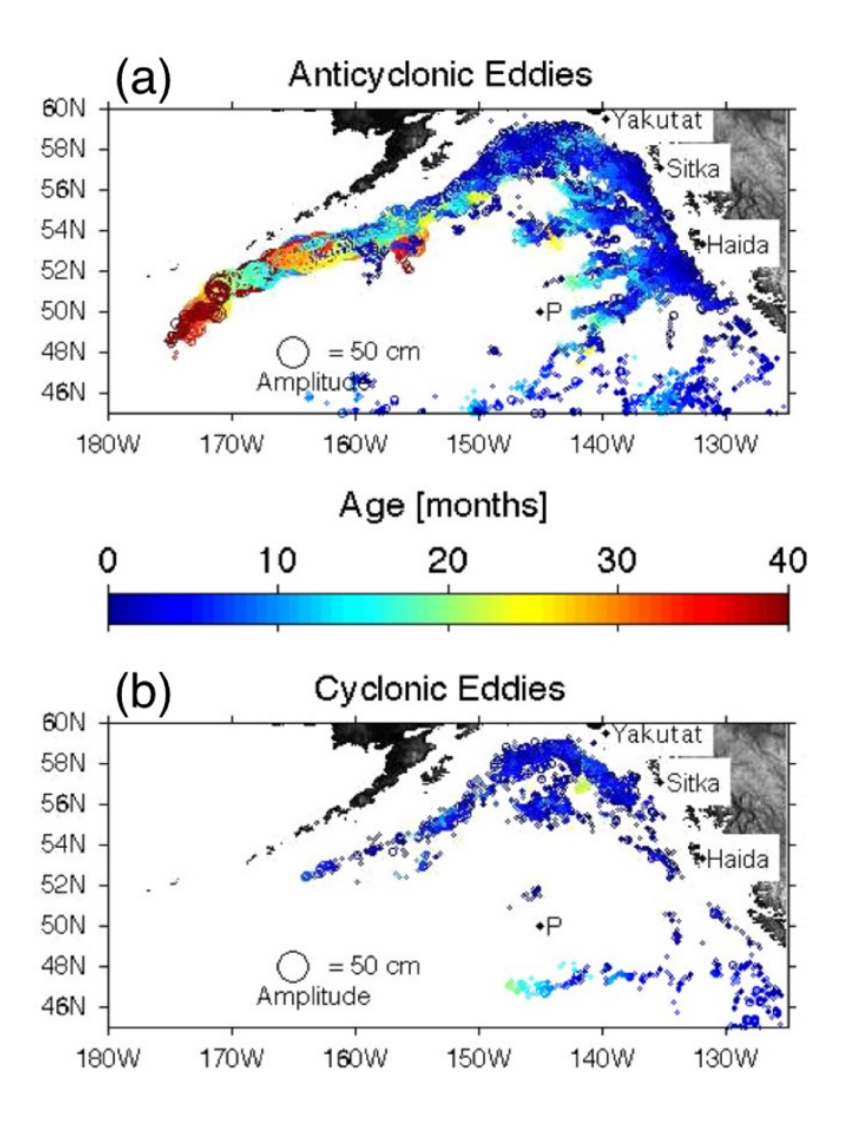


Fig. 11. Map of (a) anticyclonic and (b) cyclonic eddy amplitudes (circle radius), ages (color), from January 2003 to April 2012. From Lyman and Johnson (2015).

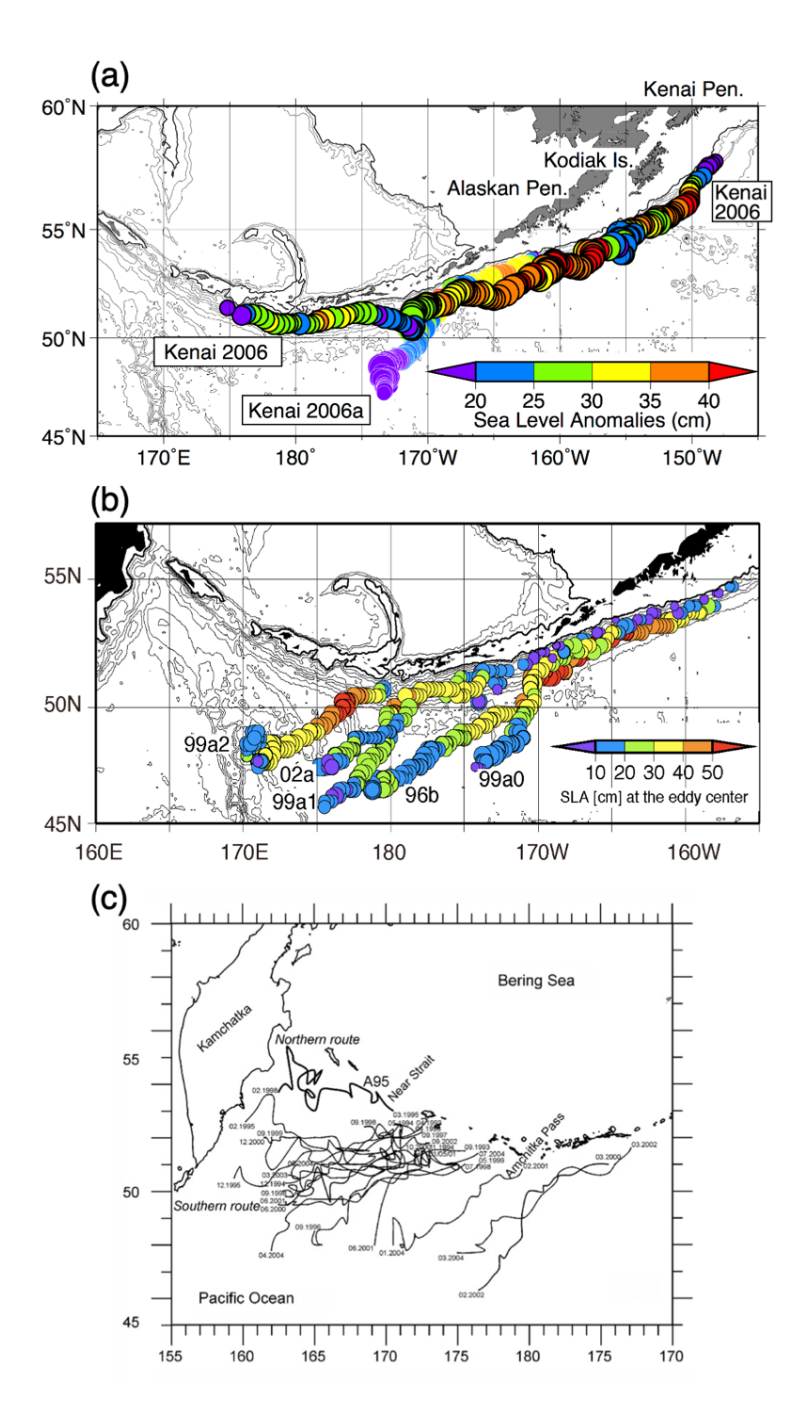


Fig. 12. (a) Trajectories of Kenai 2006 and Kenai 2006a (adapted from Ueno et al., 2012). Colors represent SLA (cm) at the eddy and the radius of each circle in the map mostly corresponds to an Okubo-Weiss radius. (b) Trajectories of long-lived Alaskan Stream eddies propagating westward along the Alaskan Stream (after Ueno et al., 2009, © American Meteorological Society). Shading represents sea level anomalies (cm) at the eddy center. (c) The track of Aleutian eddies, based on mesoscale altimetry (reprinted from Rogachev et al., 2007, with permission from Elsevier).

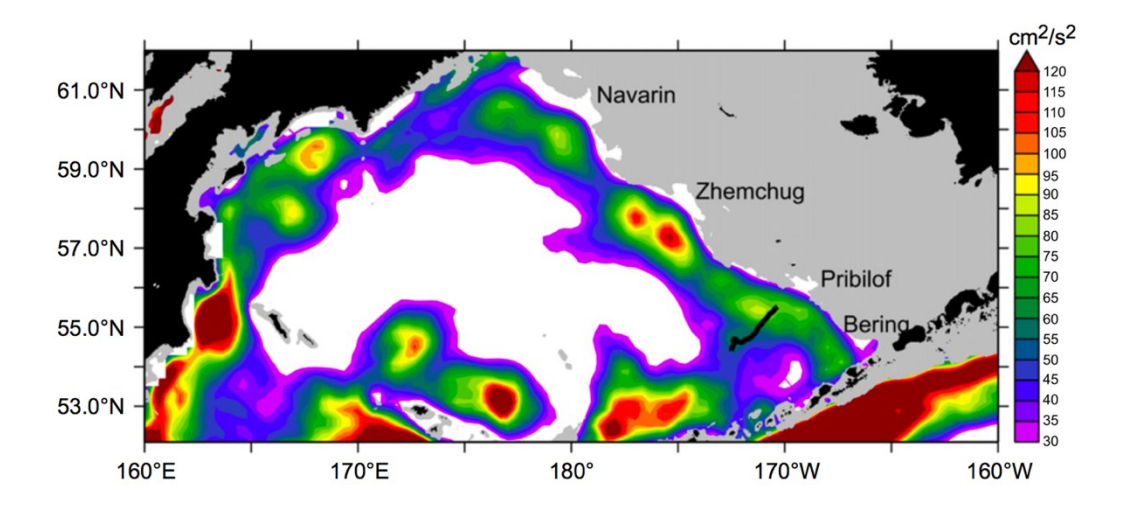


Fig. 13. (a) EKE (cm² s⁻²) averaged over full years (1993–2009) calculated from AVISO altimetry data. Gray shading denotes shelf (< 200 m). Black line shows trajectory of 1997 Pribilof Eddy (15 June–27 August 1997) calculated from drifters. Reprinted from Ladd et al. (2012), with permission from Elsevier.

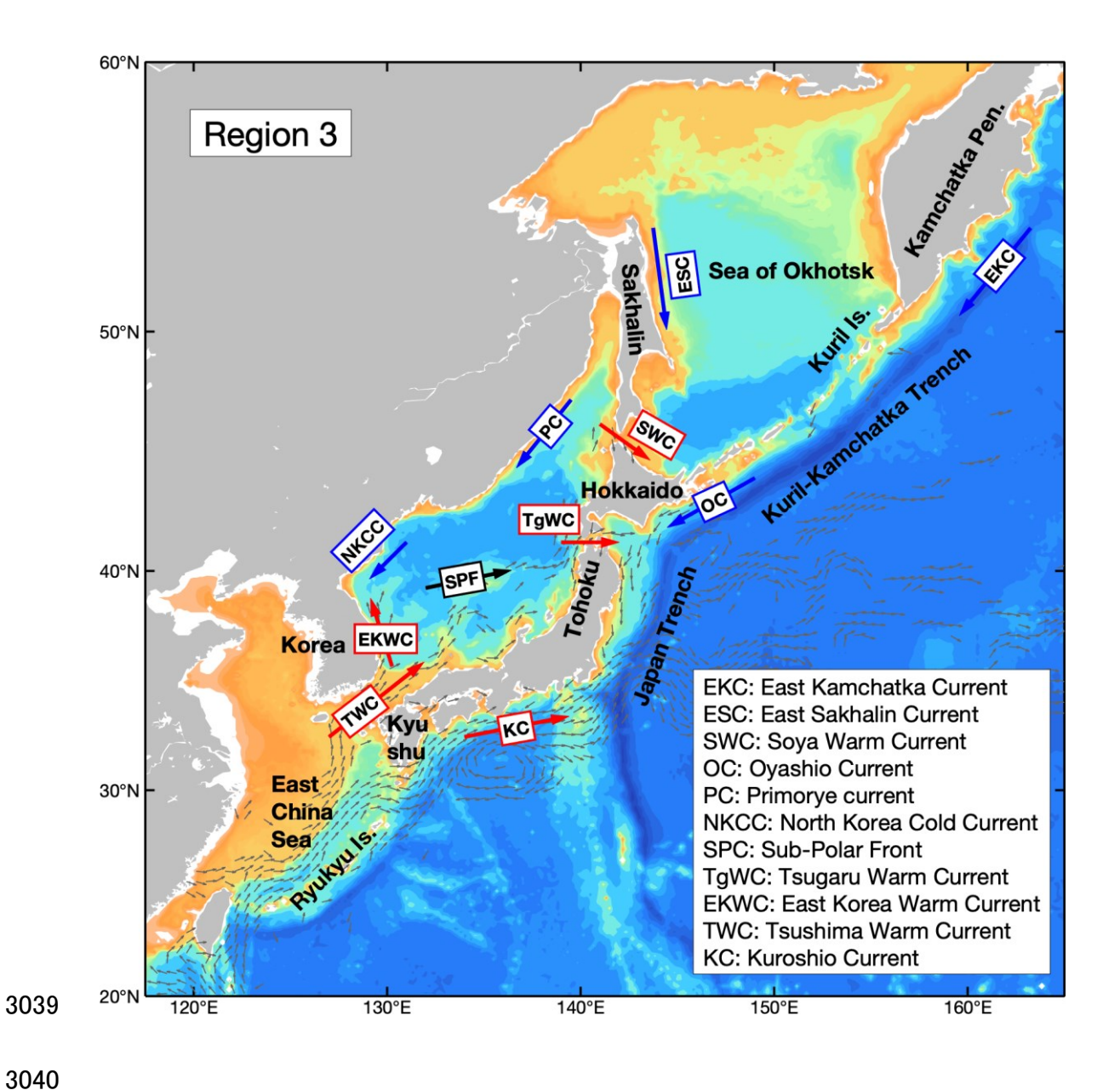


Fig. 14. As in Fig. 7 but for the western boundary of the North Pacific and marginal seas (Region 3). In this figure, gray arrows indicate the direction of mean surface geostrophic velocity whose speed is stronger than 0.1 m s⁻¹.

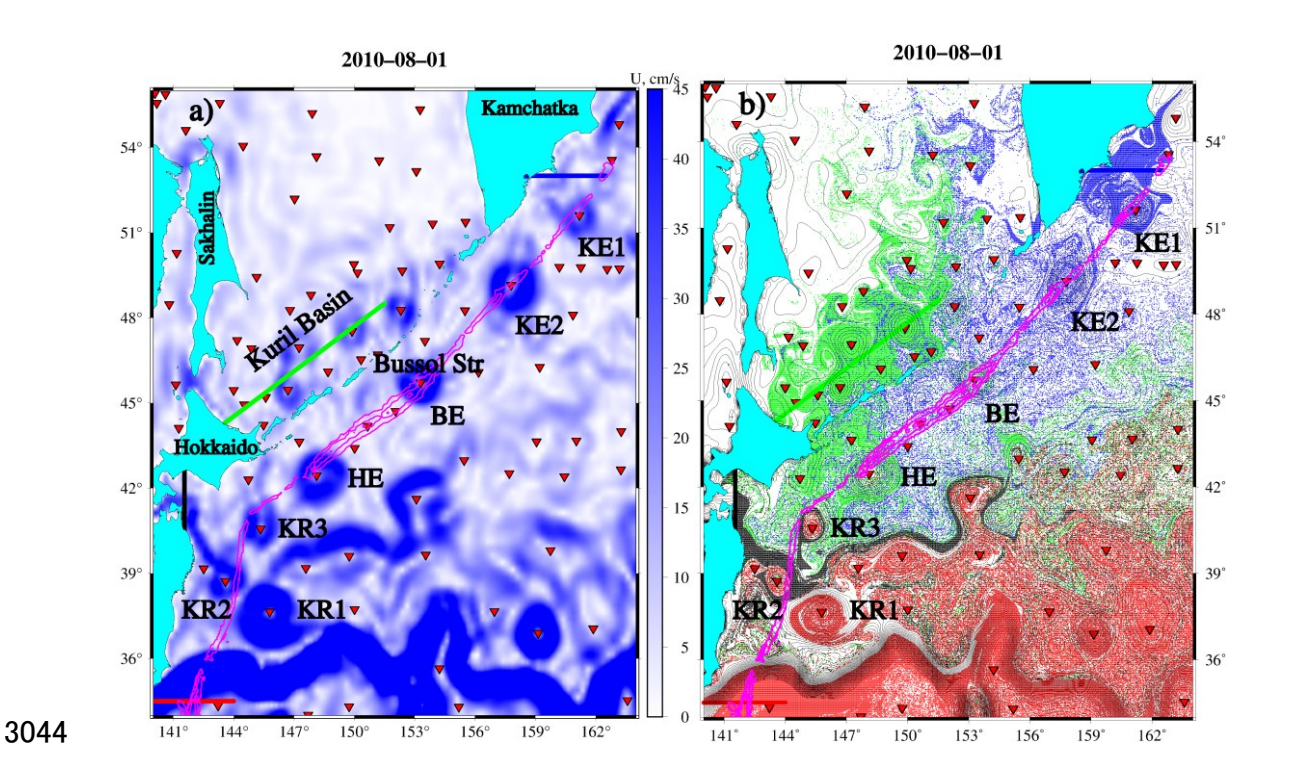


Fig. 15. (a) Snapshot current speed (cm/s) and (b) Lagrangian origin map on August 1, 2010, based on AVISO altimetry. Centers of anticyclonic features on this date are marked by triangles. Marked in (b) are Kuroshio rings as KR1-3, Hokkaido eddies as HE, Bussol' eddies as BE, Kamchatka eddies as KE1-2. (b) Colors mark fluid particles which crossed the sections of the same color shown in (a) during two years before the observation date. Isobaths from 7 to 10 km are shown by magenta contours. The origin of particles in the white areas could not be

determined.

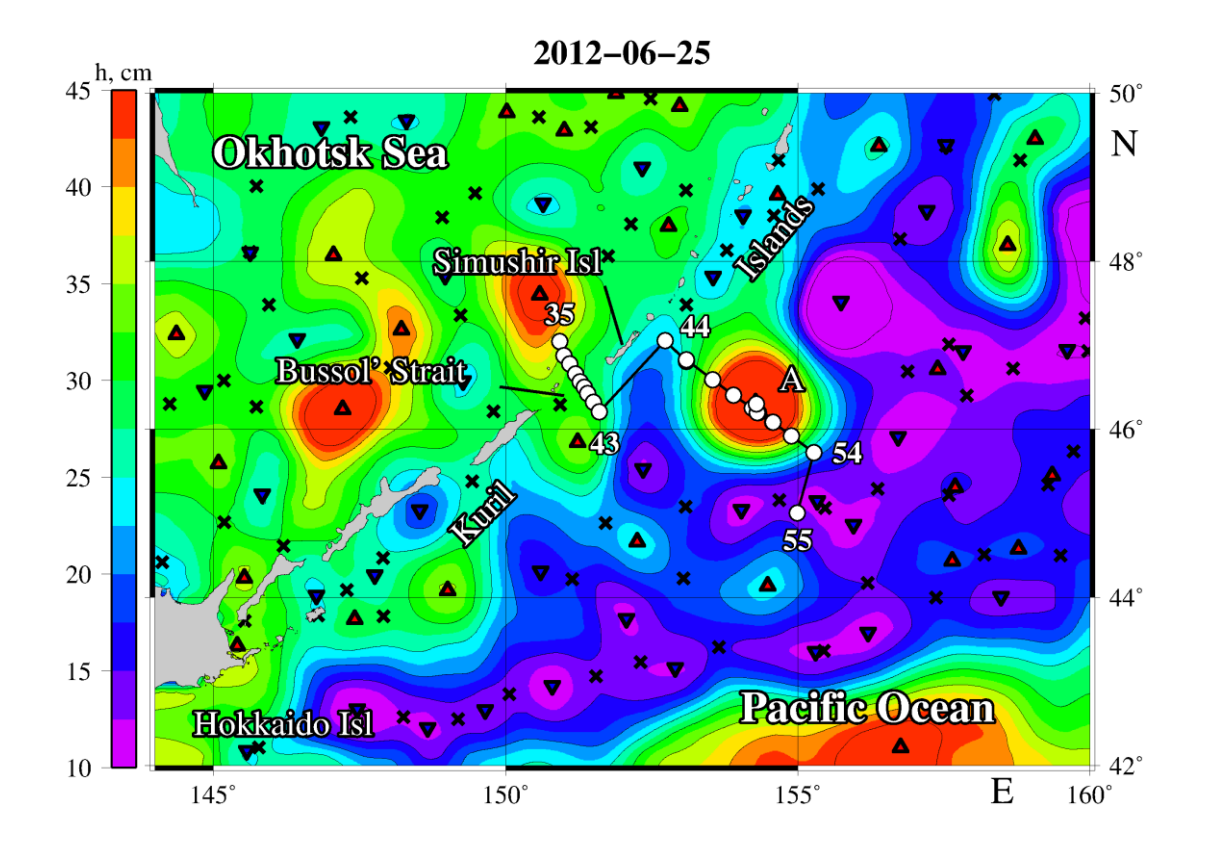


Fig. 16. SSH field showing the Bussol' eddy (A) sampled in a cruise in 2012 (white circles, Prants et al, 2016) and 'red' anticyclonic eddies with SSH > 45 cm in the Kuril Basin. Up(down)ward oriented triangles indicate the centers of anticyclonic (cyclonic) features on June 25, 2012. Reprinted from Prants et al. (2016), with permission from Elsevier.

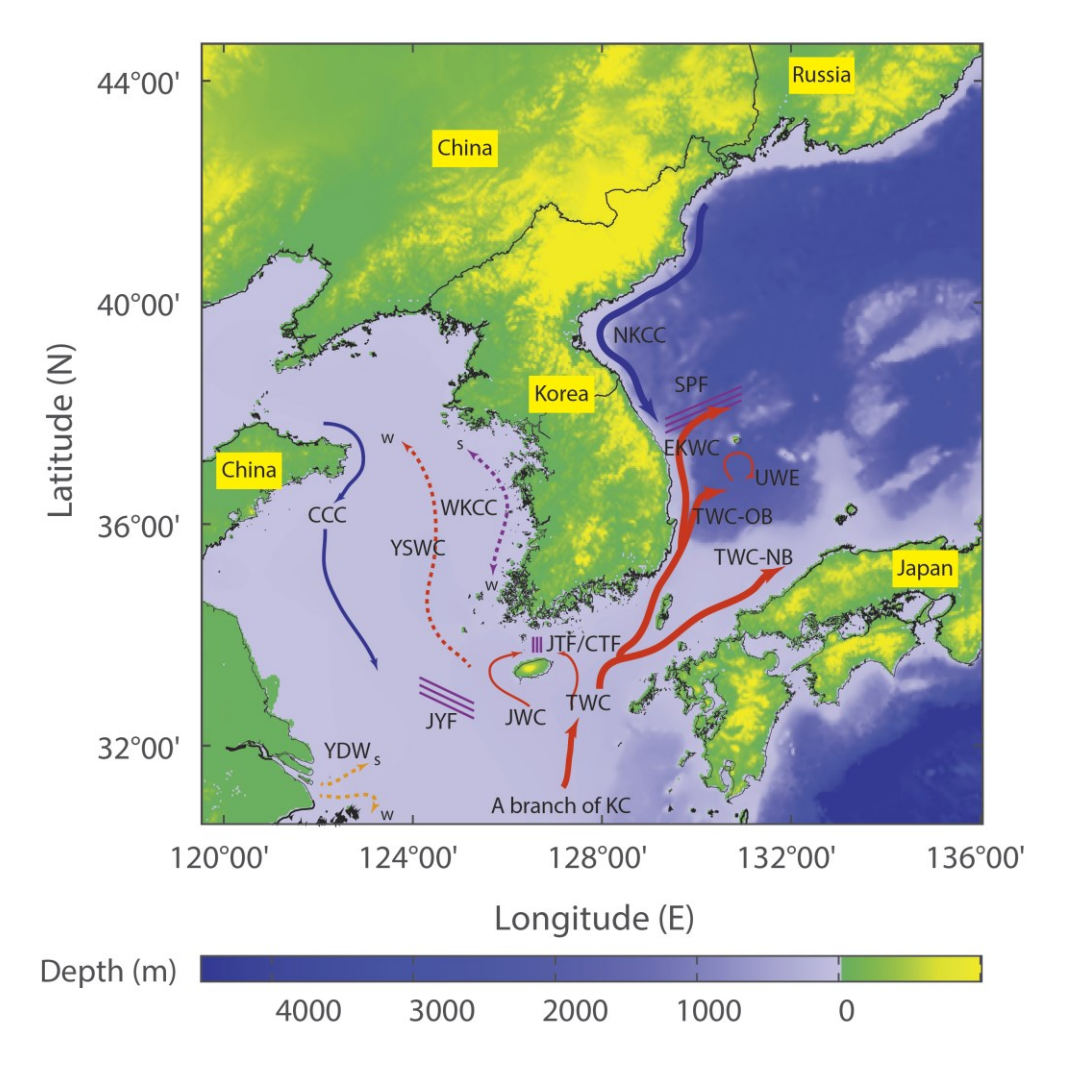


Fig. 17. Schematic of the regional circulation around the Korean Peninsula. Blue, red, purple, and orange colors indicate the water temperature of cold, warm, fronts, and riverine waters, respectively. Solid and dashed curves denote the persistent and seasonal currents, respectively (s and w indicate the directions of currents in summer and winter, respectively). Acronyms of primary regional currents are listed in the order of the Yellow Sea Warm Current (YSWC), West Korea Coastal Current (WKCC), Chinese Coastal Current (CCC), Jeju Warm Current (JWC), Jeju Tsushima Front (JTF)/Cheju Tsushima Front (CTF), Jeju Yangtze Front (JYF), Yangtze Diluted Water (YDW), Kuroshio Current (KC), North Korea Cold Current (NKCC), Tsushima Warm Current (TWC), Tsushima Warm Current-Nearshore Branch (TWC-NB), Tsushima Warm Current-Offshore Branch (TWC-OB), East Korea Warm Current (EKWC), Subpolar Front (SPF), and Ulleung Warm Eddy (UWE). Adapted from Lee et al. (2019).

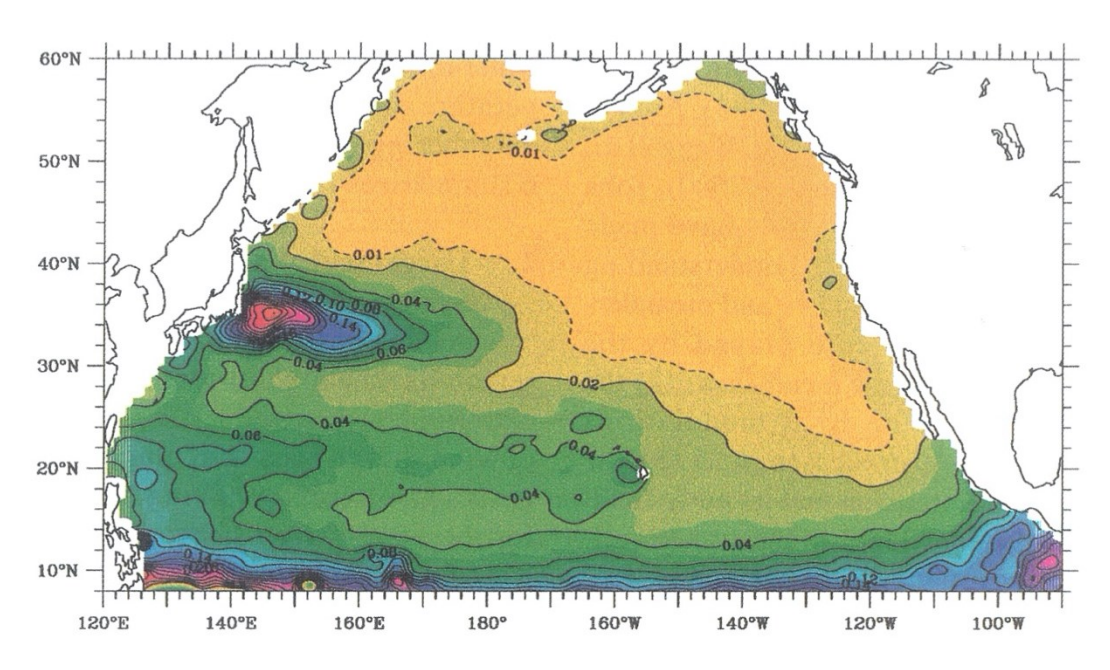


Fig. 18. EKE distributions in the North Pacific Ocean from the T/P SSH data of October 1992 to November 2000 after removing signals longer than the annual period. Contour intervals are 0.02 m²s⁻² for solid lines; dashed lines denote the 0.01 m²s⁻² contours. Reprinted by permission from Springer Nature: Qiu (2002).